INVESTIGATION OF THE EFFECT OF BISMUTH ON THE SQUEEZE CAST ZA-27 ALLOY

by

Uğur Osman Bozer

B.S. in M.E., Kocaeli University, 1999

Submitted to the Institute for Graduate Studies in
Science and Engineering in partial fulfillment of
the requirements for the degree of
Master of Science

Graduate Program in Mechanical Engineering

Boğaziçi University

2006

ACKNOWLEDGEMENTS

I wish to thank to Prof. Dr. Mahmut A. Savaş, my thesis supervisor for his invaluable help and guidance and to Prof. Dr. Sabri Altıntaş for his suggestions and interest during this study.

I also wish to thank to my chief in the Diler Steel Plant Gebze, Mehmet Demirci for his help and patience. Also, I wish to thank to Özgür Başkaya for his guidance and help in the experimental work, and to the research assistants in the Material Laboratory of Mechanical Engineering Department of Boğaziçi University, especially to Nazım Mahmutyazıcıoğlu for his invaluable help.

I also wish to thank to Fatma Başaran for her support and encouragement during this thesis.

Besides, I am grateful to my family; my mother Şerife Bozer, my sisters Aslıhan and Neslihan for their understanding and support during this work.

Especially I am grateful to my father Hasan Bozer for his invaluable help, worthy support and encouragement.

ABSTRACT

INVESTIGATION OF THE EFFECT OF BISMUTH ON THE SQUEEZE CAST ZA-27 ALLOY

Squeeze casting is specified as a technique where solidification is promoted under high pressure within a re-usable die hence, combining the permanent mould casting and die forging in a single operation. Squeeze casting has a greater potential to produce less defective cast components contrary to the other conventional casting techniques.

In the present study, the aim was to search for the improvement of the mechanical properties of the ZA-27 alloy in three different pressure ranges in conjuction with the addition of various percentages of bismuth element. For this purpose; ZA-27, ZA-27+0.5 wt%Bi, ZA-27+1.0 wt%Bi, ZA-27+1.5 wt%Bi, i.e. in total 54 samples were cast under 0, 50 and 100 MPa squeezing pressures. Three sets of the castings (36 pieces) were machined for the tension test, microstructure examination and machinability test, and the remainder castings were prepared for hardness test, chemical composition determination and surface roughness. While doing this thesis, 36 tension tests, 12 SEM microstructure analyses were done. 85 SEM photographs, 140 optical photographs were taken to understand the microstructure-property relations, A lot of chip lengths were measured from 12 different type of parts to understand the machinability characteristics, 288 Brinell hardness measurements were taken from 12 parts to understand hardness variation, 120 roughness measurements were done in 12 parts to determine roughness variation, density calculations of 29 parts were done to determine the effect of squeezing pressure on density.

It was found that, when the bismuth concentration was increased the machinability characteristics were increased, too. Also, the color of the bismuth added castings were darker than the pure ZA-27 alloys. As the squeezing pressure was increased, the porosity levels of each batch were decreased and the densities were increased. It was seen that while applying squeezing pressure to the semi-solid mixture, the lower part of the die solidified before the upper part. To eliminate this, a batch of glass wool was put under the die for insulation.

ÖZET

BİZMUTUN SIKIŞTIRMA DÖKÜMLE DÖKÜLMÜŞ ZA-27 ALAŞIMINA ETKİSİNİN İNCELENMESİ

Sıkıştırma döküm; katı-sıvı bölgesinde katılaşmakta olan bir alaşımın yüksek basınç altında ve tekrar kullanılabilen bir kalıp içerisinde yapıldığı döküm anlamına gelir. Bu döküme ayrıca hassas dökümle dövme işleminin tek operasyonda birleştirilmesi olarak da bakılabilir ve bu nedenle ergiyik dövme olarak anıldığı da olur.

Bu çalışmanın amacı ZA 27 alaşımının üç farklı basınç aralığında, çeşitli oranlarda bizmut eklenmesi sonucu mekanik özelliklerde ve talaşlı işlenebilirlikte ortaya çıkan davranışlarını incelemektir. Bu amaçla, saf Çinko Alüminyum alaşımı (ZA 27) ile ZA-27+%0.5 Bi, ZA 27+%1.0 Bi, ZA 27+%1.5 Bi alaşımlarından en az 4 set ve 0-50-100 MPa basınçlarda olmak üzere toplam 54 parça dökülmüştür. Bu parçaların her bir türünden 3'er seti işlenebilirlik ve çekme deneyinde kullanılmak üzere tornalanmıştır. Ayrıca, bu 3 set malzemede mikroyapı incelemesi yapılmıştır. Kırılma yüzeyleri taramalı elektron mikroskobunda incelenmiştir.

Diğer 1 set malzemede ise sertlik dağılımı, kimyasal bileşim ve yüzey pürüzlülüğü değerlerine bakılmıştır. Çıkan sonuçlara göre, artan bizmut miktarının, malzemenin işlenebilirliğini arttırdığı gözlenmiştir. Belirli bir yüzdeden (monotektik bileşimden) sonra artan bizmut miktarının, çok küçük talaş boyutu (toz) oluşturması sebebiyle malzeme işlenebilirliğini olumsuz etkilediği gözlemlenmiştir. Buna ek olarak, alaşımın içerdiği bizmut miktarının artmasıyla dökümlerin dış renginin de koyulaştığı görülmüştür.

Sıkıştırma basıncındaki artışa paralel olarak malzemelerin içindeki boşluk miktarının azaldığı ve malzemenin yoğunluğunun arttığı gözlemlenmiştir. Potadan dökülen ergiyik alaşıma sıkıştırma işlemini uygularken, kalıbın alt kısmındaki ergiyiğin daha hızlı katılaştığı ve bu sebeple alt kısmın yeterince sıkıştırılamadığı gözlemlenmiştir. Bu olumsuzluğu gidermek için kalıbın altına bir miktar cam yünü yerleştirilmiş, bu bölgenin soğuması yavaşlatılmış ve deney parçalarının tümünün sıkıştırılabilmesi sağlanmıştır.

TABLE OF CONTENTS

LIST OF FIGURES

LIST OF TABLES

LIST OF SYMBOLS / ABBREVIATIONS

C	Number of components
C_{Al}	Weight percentage of the Al metal in the ZA alloy
C^i	Specific heat of the particle
C_m	Monotectic composition
C_o	Composition
C^p	Specific heat of the particles
C_s	Chvorinov constant
C_{Zn}	Weight percentage of the Zn metal in the ZA alloy
d	Density
d_1	Primary dendrite arm spacing
d_2	Secondary dendrite arm spacing
D^M	Density of the melt
g	Gravitational Acceleration
h	Undeformed chip thickness
h_c	Chip thickness
Kıc	Fracture toughness
L	Liquid phase
I_c	A chip of measured length
L_f	Latent heat of fusion (J/kg)
m_1, m_2	Weight of elements
m_a	Mass of the specimen in air
m_w	Mass of specimen in water
n	Angular speed
P	Applied pressure (MPa)
P_c	Cutting force
P_h	Compressive force
P_n	Shear force

P_R	Resultant force
P_t	Thrust force
R_k	Material ratio curve parameter (μm)
R_{max}	Largest peak to valley height (mm)
R_z	Average height of profile (μm)
r	Radius
r_c	Cutting ratio
S	Surface area of the casting
T	Temperature
T_E	Melting point
T_f	Equilibrium freezing temperature (˚K)
T_l	Liquidus temperature of the alloy
T_m	Monotectic temperature
T_s	Solidus temperature of the alloy
t_s	Total solidification time
V	Volume of the casting
V_l	Specific volume of the liquid
V_s	Specific volume of the solid
$\bar{x}$	Some parameter of x
W_{Al}	Weight of Al pieces
W_{Zn}	Weight of Zn pieces

α	Solid phase
ΔH_f	Latent heat of fusion
ΔT	Temperature difference due to applied pressure
$\varepsilon_f^{\%}$	Elongation at fracture
ϕ	Outer dimension of the test bar
μ	Viscosity
θ	Clearance angle

ρ	Calculated density
ρ_l	Liquidus density (kg/m^3)
ρ_s	Solidus density (kg/m^3)
σ_{uts}	Ultimate tensile strength (N/mm2)
σ_{ys}	Yield strength (N/mm2)
$\sigma_{0.2}$	Yield strength
σ_f	Fracture strength
υ	Cutting speed (m/min)

ASTM	American Society for Testing of Materials
DC	Direct Casting
F	Forging
MMC	Metal Matrix Composite
ZA	Zinc Aluminum Alloy
ZA-27	Zinc-27 %wt Aluminum Alloy

1. INTRODUCTION

To date, little attention has been given to the bismuth addition into squeeze casting alloys except some researches [1, 2, 3]. In the current work, the general aim was to increase the machinability of the popular ZA-27 alloy without harming its mechanical properties. Since bismuth forms monotectic systems both with zinc and aluminum, it was hoped that the chip length of the ZA-27 alloy would be reduced as it was achieved in the commercial free cutting aluminum alloys. Bismuth is the most diamagnetic of all metals, and the thermal conductivity is lower than any metal, except mercury. It has a high electrical resistance, and has the highest Hall Effect of any metal (i.e., greatest increase in electrical resistance when placed in a magnetic field). "Bismanol" is a permanent magnet of high coercive force, made of MnBi, by the U.S. Naval Surface Weapons Center. Bismuth expands 3.32% on solidification. This property makes bismuth alloys particularly suited to the making of sharp castings of objects subject to damage by high temperatures [4]. In terms of mechanical properties, it is a brittle material.

Squeeze casting is also known as liquid metal forging, squeeze forming, extrusion casting and pressure crystallization. It is a casting process in which metal is solidified under the direct action of pressure and essentially a combination of gravity die-casting and closed die forging can be achieved. The major advantages of squeeze casting are:

- Parts produced are without gas porosity or shrinkage porosity;
- Feeders or risers are not required and therefore no metal wastage occurs;
- Alloy fluidity (castability) is not critical in squeeze casting as both common casting alloys and wrought alloys can be squeeze cast to finished shape with the aid of pressure;
- Squeeze castings can have mechanical properties as good as wrought products of the same composition [5].

- Other advantages include fine structure, heat-treatable, weldable, good surface finish, high productivity, applications for composite fabrication, and can cast special alloys [6]. Casting quality is compared with the other casting techniques in Table 1.1.

Table 1.1. Casting quality with respect to the casting technique [6]

	Low Pressure Die Casting	High Pressure Die Casting	Vacuum Die Casting	Thixomoulding	Semi Solid Forging	Squeeze Casting
Cycle Time	C	B	C	A	D	B
Surface Finish	C	A	C	A	A	A
Gas Entrapment	B	D	B	B	B	A
Shrinkage Pores	D	D	D	A	A	A
Heat Treatable	A	D	A	A	A	A
Weldable	A	D	A	A	A	A
KEY	A= GOOD, D=POOR					

Among the zinc-based foundry alloys used as matrix materials, the ZA family of alloys has been particularly popular during recent years. ZA-27 alloy, developed by the Canadian Organisation of Naranda Mines Ltd, is part of a new family of zinc-based foundry alloys characterized by low initial cost, excellent foundry castability, good mechanical properties and good machining properties. These properties combine to make this alloy suitable for a wide range of purposes both in sand casting and die casting. The other members of the family, namely ZA-8 and ZA-12 alloys, are moderate to high strength materials, while ZA-27 is a high strength alloy'. In some cases, the properties can be equivalent to those of aluminum alloys [7].

The alloy composition, casting method and microstructure are important to increase simultaneously the mechanical properties, and machinability characteristics of ZA-27 alloy. Thus, this work includes the preparation of alloy composition ZA-27, ZA-27+0.5 wt%Bi, ZA-27+1.0 wt%Bi, ZA-27+1.5 wt%Bi. At least four samples for each composition were prepared under 0, 50 and 100 MPa pressures. Three sets of the castings were machined for tension test, microstructure examination and machinability test, and remainder castings were prepared for hardness test, chemical composition test and surface roughness. The die temperature was selected 285˚C, which is near the eutectic temperature of the system. This work aims to detect the effect of bismuth on the tensile and yield strengths of ZA-27 alloy. Another aim was to examine the effect of squeezing pressure on the castings.

2. LITERATURE SURVEY

2.1. Squeeze Casting

Squeeze casting is a process by which molten metal solidifies under applied pressure that is maintained until the end of solidification. The closed dies are positioned between the plates of hydraulic press. By pressurizing liquid metals while they solidify, near-net shapes can be achieved in sound, fully dense castings. The dimensional accuracy of squeeze castings is similar to those of die-casting, 0.25 mm in 100 mm to 0.6 mm in 500 mm. The applied pressure and the instant contact of the molten metal with the die surface produce a rapid heat transfer condition that yields a pore-free fine-grain casting with mechanical properties approaching those of a wrought product. However, the process is much simpler, more economical and more efficient in its use of raw material. Due to the high pressure, porosity is eliminated and microstructural refinement is achieved to a much greater extent than any other casting processes. The microstructure refinement and integrity made possible by squeeze casting allow a variety of secondary operations to be conducted, including welding and solution heat treatment [8].

2.1.1. Definition

Casting is the most economical route to transfer raw materials into readily usable components. However, one of the major drawbacks for conventional or even more advanced casting techniques, e.g., high pressure die-casting -is the formation of defects such as porosity. Furthermore, segregation defects of hot tears, A and V segregates and banding could be potential crack initiators during service operation of the as-cast components. New casting techniques have, therefore, been developed to compensate for these shortcomings. Of the many such casting techniques available, squeeze casting has greater potential to create less defective cast components [6].

Squeeze casting (SC) is a generic term to specify a fabrication technique where solidification is promoted under high pressure within a re-usable die. It is a metal-forming process, which combines permanent mould casting with die forging into a single operation where molten metal is solidified under applied hydrostatic pressure. Although squeeze casting is now the accepted term for this forming operation, it has been variously referred to as “extrusion casting”, “liquid pressing", ”pressure crystallisation" and ``squeeze forming". The idea was initially suggested by Chernov in 1878 to apply steam pressure to molten metal while being solidified. However, in spite of its century old invention, commercialisation of squeeze casting has been achieved only quite recently and is mainly concentrated in Europe and Japan. It is mainly used to fabricate high integrity engineering components with or without reinforcement. Hartley reported a technique developed by GKN Technology in UK for the pressurised solidification of Al alloy in reusable dies. In this process a die set is placed on a hydraulic press and preheated, and the exact amount of molten alloy is poured into the lower half of the open die set, the press closed so that the alloy fills the cavity and the pressure maintained until complete solidification occurs (31± 108 MPa pressure). External undercut forms can be produced, and using retractable side cores, through-holes are possible. Since the as-fabricated components can be readily used in service or after a minor post-fabrication treatment, squeeze casting is also regarded as a net or near net-shape fabrication route [6].

Parallel to commercialisation, there are research centers throughout the world that are actively researching further development and exploitation of this net or near net shape fabrication process. This is evidenced by the publication of more than 700 papers in various engineering and scientific journals. These are mainly related to aluminum and magnesium-based alloys with special emphasis on metal matrix composites MMC’s. According to Crouch, squeeze casting is now the most popular fabrication route for MMC artifacts. The annual 12±15% growth rate of MMC’s in the automotive, aerospace, sport and leisure goods and other markets is a clear indication of better usage of advanced manufacturing routes such as squeeze casting [6].

Generally, the SC-fabricated engineering components are fine grained with excellent surface finish and have almost no porosity. They come in a variety of shapes and sizes. The mechanical properties of these parts are significantly improved over those of

conventional castings and more sophisticated casting routes of pressure or gravity die-casting. It is further claimed that SC-fabricated components have superior weldability and heat treatability. In addition, since squeeze casting may be carried out without any feeding system, runners, gates, etc., and shrinkage compensating units, risers, and the yield is quite high with almost no scrap for recycling. Finally, in contrast to forging, squeeze cast components are fabricated in a single action operation with lesser energy requirements.

The squeeze forming (or casting) process has many advantages. The main advantages of the process are smoother surfaces of the cast parts, reducing the mushy zone during solidification, fewer defects and higher component strength due to rapid solidification rates that are achieved. The process has a high yield since there are no feeding and filling systems attached to the casting [9].

Two different types of squeeze casting technology have evolved, based on different approaches to metal metering and metal movement during die filling. These have been given the names “direct” and “indirect”. Direct squeeze casting is sometimes termed liquid-metal forging since it is accomplished in equipment more akin to that used for forging than to that used for die casting. It is a process in which liquid metal is poured into a lower die segment contained within a hydraulic press, the upper die segment is then closed over it and high pressure (usually 100 MPa or more) is applied over the entire cavity until the part is solidified. Both the direct squeeze casting and indirect squeeze casting have advantages and disadvantages [8].

Direct Squeeze Casting: In the case of the direct squeeze casting, the melt is poured directly into an open die, and a hydraulic ram is moved down into the melt to apply the pressure. The biggest advantage of direct squeeze casting process is that pressure is applied to the entire surface of the liquid metal during freezing, producing castings of full density. This technique, inevitably, gives the most rapid heat transfer, yielding the finest grain structure but does not control the die filling stage. This leads to turbulent flow and the entrapment of brittle surface oxide films. The inherent time delay occurring after the metal is poured and prior to pressurization with the ram often leads to premature solidification. A highly accurate metering system is needed to control the dimensions of the casting.

Indirect Squeeze Casting: Indirect squeeze casting, on the other hand, is akin to die casting. Is performed in die-cast-like equipment (vertical or horizontal) and tooling. An example of one version of indirect squeeze casting is the vertical process offered by Ube of Japan [6].

Indirect squeeze casting has proven to be among the more capable processes for such automotive safety components as steering knuckles. It is especially useful for heavier-walled parts such as knuckles but considerably more limited for thin parts like chassis frame nodes or brackets. In indirect squeeze casting the pressure is more difficult to apply compared to direct squeeze casting. The melt is injected into the bottom of the die cavity with a hydraulic ram. The metal flow can be controlled via the injection speed and pressure application begins as soon as the die is filled. The casting forms inside a closed die cavity and the dimensions of the casting are easier to control. The use of a highly accurate metering system is not required. As a result, the indirect squeeze casting process has seen more commercial use than the direct process in die casting industry.

Although these are two distinct versions of squeeze casting, direct and indirect, both versions utilize the essentials of the process; molten metal is introduced to casting cavities with minimum turbulence and solidifies under high pressure within very robust (usually ferrous) closed dies. High pressure and intimate contact of molten alloy with metal die surfaces produce very rapid solidification, small secondary dendrite arm spacing (SDAS), minimum porosity and excellent mechanical properties.

2.1.2. Process Outline

The process of squeeze casting involves the following steps [6]:

1. A pre-specified amount of molten metal is poured into a preheated die cavity, located on the bed of a hydraulic press.

2. The press is activated to close off the die cavity and to pressurize the liquid metal. This is carried out very quickly, rendering solidification of the melt under pressure.

3. The pressure is held on the metal until complete solidification. This not only increases the rate of heat flow, but also most importantly may eliminate macro / micro shrinkage porosity. In addition, since nucleation of gas porosity is pressure-dependent, the porosity formation due to dissolve gases in the molten metal is restricted.

4. Finally the punch is withdrawn and the component is ejected.

2.1.3. Mechanics of Squeeze Casting

The Die: A most crucial aspect in permanent mould castings such as die-casting or squeeze casting is the die itself and, most importantly, the design of the die including the selection of a suitable die material, the manufacturing process, appropriate heat treatment and the maintenance practice. Squeeze casting dies are exposed to severe thermal and mechanical cyclic loading, which may cause thermal fatigue, cracking, erosion, corrosion, and indentation. The nature and features of a die are greatly influenced by the particular alloy to be cast. Currently, H13 tool steel is a widely used material of constructions but generally die steels should have good hot hardness, high temper resistance, adequate toughness and especially a high degree of cleanliness and uniform microstructure.

The Key Features of the Casting Process: Two basic forms of the process may be distinguished, depending on whether the pressure is applied directly on to the solidifying cast product via an upper or male die (punch) or the applied pressure is exerted through an intermediate feeding system as schematically shown in Figure 2.1. : (i) the direct squeeze casting mode, and (ii) the indirect squeeze casting mode.

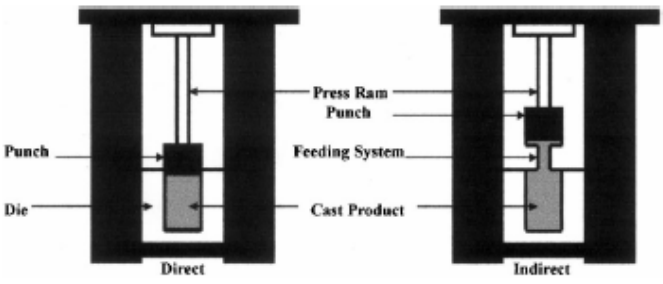

Figure 2.1. Basic forms of squeeze casting process [6]

For the direct mode, two further forms may be distinguished based on liquid metal displacement initiated by the punch movement: (i) without metal movement, and (ii) with metal movement.

The first form is suitable for ingot type components where there is no metal movement, whilst the second type involving metal movement, also known as the backward process, is more versatile and can be used to cast a wide range of shaped components. In addition to the molten metal displacement forms, the squeeze casting process may also be classified based on the following features.

Type of equipment: A variety of squeeze casting machines are in use in various parts of the world. They are either designed by the researchers themselves, the so-called home-made, or manufactured by machine tools companies on a mass production basis. The direct SC-machines are simple and straight forward but the indirect ones generally fall into the following categories of: (i) vertical die closing and injection, (ii) horizontal die closing and injection, (iii) horizontal die closing and vertical injection, and (iv) vertical die closing and horizontal injection.

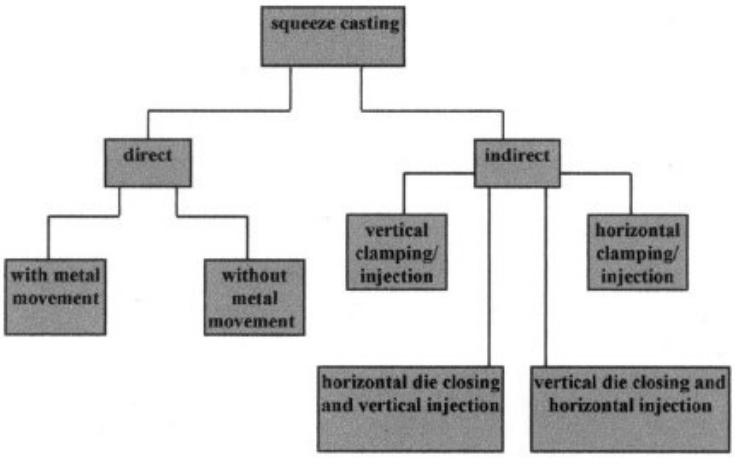

Figure 2.2. Block diagram to show the squeeze casting classifications [6]

Timing of Pressure Application: Although squeeze casting is regarded as the pressurisation of molten alloy, it may also be used for shaping semi-solids and, therefore, a further classification may be envisaged as:

Before the beginning of crystallisation, and after the beginning of crystallisation, which may also be described as semi-solid pressing. Figure 2.2. summarizes the various modes of the squeeze casting process

2.1.4. Process Parameters

The most important process parameter is the alloy itself. The composition and physical characteristics of the alloy are of paramount importance due to their direct effects on the die life. These include the melting temperature, and thermal conductivity of the alloy together with the combined effect of the heat-transfer coefficient and soldering onto the die material. Furthermore, the alloy dictates the selection of casting parameters such as die temperature, which has direct consequence on the die life. Therefore, squeeze casting is usually employed for low melting temperature alloys of aluminum and magnesium [6].

In addition to the composition of a casting alloy, which determines its freezing range and affects the quality of finished components, the casting parameters should also be controlled very closely to achieve a sound casting. The most dominant process parameters are die temperature and pouring temperature, and superheat, although the level of applied pressure is also important. Since the metal is cast under pressure, the inherent castability of the alloy is of little or no concern. Other important parameters include the cleanliness of the metal in relation to the presence of inclusions, metal movement within the die which may induce turbulence, the die coat, and the time interval over which the pressure is applied, i.e., the so-called dead time. The die temperature is usually held at between 200°C and 300°C for aluminum and magnesium alloys, whilst the applied pressure varies between 50 and 150 MPa. The lubrication medium, i.e., the die coat, is usually graphite based. Heat-transfer coefficients are extremely high due to the casting metal being pressed against the die wall [6].

2.1.5. Limitations of Squeeze Casting

Squeeze casting has a few shortcomings or disadvantages:

- Relatively poor tool life (melt temperatures during squeeze casting are typically 700 to 730 ˚C) that is quite a bit higher than is typical of die casting (650 to 660 C), thus

the ΔT between die and melt is higher; it is that ΔT that drives the onset of thermal fatigue of tool surfaces. While selection of the material of the mold, this thermal fatigue risk should be considered. So, generally H13 high temperature steel is selected for mold material. If the material isn't high temperature resistant, creep formation occurs and useful usage time of the mold decreases.

- Costly de-gating and high capital cost, i.e., large in-gates must be sawed from cast parts.

- Limited suitability for thin-walled or highly detailed parts.

- Limited suitability for producing complex shapes.

- Limited cavity count (high pressures limit the projected area that a given machine tonnage can accommodate), limited maximum size and weight.

- As with most other high pressure processes, limited ability to accommodate disposable internal cores.

2.2. Zinc Alloys

Zinc alloys' high strength and hardness, means that it is the ideal alternative to machined, pressed, stamped and fabricated items. This section covers an explanation of zinc alloys' properties and uses. Tables below that show their properties and composition, as are graphs showing their behaviour at various temperatures and stresses.

Zinc Alloy Characteristics:

- High strength and hardness
- Excellent electrical conductivity
- High thermal conductivity
- Lowest cost raw material

- High dimensional accuracy and stability
- Excellent thin wall capability
- Ability to cold form, which eases joining
- High quality finishing characteristics
- Outstanding corrosion resistance
- Full recyclability

Table 2.1. Main characteristics of ZA alloys [10]

Characteristic	Zamak Die-casting Alloy				ZA Die-casting Alloy		
	2	3	5	7	ZA-8	ZA-12	ZA-27
Resistance to Hot Cracking	1	1	2	1	2	3	4
Pressure Tightness	3	1	2	1	3	3	4
Casting Ease	1	1	1	1	2	3	3
Part Complexity	1	1	1	1	2	3	3
Dimensional Accuracy	1	1	1	1	2	2	3
Dimensional Stability	4	2	2	1	2	3	4
Corrosion Resistance	2	3	3	2	2	2	1
Resistance to Cold Defects	2	2	2	1	2	3	4
Machining Ease and Quality	1	1	1	1	2	3	4
Polishing Ease and Quality	2	1	1	1	2	3	4
Electroplating Ease and Quality	1	1	1	1	1	2	2
Anodizing (Protection)	1	1	1	1	1	2	2
Chemical Coating (Protection)	1	1	1	1	2	3	3
Relative Scale : 1=Most Desirable, 5=Least Desirable							

2.2.1. Advantages of Zinc Based Alloys

Zinc casting alloys are versatile engineering materials. No other alloy system provides the combination of strength, toughness, rigidity, bearing performance and economical castability. Listed are zinc alloy attributes which can reduce component costs. Improving precision, quality and product performance are other zinc alloy design advantages discussed below.

Process Flexibility: Virtually any casting process can be used with zinc alloys to satisfy virtually any quantity and quality requirement. Precision, high-volume die casting is the most popular casting process. Zinc alloys can also be economically gravity cast for lower volumes using sand, permanent mold, graphite mold and plaster casting technology.

Precision Tolerances: Zinc alloys are castable to closer tolerances than other metals or molded plastics, therefore presenting the opportunity to reduce or eliminate machining. "Net Shape" or "Zero Machining" manufacturing is a major advantage of zinc casting.

Strength and Ductility: Zinc alloys offer high strengths (to 60,000 psi) and superior elongation for strong designs and form ability for bending, crimping and riveting operations.

Toughness: Few materials provide the strength and toughness of zinc alloys. Impact resistance is significantly higher than cast aluminum alloys, plastics, and grey cast iron.

Rigidity: Zinc alloys have the rigidity of metals with modulus of elasticity characteristics equivalent to other die castable materials. Stiffness properties are therefore far superior to engineering plastics.

Anti-Sparking: Zinc alloys are non sparking and suitable for hazardous location applications such as coal mines, tankers and refineries.

Bearing Properties: Bushing and wear insert in component designs can often be eliminated because of zinc's excellent bearing properties. For example, zinc alloys have outperformed bronze in heavy duty industrial applications.

Easy Finishing: Zinc castings are readily polished, plated, painted, chromated or anodized for decorative and/or functional service.

Thin Wall Castability: High casting fluidity regardless of casting process allows for thinner wall section to be cast in zinc compared to other metals. Related to that, Britnell

and Neailey [11] found that when the pressure difference used across a curved surface and equating this to the pressure due to depth, the minimum web width or no significant segregation can be estimated. This estimation has been verified for LM25. Thus components can be designed with walls of minimum thickness and minimum radius for corners for production using the squeeze casting technique.

Machinability: Fast, trouble-free machining characteristics of zinc materials minimize tool wear and machining costs.

Low Energy Costs: Because of their low melting temperature, zinc alloys require less energy to melt and cast versus other engineering alloys.

Long Tool Life: Low casting temperatures result in less thermal shock and therefore extended life for die casting tools. For example, tooling life can be more than 10 times that of aluminum dies. According to L.J.Yang [5], the best temperatures to gravity cast the aluminum alloy and the zinc alloy were 720 and 460 ˚C, respectively. For the squeeze casting of the aluminum alloy, the best temperature to use was either 690 or 660 ˚C; the former would give a better property at the top of the casting while the latter, at the bottom of the casting. However, for the squeeze casting of the zinc alloy, the best temperature was again 460 ˚C.

Clean and Recyclable: Zinc alloys are among the cleanest melting materials available. Zinc metal is non-toxic and scrap items are reusable resources which are efficiently recycled [12].

2.2.2. Zinc Die Casting Alloys

Designers of structural components should be aware of the creep limitations of zinc alloys, which are discussed below. These alloys exhibit excellent damping capacity and vibration attenuation in comparison with aluminum diecasting alloys. Aluminum, as alloying element in Zn-based alloys, greatly affects solidification behavior of the alloys [14, 15] and in turn affects their microstructure. Zn–Al alloys basically comprise a mixture

of two phases, namely α and η (Al and Zn rich solid solutions of each other, respectively), distributed in a specific manner depending on the Al content. Zinc-Aluminum binary phase diagram can be seen below.

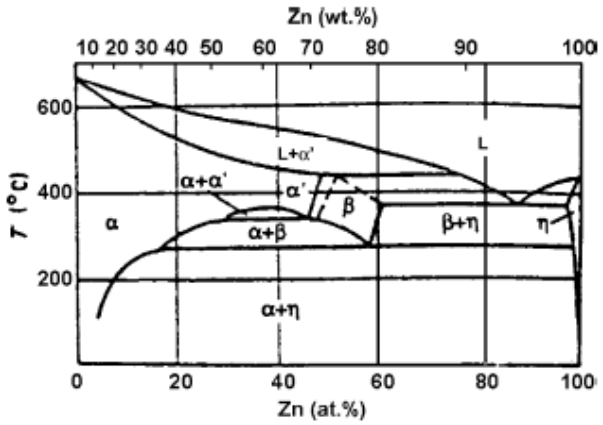

Figure 2.3. ZA binary phase diagram [13]

Microstructure of Zn–27Al has α-Al rich dendrites surrounded by α+η eutectoid (Figure 2.4.) [16]

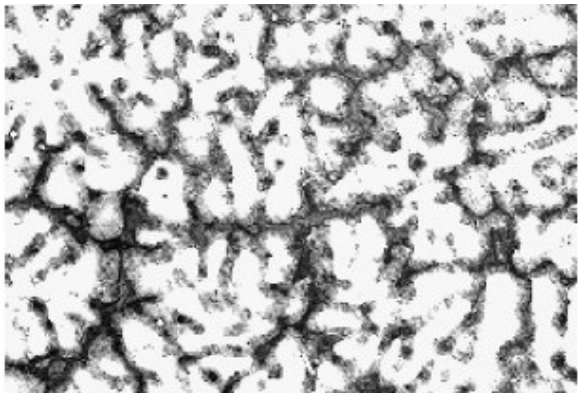

Figure 2.4. Microstructure of ZA–27 alloy [16]

Zinc Alloy 2: Zinc Alloy 2 is sometimes referred to as Kirksite. This alloy offers the highest strength and hardness of the family. However, due to the high copper content (3%), changes to the material properties occur with long-term ageing. These changes include slight dimensional growth (0.0014 mm/mm [in/in] after 20 years), lower elongation and reduced impact performance. Although this alloy exhibits excellent casting characteristics, it has seen limited use by diecasters. Its creep performance is rated higher

than the other zinc alloys and it maintains higher strength and hardness levels after long-term ageing.

Zinc Alloy 3: No. 3 Alloy is usually the first choice when considering zinc for diecasting and is the most widely used zinc alloy in North America. Its excellent balance of desirable physical and mechanical properties, superb castability and long-term dimensional stability are the reasons why most diecastings are made from this alloy. No. 3 Alloy also offers excellent finishing characteristics for plating, painting and chromate treatments. In terms of diecasting, it is the standard by which other zinc alloys are rated. Where higher strength is required, the other zinc alloys should be considered.

Zinc Alloy 5: No. 5 Alloy is the most widely used zinc alloy in Europe, with its higher copper content resulting in higher strength and increased hardness at the expense of some loss of ductility (increased elongation) compared to Alloy 3. This reduction in ductility can affect formability during secondary operations such as bending, riveting, swaging or crimping operations and should be carefully considered by the designer. Because of the wide availability of Alloy 3, component engineers often strengthen components by design modifications instead of using Alloy 5. However, when a measure of tensile performance is needed, alloy 5 castings are recommended.

Creep rates for Alloy 3 and 5 are very similar although Alloy 5 does have better creep resistance, and curves can be used for both alloys. Where temperatures above normal ambient are involved and the component must be designed to accommodate structural loads, Alloy 5 is likely to be a better choice.

Zinc Alloy 7: Alloy 7 is a modification of Alloy 3 resulting in improved casting fluidity, ductility and surface finish. Most Alloy 7 is used for special hardware applications, or when castings require extra formability during subsequent assembly operations such as crimping or staking. The higher fluidity also allows thinner walls to be cast.

Higher fluidity is sometimes desirable especially on components with intricate detail; however it does present special casting considerations. In order to avoid excessive flashing

along the tool parting lines, good die fit and close control of casting process parameters is necessary. The high ductility exhibited by this alloy also has an impact on processing, but mainly in secondary operations for flash removal and trimming.

Zinc Alloy ZA-8: The ZA alloys contain significantly more aluminum than the Zamak group of alloys with the numerical designation representing the approximate percentage of aluminum. ZA-8 was originally developed as a permanent mold alloy having excellent finishing and plating characteristics. It is particularly suitable for decorative applications. Although this alloy does not exhibit quite as good casting characteristics as the other zinc alloys, it offers significantly improved strength, hardness and creep properties. In terms of mechanical performance, this alloy has the highest creep strength of any zinc alloy and the highest strength of any hot-chamber diecast zinc alloy. This is the only ZA alloy that can be hot-chamber diecast.

Zinc Alloy ZA-27: Due to the high aluminum content of this alloy, it must be cold-chamber die-cast. This alloy has the highest strength, and the lowest density of the ZA alloys. ZA-27 provides the highest design stress capability at elevated temperatures of all the commercially available zinc-based alloys. This alloy also has excellent bearing and wear resistance properties.

According to the results of this study revealed [7] that as graphite composition was increased, there were significant increases in the ductility, ultimate tensile strength (UTS) and compressive strength of the composite, accompanied by a tremendous drop in the hardness of the material. Heat treatment was found to have a similar effect.

Zinc Alloy AlCuZinc5: This is an alloy researched and developed by General Motors, which exhibits greatly improved strength, hardness and creep performance due to the high copper and low aluminum contents. This alloy also has excellent bearing properties.

Zinc Creep: Creep (elongation under load) is defined as the time-dependent strain that takes place under a given load. There are generally, three distinct stages of creep:

- Primary - the creep strain that occurs at a diminishing rate
- Secondary - the creep strain that show a minimum and almost constant rate
- Tertiary - the creep strain that exhibits an accelerated rate, usually leading to rupture.

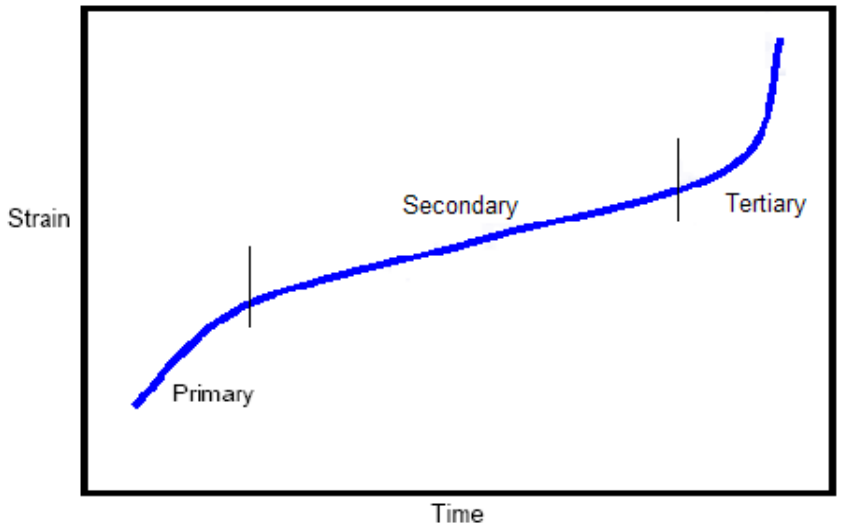

Figure 2.5. Stages of creep over time [10]

The strain rate behaviour of zinc alloys under stress is non-linear and time-temperature dependent, i.e., the ratio of stress to strain is not constant, even at low stresses, and varies with time, resulting in continuous plastic flow under applied load (creep). As a result, zinc alloys do not have a single value for elastic modulus. Yield strength (allowable stress) under sustained loading is dependent on the allowable design strain (% elongation) over the required service life. Working values for the elastic modulus and yield strength can be generated from the experimental curves for Tensile Creep Properties Alloy 3 and Beam Creep Properties Alloy 3 at room temperature. As the creep rates for Alloys 3 and 5 are very similar, the curves can be used for both alloys [10].

2.3. Material Properties of Zinc Alloys

2.3.1. Strength

ZA alloys deliver the highest tensile strength among the most widely used non-ferrous alloys and match or exceed that of most cast irons. Yield strength is a major ZA alloy attribute reaching 55,000 psi for ZA-27, that's more than twice that of A380 die cast aluminum, and significantly higher than the strongest plastics. Even ZAMAK 3, the most common alloy has a significant yield strength advantage over A380 aluminum, showing 3 times greater elongation, while maintaining greater hardness and higher stiffness [17].

2.3.2. Rigidity

Zinc alloys are rigid engineering materials. Their elastic modules are greater than those of aluminum and magnesium alloys, and are an order of magnitude greater than those of plastic. This, combined with their high strength allows the volume of individual castings to be markedly reduced, saving space and weight.

2.3.3. Toughness and Ductility

High impact strength and good ductility are qualities of zinc alloys that are rarely found in most other casting alloys. Ductility is important for bending and crimpling in post-casting assembly operations, while impact strength provides performance in rough environments. Fracture toughness is also greater than for most aluminum alloys and cast irons.

2.3.4. Hardness

ZAMAK alloys provide high hardness and abrasion and wear resistance. Optimum hardness is provided by the ZA family whose Brinell hardness ranges from 95 to 122 when die cast. These values are much higher than the 70 to 85 BHN displayed by aluminum

alloys, and much higher than the hardness values of engineered plastics. Along with high hardness, ZA alloys also exhibit excellent abrasion and wear resistance.

2.3.5. Conductivity

As zinc alloys conduct both heat and electricity, they can be used for heat dissipating devices such as heat sinks. Zinc's excellent casting fluidity permits thinner fin and cooling pin design to better dissipate heat. Zinc's excellent electrical conductivity also provides good EMI, RFI and ESD shielding.

2.3.6. Non-sparking and Non-magnetic Properties

Aluminum alloys can generate a spark when struck with a rusty iron component. All zinc alloys, except ZA-27, are classified as "non-sparking" and are the perfect low-cost alternative to bronze in potentially explosive environments.

Zinc's non-magnetic properties are ideal for use in electronics and other applications where delicate moving parts are subject to magnetic disturbances.

2.3.7. Fatigue Strength

This measure of a material's ability to withstand cyclic loading is and important design criterion. Both the ZAMAK and ZA alloys have high fatigue strengths.

2.3.8. Design (Creep) Stress

The allowable design stress or resistance to creep at room temperature, of ZA alloys is far better than for all but the most esoteric engineering plastics. The room temperature design stress of die cast ZA-27, for example, is 10,000 psi (stress required for the creep of 1% in 100,000 hours). This property allows ZA alloys to be used in applications subject to significant static loading. However, permissible design stress drops with increasing

temperature, and a careful review of all constant load applications at temperature is required to determine the suitability of zinc alloys.

2.3.9. Pressure Tightness

Soundness of castings is largely related to product design, tooling layout and process control. Die cast ZAMAK alloys, ZA-8 and ZA-12 are often used for pressure tight applications. For sand and permanent mold casting, ZA-12 is the preferred material. All zinc alloys solidify into a dense strong matrix with excellent pressure tightness.

2.3.10. Damping Capacity

All of the ZAMAK and ZA alloys have excellent damping capacity. At 20^{o}C, ZA-27, the highest damping zinc alloy, has nearly ten times greater damping capacity than A380 aluminum or mild steel. At 100^{o}C damping capacity increases and all of the zinc alloys become "HIDAMETS" (high damping metals) and have damping capacity greater than that of grey cast iron. This property makes zinc alloys the perfect choice for housings where vibration absorption is required [17].

2.3.11. Corrosion Resistance

Zinc has excellent corrosion resistance under normal atmospheric conditions, and in many aqueous, industrial and petroleum environments. Corrosion resistance can be enhanced by such treatments as plating, chromating, painting and zinc anodizing.

2.4. Design of Die-Castings

Poisson's Ratio of Zinc Alloys: Poisson's Ratio is used as one of the data inputs for Finite Element Stress Analysis. The values for zinc alloys are:

Table 2.2. Poisson's ratio values for some of zinc alloys [18]

ZAMAK Alloys	0.27
ZA-8	0.29
ZA-12	0.30
ZA-27	0.32

Shrinkage Factors for Zinc Alloys: Shrinkage occurs when metal changes from liquid to solid as well as when it cools in the die. Quoted values for die cast zinc alloys are as follows [18]:

Table 2.3. Shrinkage ratio values for some of zinc alloys [18]

ZAMAK Alloys	0.007
ZA-8	0.007
ZA-12	0.0075
ZA-27	0.008

However, these values may be affected by constraint caused by the die so that some castings or parts of the same casting may shrink differently. Larger parts are often more likely to be constrained than small parts so the designer may use a slightly lower value for large dimensions.

Toxicidity Condition: Zinc alloys are non-toxic and zinc is an essential element in the diet. Because food often contains strong acids or alkalis, it is usual to apply an additional surface finish to prevent tarnishing. However, designers should also be aware that there

might be regulations and codes of practice for a particular food or food industry that may limit the choice of materials in contact. For instance, sometimes only stainless steel may be considered acceptable [18].

2.5. Machining Parameters and Chip Formation

In the process discussed so far, the shape of the workpiece was obtained by the solidification or plastic deformation of the material. The amount of material lost in scrap was relatively small, and the scrap particles tended to be large enough and relatively easy separated by alloy type, allowing easy and economical recycling. Machining is capable of making geometric configurations, tolerances, and surface finishes often unobtainable by any other technique. However, machining removes material which has already been paid for, in the form of relatively small particles that are more difficult to recycle and are in greater danger of becoming mixed. Therefore developments often aim at reducing machining, especially in mass production. For these reasons, machining has lost some important markets, yet at the same time, it has also been developing and growing especially with the application of numerical control has captured new markets.

If absolutely essential, a machining process can be found for any engineering material, even if it may be only grinding or polishing. Nevertheless, economy demands that a workpiece be machinable to a reasonable degree. Before the concept of machinability can be explored, it is necessary to identify a basic process that of metal cutting.

2.5.1. The Metal Cutting Process

The variety of metal cutting processes is very large; nevertheless, it is possible to idealize the process of chip removal.

Ideal Orthogonal Cutting: As indicated by its name, in orthogonal cutting the cutting edge of the tool is straight and perpendicular to the direction of motion. (Figure 2.6.) In the simplest case, the workpiece is rectangular and is of large enough width w for width changes to be neglected (plane strain). Cutting is performed with a tool inclined at a *rake*

angle α, measured from the normal of the surface to be machined. To prevent excessive rubbing on the machined surface, the tool is relieved at the back of *flank* by the *clearance angle* θ [19].

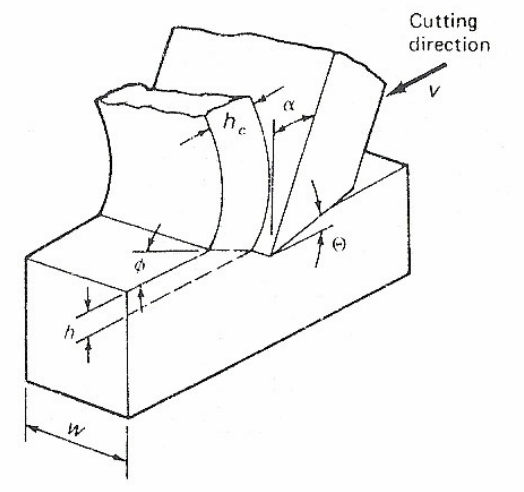

Figure 2.6. The view of zero or positive rake angle in orthogonal cutting [19]

In principle, it makes no difference whether the tool or workpiece is moved. We may visualize a stationary workpiece, with the tool moving at a *cutting speed v.* The tool is set to remove a layer of thickness h. To avoid confusion, this is not called the depth of cut, but rather the *undeformed chip thickness h.* In the simplest case, deformation takes place by intense shearing in a plane, the shear plane, inclined by the *shear angle* ϕ. The chip thus formed has a thickness h, the shear angle ϕ determines the cutting ratio r_c.

$$r_c = \frac{h}{h_c} = \frac{l_c}{l} \tag{2.1}$$

Frequently, the reciprocal value of r_c, called the chip compression factor, is quoted. Both can be obtained from measured chip thickness or, if the chip is ragged and uneven, from the measured length l_c, or if the width of the chip has changed, from the weight of a chip measurement length.

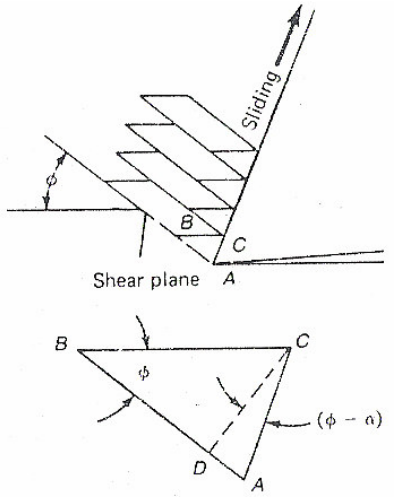

Figure 2.7. Visualisation of the chip formation as simple shearing [19]

In the ideal case all shear is concentrated in a very thin shear zone. The shear strain γ is (Figure 2.7.)

$$\gamma = \frac{AB}{CD} + \frac{AD}{CD} + \frac{DB}{CD} = \tan(\phi - \alpha) + \cot\phi \tag{2.2}$$

And, for an excessively thin shear plane, the shear strain rate γ' would be very big. In reality, the shear plane has some finite thickness Δy, typically 0.03mm and the shear strain rate can be calculated from:

$$\gamma' = \frac{v_s}{\Delta y} + \frac{\cos\alpha}{\cos(\phi - \alpha)} \frac{v_s}{\Delta y} \tag{2.3}$$

2.5.2. Chip Formation

Realistic metal cutting also differs from ideal cutting in the mode of chip formation.

In the ideal case, the shear zone is well defined, primary shear can be assumed to take place on closely packed shear planes and a continuous chip is formed. This situation is approximated under various process conditions:

- At moderately low speeds, in the presence of cutting fluid which finds access to both the rake and flank faces and acts as a lubricant, the chip slides on the rake face. The newly formed surface is smooth as is the undersite of the chip. The inner side of the chip is jagged, bearing evidence of chip formation by shearing.

- At somewhat higher speeds, heat generation causes a rise in temperatures. Friction increases until sliding at the tool face is arrested, and the system seeks to minimize the energy expenditure by finding optimum process geometry. It will be recalled that in the processes of indentation and extrusion. Sticking friction led to the formation of dead metal zones. In metal cutting too, at some intermediate speed, shearing takes place along a nose of stationary material attached to the tool face. This so called built–up edge (BUE) acts like an extension of the tool. Shear takes place along the boundary of the BUE; hence the *effective rake angle* becomes quite large and the energy consumption drops. However, a penalty is paid: dimensional control is lost and because the BUE becomes periodically unstable, it leaves occasionally lumps of metal and damaging cracks behind, and the surface finish is poor. Under certain conditions a small stable BUE may be maintained; this is desirable because it protects the tool without producing an unacceptably poor surface finish.

- With increasing speeds, the material of BUE heats up and softens, the BUE gradually disappears or rather degenerates into the secondary shear zone. The speeds at which the transition of BUE formation and secondary shear zone development occur are indicated in figure 8.4 for steel. Similar changes take place when cutting other materials; the critical speeds depend on the temperature reached in the shear zone but are also affected by adhesion between tool and workpiece materials. As in metal deformation processes, temperature effects can be normalized by reference to the homologous temperature scale.

Under special conditions, the chip may be continuous yet show a periodic change in thickness. A wavy chip exhibits roughly sinusoidal variations in thickness. Such variations are usually related to chatter (vibration) attribute to periodic variations in cutting forces. As in all machines, the imposed forces cause elastic deflections of the workpiece, tool, tool

holder, and machine tool. Any variations in forces result in a change of undeformed chip thickness and hence in a visible and measurable waviness of the machined surface.

- In regenerative chatter the source of vibration is a change in undeformed chip thickness (from waviness produced in a preceding cut by the presence of a hard spot or other irregularity) or a periodic loss of the BUE. A remedy is usually found in changing the process conditions (speed, feed, workpiece support, tool support)

- Chatter may also originate in forced vibrations due to a periodic variation of forces acting within the machine tool. (e.g. from a gearbox or coupling) or may be transmitted from an external source such as a nearby, vibrating machine tool. Vibration-isolation mountings or moving the offending machine tool eliminate the problem. Interrupted cuts in milling may also set up vibrations and uneven spacing of teeth is then helpful.

Segmented chips show a sawtooth-like waviness. The thick sections are only slightly deformed and are joined by severely sheared, thinner sections. An extreme form of this observed in materials of low heat conductivity, such as titanium. The process starts by upsetting ahead of the tool, resulting in a localized of shear. Because heat generated in the shear plane cannot dissipate, the material heats up, weakens and shears until a chip segment is moved. The process then starts again by upsetting.

Under certain conditions *discontinuous chip* forms.

- When ductile materials are cut in a very low speeds. Severe strain hardening of the material causes upsetting until sufficient strain is accumulated to initiate shear. Elastic members in the system (e.g. the tool holder) allow sudden acceleration and complete separation of a chip, to be followed by a new upsetting cycle. Cutting forces fluctuate violently; the new surface is torn (Figure 2.8.) and wavy. High adhesion and low cutting speeds that generate low homologous temperatures favor such chip formation.

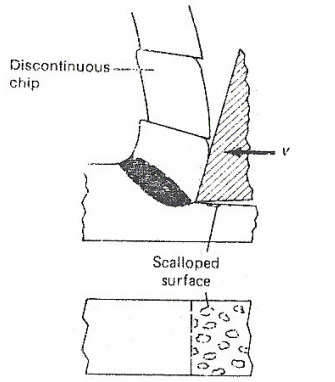

Figure 2.8. Chip formation changes with cutting speed (discontinuous chips) [19]

- Segmental chips formed at high cutting speeds may also fall apart. Discontinuous chip formation is intentionally introduced in some free machining alloys by the incorporation of inclusions or second-phase particles that serve as stress raisers and cause total separation of tightly spaced chip fragments The second phase particles or inclusions often reduce the shear strength in both the primary and secondary shear zones; thus cutting forces are low. Because chip separation is facilitated, the surface finish is good and the tendency to chatter is reduced.

- The above discussion was based on the assumption of continuous engagement of the cutting edge, as is typical of operations such as turning and drilling. In other processes, most notably milling, cutting is interrupted, with the edge emerging from the cut after limited engagement. This has advantages in terms of chip disposal but subjects the tool to impact loading.

Removal of Chips: The short chip produced in cutting free machining materials is easily removed from the cutting zone. In contrast the continuous chip formed when machining ductile materials under stable conditions is a nuisance: It is difficult to remove; it may clog up the work zone, it may wrap around the workpiece or tool; and it may present danger to the tooling, machine and operator alike.

A partial remedy is found in chip breakers. With some materials, they impart additional strain to the chip, causing it break into shorter lengths or at least curl up into

tight coils that break frequently. At other times, the chip is forced to bend and hit an obstruction such as the tool holder, tool flank, or the workpiece itself. With one end fixed, the chip grows until bending stresses make it snap. Ductile materials always give a continuous chip, which must be chopped up or dragged out of the work zone.

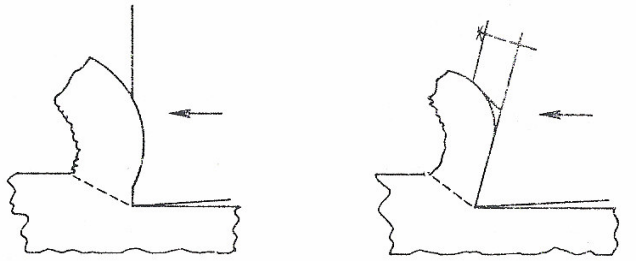

Figure 2.9. Using the groove (left) and obstruction type (right) chip breakers [19]

A chip breaker may be incorporated into the tool by giving the rake face a curvature, away from the cutting edge as in the left side of the Figure 2.9. or a separate chip breaker may be attached to the rake face as right side in Figure 2.9. Chip breakers have, in general, little effect on cutting forces but, if moved too close to the cutting edge, they localize heat at the edge and may cause rapid loss of the tool because of overheating. The natural curvature of chips is a function of many process variables; in general, the chip curl radius becomes smaller (the chip is tighter) with increasing *h* and decreasing speed. Correspondingly, chip breakers work most efficiently at specific undeformed chip thicknesses and speeds.

2.5.3. The Basics of Chip Formation

Some basic information about the chip formation is given below [20].

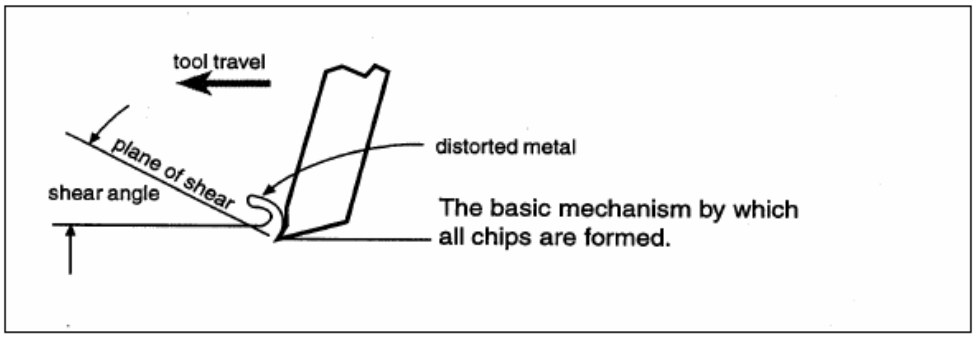

Figure 2.10. The basic chip forming mechanism [20]

Discontinuous Chips:

- Typically associated with brittle metals like cast iron.
- As feed is increased, some compression takes place.
- As the chip starts up the chip-tool interference zone, increased stress occurs until the metal reaches a saturation point and fractures off the work-piece.

Conditions Which Favor a Discontinuous Type of Chip:

- Brittle work material
- Small rake angles on cutting tools
- Coarse machining feeds
- Low cutting speeds
- Major disadvantage—could result in poor surface finish

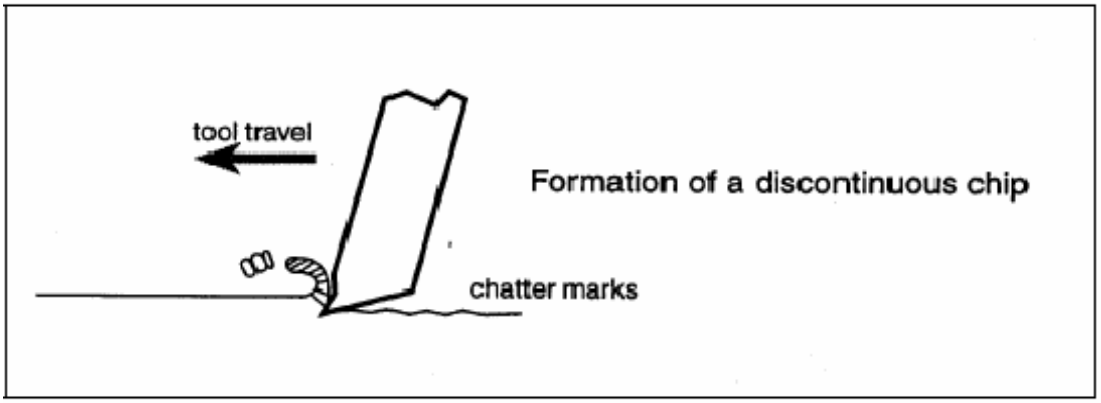

Figure 2.11. Discontinuous chip formation [20]

Continuous Chips:

- Continuous “ribbon” of metal that flows up the chip-tool zone.
- Usually considered the ideal condition for efficient cutting action.

Conditions Which Favor a Continuous Type of Chip:

- Ductile workpiece
- Fine feeds
- Sharp cutting tools
- Larger rake angles
- Proper cutting speeds
- Proper coolants

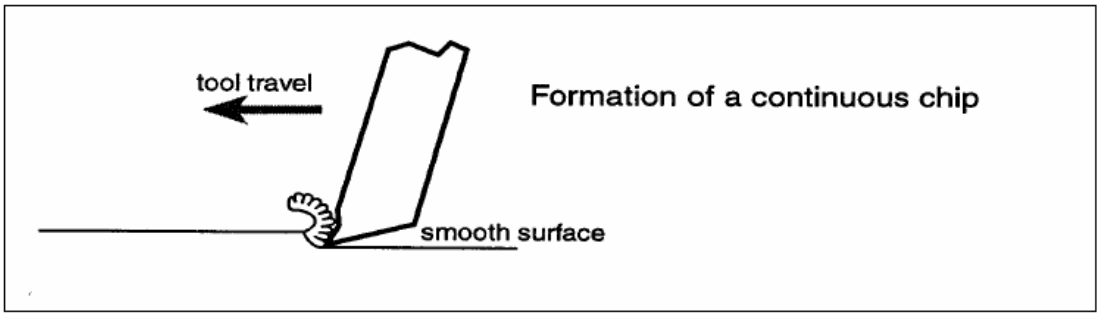

Figure 2.12. The basic chip forming mechanism [20]

Continuous Chips with a Built-Up Edge (BUE): Same process as continuous, but as the metal begins to flow up the chip-tool zone, small particles of the metal begin to adhere or weld themselves to the edge of the cutting tool

As the particles continue to weld to the tool it effects the cutting action of the tool including the beginning of gauling

Conditions Which Favor a BUE Type of Chip: This type of chip is common in softer non-ferrous metals and low carbon steel. BUE chip formation increases as the tool begins to dull.

Problems Associated With BUE Chip Formation: Welded edges break off and can become embedded in work-piece

- Decreases tool life
- Can result in poor surface finishes

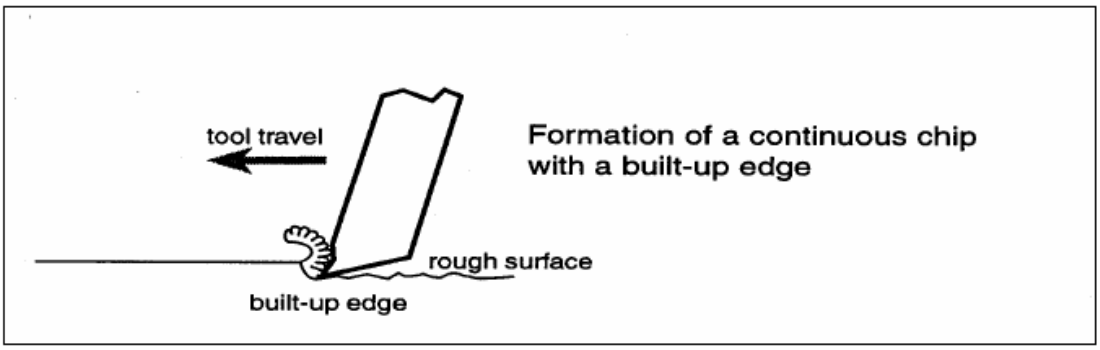

Figure 2.13. Formation of a continuous chip with a built-up edge [20]

2.5.4. Surface Quality

Machining aims to make a part of given geometry, to specified dimensions and dimensional tolerances. To permit proper function of the part, the surface finish is also specified. Beyond these geometrical considerations, it is also important that the surface produced should be free of defects such as cracks, have no harmful residual stresses, and not be subjected to undesirable metallurgical changes. These are particularly important aspects when the part operates in a hostile environment, is subject to fatigue loading, or when its failure could have catastrophic consequences. With the growth of such critical applications, particularly in the aerospace industries, the term surface quality has acquired a complex meaning.

Surface Roughness : The surface formed in simple orthogonal or oblique cutting is ideally, perfectly smooth (roughness is zero) When a tool of R radius is moved by the feed *f* between successive cuts, the ideal transverse roughness can be calculated approximately by considering the geometry. The peak to valley height is

$$R_{\max} = \frac{f^2}{8R} \tag{2.4}$$

The arithmetic average for a triangular roughness is Ra= R_{max}/4; hence

$$R_a \approx \frac{f^2}{32R} \tag{2.5}$$

The longitudinal roughness will still be zero. Similar relationships can be developed for other processes. Superimposed on the ideal roughness are features introduced by the chip forming process itself. This results in a measurable roughness in the longitudinal direction and modification of surface profile. (and hence of roughness values) in the transverse direction. Several features may be observed:

In cutting at very low speeds and typically also with all discontinuous chip formation, the surface is scalloped as in Figure 2.8 and cracks may develop transverse to the cutting direction.

In cutting with an unstable BUE, heavily strain hardened fragments are welded to the surface, covering some 5-10% of it.

When a continuous chip is formed without a BUE, the surface configuration comes close to the ideal one, even though localized wear of chipping of the tool edge gives some roughness increase in the transverse direction.

Chatter introduces a periodic variation of surface geometry which is readily visible and shows up as waviness on a recorded longitudinal trace.

The surface finish changes in the course of cutting and, in general, deteriorates with the progression of wear. Indeed, tool life is sometimes specified as the time for which an acceptable finish is produced.

Surface Integrity: The term surface integrity has been introduced to indicate the absence of undesirable features on the surface as well as in the subsurface region of the workpiece.

Strain hardening of a surface layer is a natural consequence of chip formation. A residual stress may also be generated which is most of the time compressive and thus beneficial.

Cracks formed in low-speed cutting are harmful, as are those sometimes found when cutting with an unstable BUE.

Some aspects of surface integrity can be evaluated only by destructive techniques (metallography), whereas others can be explored under the microscope, particularly SEM. On the basis of such tests, cutting conditions that ensure good surface integrity can be specified. For the most critical applications, NDT techniques – including x-ray analysis for residual stresses are employed. Some Irish researchers applied finite element method for evaluation of the effects of initial stresses developed during the pressurized casting process. The finite element method is employed and a few 3D numerical examples are presented in this research [9].

2.6. Applications of ZA Alloys

Zinc die-castings are extensively used for gears varying in size from the tiny pinions used in instruments and switches, to sprockets for chain drives and gear racks for washing machines. In most cases, the teeth are cast to size; however, for special applications they may be machined by hobbing, broaching, etc.

Die cast zinc alloys do not have as good thermal conductivity as extruded aluminum. However, die-casting brings several advantages that can outweigh this fact

More efficient fin design is possible than with extrusions.

The fins are integral with the chassis resulting in a more efficient heat path, with no joints or interfaces.

One die-casting acts as chassis, heat sink, and container for both protection and EMI shielding. So they can be used as heat sinks.

2.7. Microstructure and Properties of Squeeze Cast Alloys

As mentioned before, squeeze cast products have superior mechanical properties to their conventionally cast counterparts due to higher density, finer grain size and more homogenous microstructure. Furthermore, thermal limitations of the die restricts squeeze casting to mainly light and low melting point alloys of aluminum and magnesium, although there are reports that copper alloys, cast irons and steels have also been squeeze cast. Table 2.4. summarizes the alloys used for squeeze casting.

Table 2.4. List of alloys used for squeeze casting [6]

SC ALLOYS				
FERROUS ALLOYS		**NONFERROUS ALLOYS**		
STEELS	CAST IRONS	COPPER ALLOYS	Al. ALLOYS	Mg. ALLOYS
		METAL MATRIX COMPOSITES		

The application of pressure has a significant effect on the morphology of the phases in squeeze cast alloys as, for instance, there is a tendency for flake graphite to transform to compacted graphite with increasing pressure. In the case of Al-Si alloys, fibrous silicon is the likely morphology.

Some authors found it essential to design alloys specifically for SC conditions. New alloy system of Al-Si-Cu-Mg which posses good castability and excellent mechanical properties was examined by Lee et al to optimize its composition for squeeze casting [21]

Table 2.5. Tensile properties of conventional and squeeze cast alloys [6]

Alloy	**Yield Strength (MPa)**	**Tensile Strength (MPa)**	**Elongation (%)**
AA603-T6	260	350	≥10
A356-T6	220	300	≥10
LM24 (SC)	-	210±5	2-2.5
7010 CHILL CAST-T6	468-488	523-526	4.7-5.9
7010 SC-T6	470-490	550-563	10-14

The selected alloy was Al + 12 wt.%Si + 3wt.%Cu + 0.7wt.%Mg that showed 10 ± 20% improvement in hardness, tensile strength, and elongation over those of gravity cast products. Modification with Sr, Ti, and B of this alloy resulted in 40% increase of elongation, although no significant change in wear resistance was found. Yen and Evans [22] patented an Al casting alloy that consists of, by wt.%: 7.0±13.0 Cu, 0.4±1.2 Mn, 0.21±0.40 V, 0.31± 0.70 Zr; impurities are limited to: <0.6% Si, <0.8% Fe, <0.2% Zn, <0.1% Mn, <0.2% Ni, the remainder being essentially Al. The alloy has a tensile strength of 420 MPa, yield strength of 340 MPa, a tensile elongation of 6%, and a tensile modulus of elasticity of 80 GPa. A new Mg alloy specifically designed by Chadwick [23] for the squeeze casting process has been tested to show excellent creep and high temperature fatigue properties. The alloy, which was patented in 1987, contained 10± 25%Zn, 0.5±5% Cu and 0.25±4% Si. Additions may include up to 1% Ca with a preferred 0.3% Ca and 0.002±0.005% Be.

Squeeze casting process gives new opportunities to fabricate advanced materials, especially in the field of composites. There are a large number of publications devoted to MMCs fabricated by squeeze casting. Squeeze casting may also be used to fabricate bi-metals where, for instance, cast iron inserts can be incorporated to increase wear resistance in Al alloy components. Applications to date have been wheels, pistons and brake discs. Some Indian researchers [24] fabricated Beryl/Al–Si–Mg composites containing 2.0–10.0% of beryl particles by squeeze casting. They have found that new composites also have improved wear resistance when compared to gravity cast composites. Squeeze cast composites with 6 wt.% of beryl particles showed almost 1.2 times reduced adhesive wear rate at 2400m sliding distance when compared to that at 600 m.

2.8. Alloy Selection

There are two basic families of zinc casting alloys: ZAMAK alloys and ZA alloys. The ZAMAK alloys were developed for pressure die casting during the 1920's and have seen widespread usage since then. It is for this reason that specifies often relates zinc as synonymous with die casting. However, the development of the ZA (Zinc-Aluminum) alloys during the 1970's have radically changed zinc's product design and manufacturing capabilities.

ZA alloys were initially developed for gravity casting. Their mechanical properties compete directly with bronze, cast iron and aluminum using sand, permanent mold and plaster mold casting methods. Distinguishing features of the ZA alloys are their high aluminum content and excellent bearing properties. [12]

During the 1980's, ZA alloys evolved as valuable die casting materials. It is important to note that when considering a ZA alloy for die casting, only ZA-8 can be hot chamber die cast that is highly automated and the most efficient die casting process. ZA-12 and ZA-27 require special melting procedures and must be die cast like aluminum using the less efficient cold chamber die casting process. The ZAMAK alloy family is identified by their numbers 3, 5, 7, and 2. ZA alloys consist of ZA-8, ZA-12 and ZA-27.

NO.3: This alloy is usually the first choice when considering zinc for die casting. Its excellent balance of desirable physical and mechanical properties, superb castability and long-term dimensional stability. It is therefore the most widely available alloy from die casting sources. ZAMAK No. 3 also offers excellent finishing characteristics for plating, painting and chromate treatments. It is the "standard" by which other zinc alloys are rated in terms of die casting.

NO. 5: These alloy castings are stronger and harder than No. 3. However, these improvements are tempered with a reduction in ductility which can affect form ability during secondary bending, riveting, swaging or crimping operations. No. 5 contains an addition of 1% copper which accounts for these property changes. However, when an extra measure of tensile performance is needed, No. 5 alloy castings are recommended. The alloy is readily plated, finished and machined comparable to No. 3 alloy.

Table 2.6. General design features of zinc alloys, which can influence material selection [12]

Comparison Ratings*	No.3	No.5	No.7	No.2	ZA-8	ZA-12	ZA-27
Die Castability**	E	E	E	E	VG	VG	G
Sand Castability	NR	NR	NR	G	G	E	F
Perm. Moldability	NR	NR	NR	G	VG	E	F
Strength	G	G	G	VG	VG	E	E
Ductility	E	VG	E	VG	VG	G	F
Impact	E	E	E	G	VG	G	F
Bearing/Wear	G	G	G	VG	VG	E	E
Machinability	E	E	E	E	E	VG	G
Pressure Tightness	E	E	E	E	VG	E	F
Plating	E	E	E	E	VG	G	NR***
Zinc Anodizing	E	E	E	E	E	E	VG
Chromating	E	E	E	E	VG	G	F
Painting	E	E	E	E	E	E	E
Dimensional Stability	E	E	E	VG	VG	VG	F
Anti-Sparking	E	E	E	E	E	E	F****
E = excellent VG = very good G = good F = fair NR = not recommended							
*General performance ratings which can vary depending upon process selection							
**Alloy Nos. 3,5,7,2, & ZA-8 are hot chamber die cast, Z-12 & ZA-27 are cold chamber die cast							
***ZA-27 can he plated using special techniques, however it is not normally recommended for plating							
****High aluminum content of ZA-27 reduces anti-sparking rating							

Alloy Selection Guide: Numerous factors influence material selection. Most important are mechanical properties, choice of casting process, and manufacturing characteristics. Rated are the general design features of zinc alloys, which can influence material selection.

2.9. Importance of Alloy Chemistry

Casters often made various metallic additions at the zinc alloy pot with little concern about their overall affect on the castings. Components made from these commercial and "custom" alloys typically failed prematurely due to growth, distortion and cracking. The reasons for their failure are well known today, and are discussed in detail below [25].

It was not until the 1920's and 1930's that alloy composition and the effects of impurities were thoroughly researched. The New Jersey Zinc Company quickly discovered the importance of controlling the alloying elements within a specified range and of using a pure grade of zinc1. Zinc purity was of great importance because impurities such as lead and cadmium, which were common in most grades of zinc at the time (and still in lower purity zinc grades); promote intergrannular corrosion in zinc-aluminum die casting alloys. While tin is not present in any refined zinc grades, it was found in zinc die casting alloys at the time due to contamination by tin die castings, solder or other tin containing materials. The commercial availability of Special High Grade zinc (99.99% pure) in 1929 made the development of suitable zinc die casting alloys both possible and practical. Over the next several years further studies and developments by The New Jersey Zinc Company led to the introduction of the commercial die casting alloys that are still in use today. These alloys were patented under the "Zamak" trademark in the '30s (trademark originally owned by New Jersey Zinc) and are commonly known as 2, 3, 5 and 7. Table 2.7. lists the chemical compositions as per ASTM B86 for castings made from these alloys. Note that all the alloys have defined ranges for the alloying elements, and low impurity limits for lead, cadmium and tin. Aluminum is the main alloying element in all common zinc die casting alloys. It serves to strengthen the alloys and renders the Zamak and ZA-8 alloys hot chamber die castable by lowering their melting points. The lower melting and casting temperatures result in minimal attack of the iron and steel components associated with the hot chamber process. Aluminum also significantly increases the fluidity of the alloys. Low aluminum levels cause a reduction in alloy fluidity and inferior mechanical properties in castings. Aluminum levels above the specification cause a loss of impact strength and often result in brittle castings. Magnesium is added to zinc-aluminum alloys to help prevent intergranular corrosion when castings are exposed to warm, humid environments. Intergranular corrosion is the process whereby individual boundaries around the grains corrode preferentially to the grains themselves.

Table 2.7. Chemical composition of zinc alloy die castings as per ASTM B86 [25]

Element wt %	Common Name						
	No. 2	No. 3	No. 5	No. 7	ZA-8	ZA-12	ZA-27
Aluminum	3.5-4.3	3.5-4.3	3.5-4.3	3.5-4.3	8.0-8.8	10.5-11.5	25.0-28.0
Magnesium	0.02-0.05	0.02-0.05	0.03-0.08	0.005-0.02	0.015-0.03	0.015-0.03	0.01-0.02
Copper	2.5-3.0	0.25	0.75-1.25	0.25	0.8-1.3	0.5-1.2	2.0-2.5
Iron	0.1	0.1	0.1	0.075	0.075	0.075	0.075
Lead	0.005	0.005	0.005	0.003	0.006	0.006	0.006
Cadmium	0.004	0.004	0.004	0.002	0.006	0.006	0.006
Tin	0.003	0.003	0.003	0.001	0.003	0.003	0.003
Nickel	-	-	-	0.005-0.02	-	-	-

Residual lead and cadmium in pure refined zinc as well as other elements such as tin, bismuth and mercury have extremely low solid solubility in zinc die casting alloys. Their low solubility coupled with lower melting points results in their solidifying in the grain boundaries. The presence of small particles of these metals in the grain boundaries can create electrochemically active cells in moist environments. The addition of magnesium makes these metals inactive when they are present at or below specified limits. Below the minimum specified level, magnesium does not provide protection and at levels above those specified, the alloys are less fluid and have an increased tendency towards hot shortness. Copper improves the hardness, and tensile and creep strengths of zinc-aluminum alloy die castings. At high levels of copper (above 1.25 percent) the alloys are prone to reduced impact strength and dimensional instability (castings grow moderately) with ageing. At levels normally encountered, iron has little or no effect on the properties of zinc alloy die castings. While the standard allows for some pick up, iron's low solubility (0.02 percent) results in excess iron reacting with aluminum to form $FeAl_3$ which floats and concentrates in top dross. Proper skimming practice will help prevent entrapment of these iron-aluminum intermetallics in castings where they could cause machining problems.

Lead, cadmium and tin are the most common impurities that affect the quality of zinc alloy castings. At levels below those specified in the standard, the magnesium serves to eliminate their effect. However, at higher levels magnesium becomes ineffective in preventing intergranular corrosion of castings. Figure 2.14. shows the effect of high levels

of lead in a No. 3 alloy casting exposed to a warm, moist environment. Note that the casting has swollen and cracked severely due to intergranular corrosion. At levels significantly above those specified, lead, tin and cadmium will also cause severe hot-shortness during casting because of their low melting points.

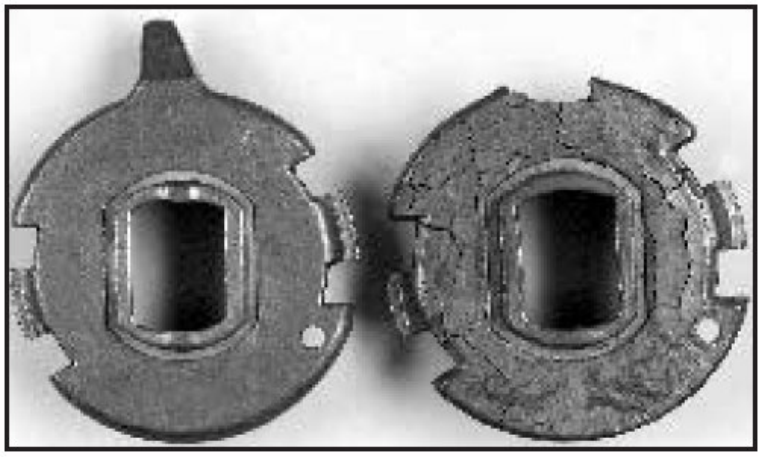

Figure 2.14. Casting on right shows the effect of high impurities [25]

Most National Standards, including ASTM B86 also specify limits on nickel, chromium, silicon and manganese. Nickel and chromium can be present because of remelting chrome plated castings. Silicon and manganese may come from aluminum used to produce the alloys, or from dissolution of alloy steels used in the die casting process. Analysis for these elements is only required where it is suspected that gross contamination has occurred. Generally, analysis is not required since the levels at which they would normally be encountered are not detrimental.

Mechanical deformation increases the tensile strength of the fractionally melted alloy twice that of the as cast alloy. Tensile strength of the alloy is improved by ageing about 275 °C eutectoid temperature prior to deformation process. The higher strength is achieved at below this temperature. Ageing process reduces the strength of the alloys, notably the fractionally melted specimens which are deformed by swaging [26].

2.10. Theoretical Background: Effect of Pressure on the Solidification of a Freezing Alloy

The application of pressure during solidification would be expected to affect phase relationships in an alloy system. This may be deduced by considering the Clausius-Clapeyron equation [3],

$$\frac{\Delta T_f}{\Delta P} = \frac{T_f \left(V_l - V_s\right)}{\Delta H_f} \tag{2.6}$$

Where T_f is the equilibrium freezing temperature, V_l and V_s are the specific volumes of the liquid and solid, respectively, and ΔHf is the latent heat of fusion. Substituting the appropriate thermodynamic equation for volume, 2 the effect of pressure on freezing point may roughly be estimated as follows:

$$P = P_0 \exp\left(\frac{-\Delta H_f}{RT_f}\right) \tag{2.7}$$

Where P_0, ΔHf and R are constants. Therefore, T_f should increase with increasing pressure. On a mechanistic approach, such change in freezing temperature is expected due to the reduction in interatomic distance with increasing pressure and thus restriction of atomic movement, which is the prerequisite for melting/freezing. The inter-solubility of constituent elements together with the solubility of impurity and trace elements is also expected to increase with pressure. The above mentioned theoretical predictions have been proven experimentally where a liquidus temperature rise of up to 9°C has been reported for pure Al/Si binary alloys at a pressure of 150 MPa. Furthermore, the eutectic point moves to the left, i.e., to higher Si contents. The consequences of such changes in the phase diagrams area significant improvement in the microstructure and mechanical properties of SC-fabricated components. As reported by Chadwick and Yue [27] and Franklin et al. [28], grain refinement is quite noticeable in squeeze cast parts. However, their interpretation of such requirement is sharply different. Chadwick and Yue have claimed that pressure has no effect on grain refinement, the observed fine grained structure of squeeze castings being

principally due to the increase in heat-transfer coefficients, i.e., greater cooling rates for the solidifying alloy due to reduction in the air gap between the alloy and the die wall and thus more effective contact area. Franklin et al., however, have suggested the opposite, where the application of pressure brings about undercooling in an initially superheated alloy (see Figure 2.15.) and thus increases nucleation frequency so bringing about a finer grain size.

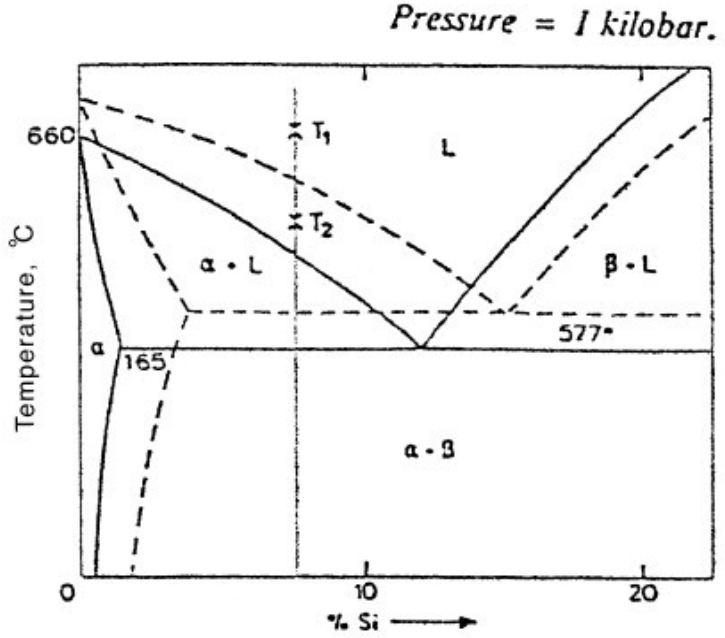

Figure 2.15. The effect of rapid cooling and the application of pressure on the Al-Si phase diagram [13]

In the opinion of the present authors, both hypotheses are valid and are active simultaneously at a time but one may dominate the other at any instant during solidification. The size of the air gap between the solidifying alloy and the die wall and the degree of undercooling, the two main features for fine structure, are dependent on such process parameters as the pressure, the timing of its application and the chemistry of the solidifying metal. Certainly, the application of pressure reduces the air gap between the solidifying metal and the metallic mould and thus increases the contact area; effecting improvement in the heat-transfer coefficient, but this may not be the dominant mechanism. This is in line with studies carried out by Gethin et al. [29] who employed numerical modeling to simulate the flow and heat-transfer characteristics of molten metal during squeeze casting. They reported small changes in the thermo-physical properties of the molten metal with applied pressure. The timing of pressure application is critical, since if it

is applied at a temperature of $T > T_m$. ΔT, ΔT being the expected increase in T_m due to pressure, the effect of undercooling is negligible and thus increase in the heat transfer coefficient is the dominant mechanism. If however, the pressure is applied at a temperature $T_m \leq T \leq T_m + \Delta T$, then undercooling would be the dominant mechanism. The effect of undercooling is still appreciable if pressure is applied at the beginning of crystallisation, i.e., at a temperature $T < T_m$. The composition of the solidifying alloy is also quite important as, for instance, in case of aluminum alloys, the presence of some trace elements of Sr, P, Na or even Ti or B could have tremendous effects on the scale of the microstructure.

Irrespective of the mechanism responsible for grain refinement, investigation on Al-Li, Al-Li-Zr, Al-Li-Zr-Ti-B, Al-Li-Cu-Zr, Al-Cu, Al-Si and pure Al have shown improved mechanical properties of squeeze cast components with increasing pressure. For instance, Balan et al. [30] studied the effect of applied pressure (1-75 MPa) on LM6 Al-Si alloy and reported an increase of about 3.4% in density, 63% in UTS, 2.6% in percentage elongation and 50% in hardness with increasing applied pressure. Such remarkable improvement was mainly due to microstructural alteration through refinement of the primary α-phase and modification of the silicon phase. Similar results were obtained for pure aluminum.

In general, the fine structure and superior mechanical properties of SC-components are due to the following factors:

- Changes in undercooling of the molten alloy,
- Changes in the composition and percentages of the forming phases of the solidifying alloy,
- Changes in the heat-transfer coefficient between the metallic mould and solidifying alloy, and
- Changes in the density of the alloy due to reduction of porosity.

3. EXPERIMENTAL STUDY

3.1. Materials Used

In the experiments commercial grade pure aluminum and commercial grade pure zinc ingots were used. Aluminum was Etial 7, i.e. %99.7 purity. Zinc was %99.95 purity and Bismuth shot was %99.99 purity.

Table 3.1. Chemical composition of the Etial 7 Aluminum

Al	Si	Fe	Cu	Mn	Mg	Cr	Ni	Zn	Pb	Sn	Ti	V	Zr
99.56	0.054	0.083	<0.015	0.017	<0.036	<0.015	<0.017	<0.070	<0.078	<0.040	0.009	0.012	<0.0019

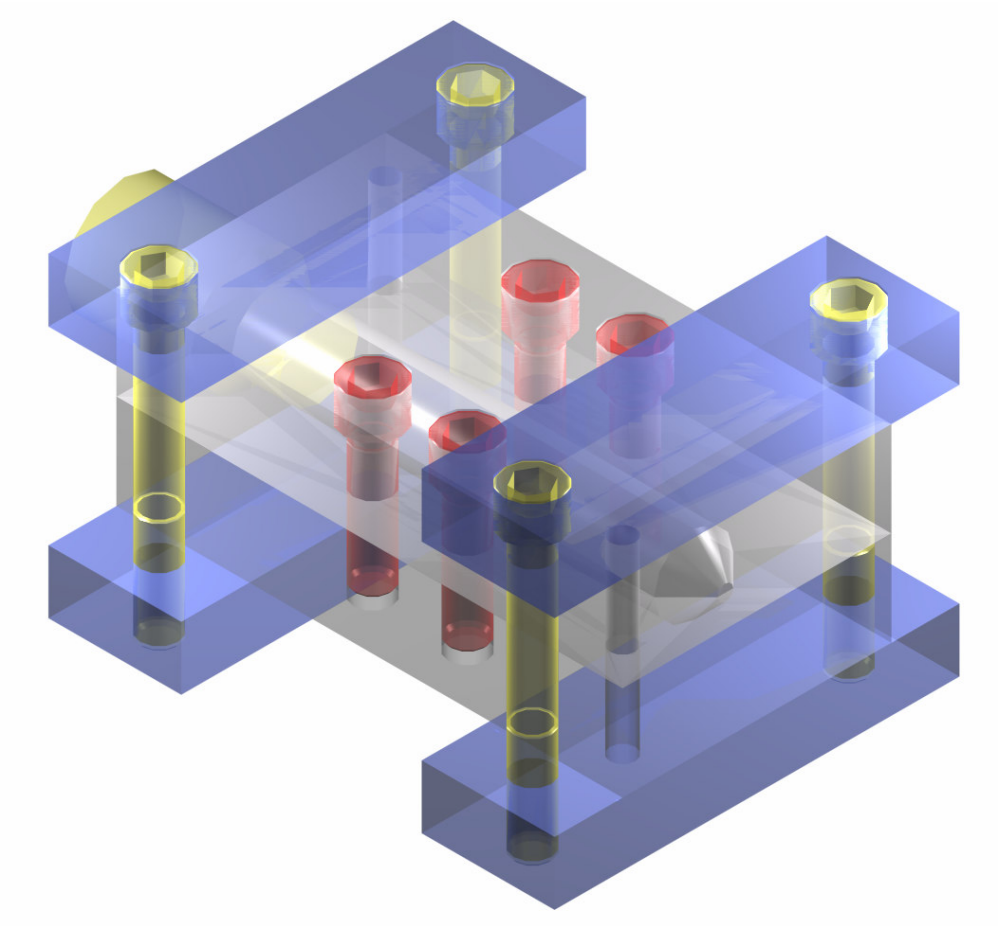

Figure 3.1. 3D drawing of the squeeze casting die

The industrial type DIN1040 steel was used for the manufacturing of dies and punches. Before starting the manufacturing, 3D models of the dies and punches were designed in Mechanical Desktop Power Pack Program. After drawing the 3D models, 2D drawings were extracted using same program. Later, dimensions were attached, arrangements were done. After the latest arrangements, print outs of these 3D and 2D drawings were obtained.

These print outs were given to the workshop; hence the dies and punches were manufactured. After machining, the flat inner sides, the dies were grinded in order to prevent of the leakage of the molten ZA-27. Before starting the casting, these parts were lubricated in order to prevent sticking and rusting. The dies were split type and the detailed drawing of the dies and punches are shown in Figure 3.2.

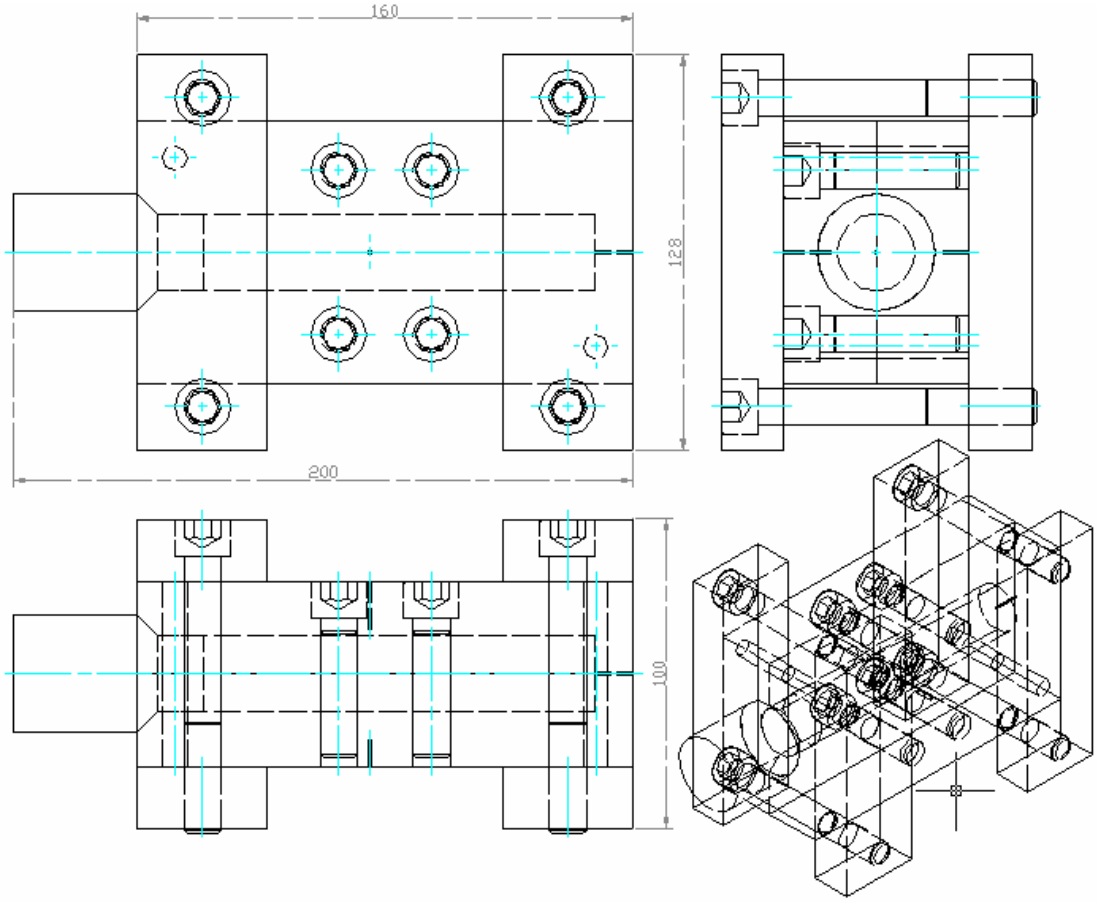

Figure 3.2. Technical drawing of the squeeze casting die

In the middle of the die a hole of 2.5 mm diameter was drilled. A K type thermocouple of 0.5 mm diameter was placed into this hole in order to measure the die temperature during squeeze casting. This hole was drilled from the outer axis of the casting hole and its approximate distance to the casting hole was about 2 mm. One of the biggest advantages to use this type of thermocouple with this diameter was fast determination of the temperatures.

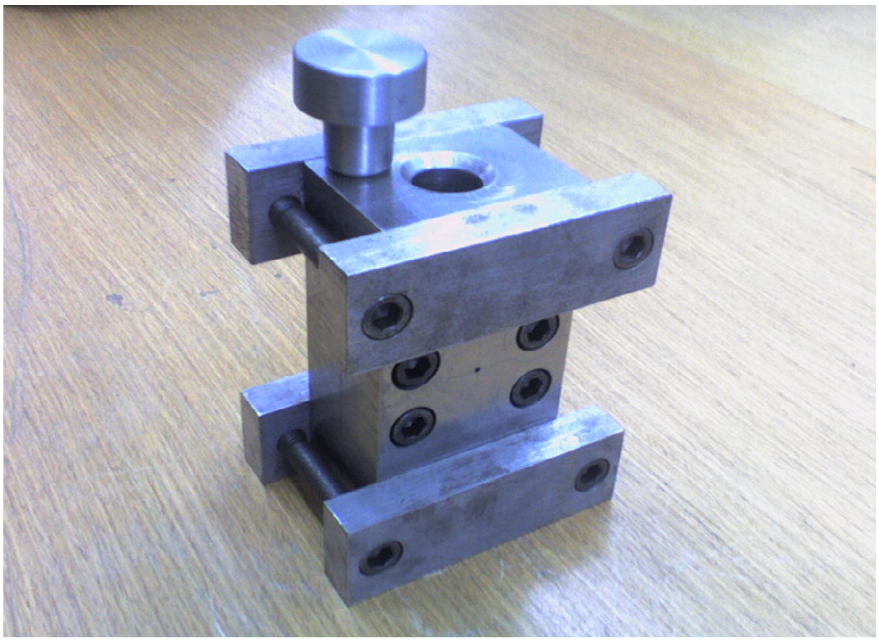

Figure 3.3. The photo of the squeeze casting die and its punch

Slicing of the Materials: Materials slicing was important to adjust the percent weight of the alloy which will be cast. The ingot aluminum and zinc were first cut into slices with a thickness of about 5 cm. Then, these big slices were cut into slices using Uzay brand hydraulic saw. After using this saw, the dimensions of the sliced parts were reduced to about 2x2x8 cm. The long and thin slices were cut into 2 or 3 pieces using a Bosch brand spiral saw. In Figure 3.4. The sliced zinc and aluminum pieces can be seen.

Figure 3.4. Long aluminum pieces after slicing with an Uzay saw

Figure 3.5. Sliced aluminum pieces using a Bosch spiral saw

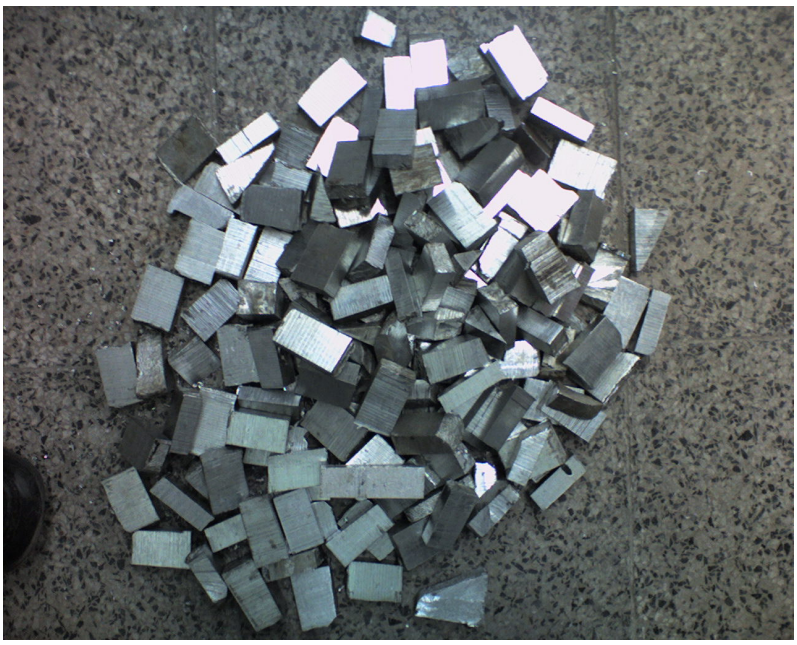

Figure 3.6. Sliced zinc pieces using a Bosch spiral saw

Each piece was weighed using the Tefal balance. The weight of each piece was written on it. After this work, these slices were categorized according to their weights and they were put into a small nylon bag. For example; those up to 10 gr were put into one nylon bag. The total weight of the zinc group is shown in the table below.

Table 3.2. The total number and total weight of the sliced materials (Zinc)

Zinc	
Size (gr)	Total Weight of The Size (gr)
0-10	89
10-25	806
25-40	1500
40-50	1930
50-60	1805
60-70	1850
70-80	1405
80-100	1480
100-110	1140
110-120	1720
120-140	1555
140-213	2460
Total Weight	17740

In order to have the right composition of the material, it was essential to add the materials in required weight. In the Table 3.3 the composition of the melts required seen.

Table 3.3. Composition calculation of the melts in required weights

MATERIAL COMPOSITION	Bismuth				Zinc				Aluminum			
	% Weight	Density (gr/cm^3)	Weight (gr)	Real Weight Ratio	% Weight	Density (gr/cm^3)	Weight (gr)	Real Weight Ratio	% Weight	Density (gr/cm^3)	Weight (gr)	Real Weight Ratio
%0 Bi + ZA27	0	9,8	0,00	0	73	7,14	316,6	0,73	27	2,7	117,1	0,27
%0,5 Bi + ZA27	0,50	9,8	2,18	0,005	72,64	7,14	316,0	0,72635	26,87	2,7	116,9	0,26865
%1 Bi + ZA27	1,00	9,8	4,37	0,01	72,27	7,14	315,5	0,7227	26,73	2,7	116,7	0,2673
%1,5 Bi + ZA27	1,50	9,8	6,57	0,015	71,91	7,14	314,9	0,71905	26,60	2,7	116,5	0,26595

MATERIAL COMPOSITION	Total Mould Volume (cm^3)	Average Density According to Bi,Zn and Al Ratios (gr/cm^3)	Calculated Total Weight According to the Average Density (gr)	TOTAL WEIGHT (From the End, For Proof Only)	TOTAL OF WEIGHTS	PROOF OF WEIGHT RATIO			
						Bi	Zn	Al	Zn/Al
%0 Bi + ZA27	73	5,9412	433,71	433,71	433,71	0	0,73	0,27	0,27
%0,5 Bi + ZA27	73	5,960494	435,12	435,12	435,12	0,005	0,72635	0,26865	0,27
%1 Bi + ZA27	73	5,979788	436,52	436,52	436,52	0,01	0,7227	0,2673	0,27
%1,5 Bi + ZA27	73	5,999082	437,93	437,93	437,93	0,015	0,71905	0,26595	0,27

In the left column, the compositions of the melts are given such as %0.5 Bi +ZA-27. This means that the %0.5 of the total weight of a melt should be bismuth. Remaining %99.5 weight of the specimen should be ZA-27. This means 27% of the 99.5% of the specimen should consist of aluminum in weight. Similarly, 73% of the 99.5% of the specimen should consist of zinc in weight. Thus, 26.865% of the total weight of a specimen should consist of aluminum, and 72.635% of the total weight of a specimen should consist of zinc, in weight.

In the lower column of the table, total volume of the melt was calculated as 73 cm3. For calculations of the volume, equation 3.1. below was used, where d is a diameter and h is the length of a specimen hole.

$$V = \frac{\pi d^2}{4} h \tag{3.1}$$

Table 3.4. Volume calculation of the specimen

Diameter	Area	Lenght	Volume
2,5	4,908738521	14,80	72,6493301

On the right side of the volume column, the average density of one specimen according to its Bi, Zn, Al contents are given. The formula used to calculate the average density is given below.

$$d_{av} = \frac{(W_{Bi}\%)(d_{Bi}) + (W_{Zn}\%)(d_{Zn}) + (W_{Al}\%)(d_{Al})}{(W_{Bi}\%) + (W_{Zn}\%) + (W_{Al}\%)} \tag{3.2}$$

After calculating the average density, the total weight of one specimen was found from the equations below.

$$W_{total} = d_{av} V_{die} \tag{3.3}$$

Table 3.5. Total weight of the specimens according to specimen number, bismuth percentage and pressure levels

MATERIAL COMPOSITION	WEIGHT FOR ONE CASTING			WEIGHT FOR TWO CASTING			WEIGHT FOR THREE CASTING			WEIGHT FOR FOUR CASTING		
	Bi	Zn	Al	Bi	Zn	Al	Bi	Zn	Al	Bi	Zn	Al
%0 Bi + ZA27	0,00	316,6	117,1	0,00	633,2	234,2	0,00	949,8	351,3	0,00	1266,4	468,4
%0,5 Bi + ZA27	2,18	316,0	116,9	4,35	632,1	233,8	6,53	948,1	350,7	8,70	1264,2	467,6
%1 Bi + ZA27	4,37	315,5	116,7	8,73	631,0	233,4	13,10	946,4	350,0	17,46	1261,9	466,7
%1,5 Bi + ZA27	6,57	314,9	116,5	13,14	629,8	232,9	19,71	944,7	349,4	26,28	1259,6	465,9
Total Weight For One Pressure	13,11	1263,03	467,15	26,22	2526,05	934,29	39,33	3789,08	1401,44	52,44	5052,10	1868,59
Total Weight For Two Pressure	26,22	2526,05	934,29	52,44	5052,10	1868,59	78,66	7578,15	2802,88	104,88	10104,20	3737,17
Total Weight For Three Pressure	39,33	3789,08	1401,44	78,66	7578,15	2802,88	117,99	11367,23	4204,32	157,32	15156,30	5605,76

In Table 3.5. the total weight of the materials required can be seen in order to cast specimens relative to their number and number of pressure types. For example, if we want to cast 4 specimens according to the four different bismuth contents (0%, 0.5%, 1%, 1.5%),

and we also want to cast them under three different squeezing pressures (0, 50,100 MPa), then we need at least 118 gr of bismuth, 11367 gr of zinc and 4204 gr of aluminum metals. These weights were fixed and in every casting operation some amount of material was melted. So these total weights would vary up to 5% and the Table 3.6. below is prepared.

Table 3.6. The weights of the melts including 5% added weights

MATERIAL COMPOSITION	% 5 ADDED WEIGHT FOR ONE CASTING			% 5 ADDED WEIGHT FOR TWO CASTING			% 5 ADDED WEIGHT FOR THREE CASTING			% 5 ADDED WEIGHT FOR FOUR CASTING		
ADD (%) 5	Bi	Zn	Al	Bi	Zn	Al	Bi	Zn	Al	Bi	Zn	Al
% 0 Bi + ZA27	0,00	332,4	123,0	0,00	664,9	245,9	0,00	997,3	368,9	0,00	1329,7	491,8
% 0,5 Bi + ZA27	2,28	331,8	122,7	4,57	663,7	245,5	6,85	995,5	368,2	9,14	1327,4	491,0
% 1 Bi + ZA27	4,58	331,3	122,5	9,17	662,5	245,0	13,75	993,8	367,6	18,33	1325,0	490,1
% 1,5 Bi + ZA27	6,90	330,6	122,3	13,79	661,3	244,6	20,69	991,9	366,9	27,59	1322,6	489,2
Total Weight For One Pressure	13,77	1326,18	490,50	27,53	2652,35	981,01	41,30	3978,53	1471,51	55,06	5304,71	1962,01
Total Weight For Two Pressure	27,53	2652,35	981,01	55,06	5304,71	1962,01	82,59	7957,06	2943,02	110,12	10609,41	3924,03
Total Weight For Three Pressure	41,30	3978,53	1471,51	82,59	7957,06	2943,02	123,89	11935,59	4414,53	165,18	15914,12	5886,04

More details about the casting parameters are listed in the Table 3.7. According to this table we can see both the number of castings per type, the bismuth content and the pressure levels. In this experiment, four types of bismuth content (%0, %0.5, %1, %1.5) three pressure levels (0-50-100 MPa), at least four castings per type was made. Considering the 5% extra addition, we needed at least 165 gr of bismuth, 15914 gr of zinc, 5886 gr of aluminum metals.

Table 3.7. The weight of melts including 5% addition (general)

MATERIALS COMPOSITION		%5 ADDED WEIGHT FOR THREE CASTING			%5 ADDED WEIGHT FOR FOUR CASTING			%5 ADDED WEIGHT FOR FIVE CASTING			%5 ADDED WEIGHT FOR SIX CASTING			%5 ADDED WEIGHT FOR SEVEN CASTING		
ADD (%) 5		Bi	Zn	Al	Bi	Zn	Al	Bi	Zn	Al	Bi	Zn	Al	Bi	Zn	Al
%0 / 0,5 / 1 / 1,5 Bi + ZA27	100 Mpa (One Pressure)	41,30	3978,5	1471,5	55,06	5304,7	1962,0	68,83	6630,9	2452,5	82,59	7957,1	2943,0	96,36	9283,2	3433,5
	0-100 Mpa (Two Press.)	82,59	7957,06	2943,02	110,12	10609,41	3924,03	137,65	13261,76	4905,04	165,18	15914,12	5886,04	192,71	18566,47	6867,05
	0-50-100 Mpa (Three Press.)	123,89	11935,59	4414,53	165,18	15914,12	5886,04	206,48	19892,65	7357,55	247,78	23871,17	8829,06	289,07	27849,70	10300,58
	0-50-75-100 Mpa (4 Pres.)	165,18	15914,12	5886,04	220,24	21218,82	7848,06	275,31	26523,53	9810,07	330,37	31828,23	11772,09	385,43	37132,94	13734,10
%0 / 0,25 / 0,50 / 0,75 / 1 / 1,25 / 1,5 Bi + ZA27	100 Mpa (One Pressure)	41,30	3978,5	1471,5	55,06	5304,7	1962,0	68,83	6630,9	2452,5	82,59	7957,1	2943,0	96,36	9283,2	3433,5
	0-100 Mpa (Two Press.)	82,59	7957,06	2943,02	110,12	10609,41	3924,03	137,65	13261,76	4905,04	165,18	15914,12	5886,04	192,71	18566,47	6867,05
	0-50-100 Mpa (Three Press.)	123,89	11935,59	4414,53	165,18	15914,12	5886,04	206,48	19892,65	7357,55	247,78	23871,17	8829,06	289,07	27849,70	10300,58
	0-50-75-100 Mpa (4 Pres.)	165,18	15914,12	5886,04	220,24	21218,82	7848,06	275,31	26523,53	9810,07	330,37	31828,23	11772,09	385,43	37132,94	13734,10

Hence, it would be beneficial to get at least 10% more material than the calculated values to compensate the losses.

These materials were put into nylon after weighing them using a Tefal balance and their contents were written onto it. For example; if, we want to cast a specimen that has a composition of 1.5%Bi+ZA-27, we should prepare 6.9 gr Bi, 330,6 gr Zn and 122,3 gr aluminum into nylon and write these values onto it. When a specimen was cast these materials would be ready in priori.

3.2. Squeeze Casting Practice

3.2.1. Preparations Before a Casting Operation

There were some preparations that should done and some auxiliary equipment should be made ready before a squeeze casting operation.

Melting Furnace: This furnace was used to melt the materials. It was capable of reaching temperatures up to 1000˚C in a very short time, like 30 minutes. The furnace inside was made of ceramic and resistance wires wounded around it. The melting furnace was used to melt aluminum, zinc and bismuth metals.

Annealing Furnace: Annealing temperatures are much lower than the melting temperatures of metals. This furnace is not capable of reaching high temperatures. Maximum allowable working temperature for this furnace is about 700˚C. The furnace temperature increases up to 700˚C in 2.5-3 hours. This furnace inside is made of thin metal and, resistance wires are wounded around this thin metal case. The squeeze casting dies and the punch were heated in this furnace.

Crucible: Crucible is one of the main auxiliary tools to melt an alloy. This tool was made of graphite. Graphite is an inert material and doesn't react with the metals. It is also durable to high temperatures and it doesn't lose its main composition at high temperatures.

In the experiments an A4 type graphite crucible was used. This crucible was capable of melting two sets of ZA-27 alloys.

Stirring Sticks: These sticks were also made of graphite in order not to contaminate the casting alloy. The diameter of these sticks varied generally from 2 mm to 5 mm, and their length was approximately 30 cm. These sticks were very brittle and can be broken very easily. So, it would be better to buy the thickest one (5mm) of these sticks.

Safety Equipments: In casting operations the safety of the people and environmental control are very important. The temperature of the melt was approximately 800˚C and if it spilled onto human body, it would seriously harm it.

In order to protect human face, a transparent face guard made of mica should be used. This tool should be used while taking the crucible out of the furnace and putting the crucible back into the furnace.

Another important safety equipment was hand gloves. These gloves must be temperature insensitive, i.e. Asbestos gloves may be useful. Even you hold the crucible by tongs, you should use hand gloves. Because the hands approach to the hot furnace and hence they may burn. To prevent this, temperature insensitive hand gloves must be used.

Thermal Millivoltmeter and Thermocouple: A thermocouple is a sensor for measuring temperature. It consists of two dissimilar metals, joined together at one end. When the junction of the two metals is heated or cooled a voltage is produced that can be correlated back to the temperature. The thermocouple alloys are commonly available as wire. A thermocouple is available in different combinations of metals or calibrations. The four most common calibrations are J, K, T and E. Each calibration has a different temperature range and environment, although the maximum temperature varies with the diameter of the wire used in the thermocouple. Although the thermocouple calibration dictates the temperature range, the maximum range is also limited by the diameter of the thermocouple wire [31]. In our experiments 0.5 mm K type thermocouple was used. 0.5 mm is important, because if the diameter is decreased the response time of the thermocouple increases. In order to read the values which thermocouple shows we need a converting unit that converts voltage to understandable temperature values. Thermal millivoltmeter is the device which does that task.

Isolator Bricks: These bricks are made of a special clay and it has many bubbles inside (i.e. large porosity). With the help of these bubbles, the heat transfer coefficient of this brick was lowered very much. So, it didn't transfer the heat of the crucible to the floor and didn't lead to the fast cooling of the crucible, hence fast cooling of the melt in the crucible or die which would be undesirable.

3.2.2. Casting of an Unsqueezed Pure ZA-27 Alloy

Firstly, two furnaces were turned on. Nylon containing the pure ZA-27 was opened and the contents of the container were put on the table. Zinc and aluminum slices were separated on the table. Crucible was held and inside of the crucible was cleaned using a wire brush. Aluminum slices were put first into the crucible. The crucible was put into the furnace, argon was blown into the die and the cover of the furnace was closed (Please refer to Figure 3.9).

The squeeze casting die was dismantled. The two halves of the die were cleaned using a wire brush. The bottom thermocouple hole of the die wasn't used. So it was blocked using a soft thick wire made of copper or soft iron as seen in the Figure 3.7.

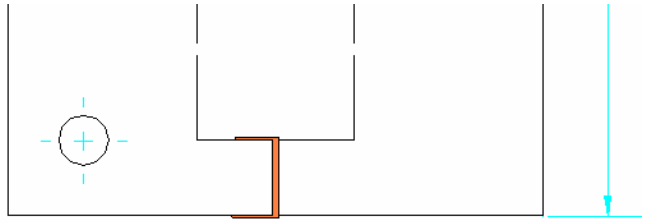

Figure 3.7. The blockage of the unused bottom thermocouple hole in the dies

The die was put into the annealing furnace. The furnace was set to 550˚C and the dies and the punch were heated.

Important Note: In order to reduce the heating time of the die and decrease the melting time of the aluminum in the crucible, it was necessary to increase the heat flux from the furnaces to the crucible or die. The melting temperature of the aluminum was

933.57K (~660˚C) and there was also an additional transformation heat (Lf) to change the aluminum from solid to liquid phase. Considering this transformation heat, we need more heat flux that means we need a furnace at higher temperatures. The higher temperature means higher heat flux from the furnace to the die or crucible. By this high energy flux, our material reaches the desired temperature in a shorter time. In order to do all these, the melting furnace was set to 800˚C, and the annealing furnace was set to 550˚C. The graphical explanation of this application is shown in Figure 3.8. below.

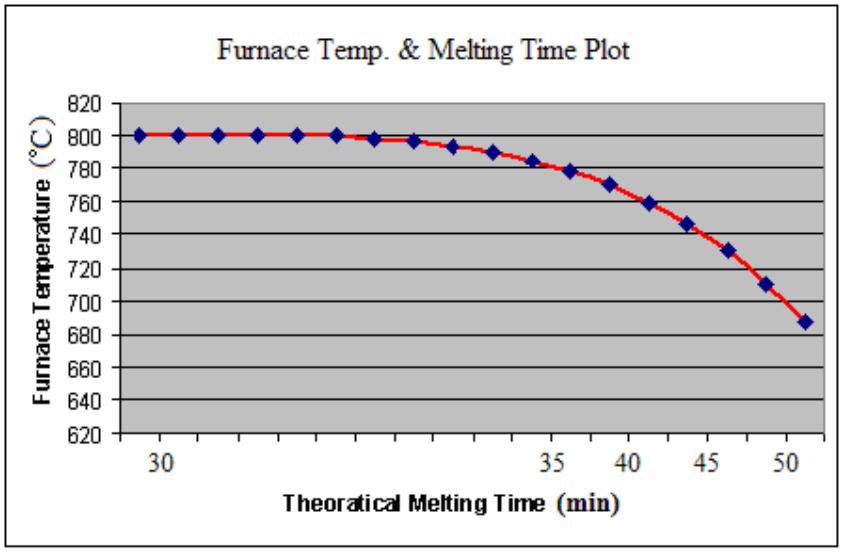

Figure 3.8. Variation of theoretical melting time versus furnace temperature

Argon Gas Sweeping: At first, the inside of the crucible and the die was swept with hot argon gas as seen in Figure 3.9.

The flow rate of the argon gas was set using a regulator unit on the tube. Using a copper pipe of 6 mm diameter, the argon gas was pre-heated. The copper pipes were wounded inside of the melting furnace. So the argon gas was heated and didn't cool the melt in the crucible.

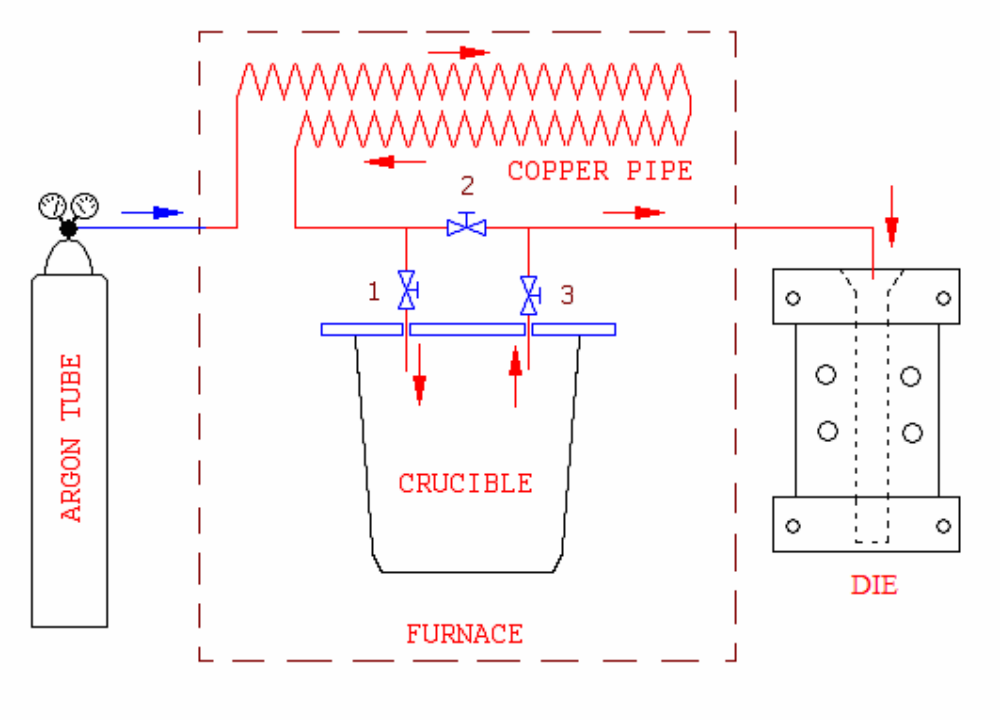

Figure 3.9. A sketch of the argon gas sweeping system used for the crucible and the die

Note: The length of the pipe should be made long enough to warm the argon gas to a high temperature. Also, the flow rate of the gas should be low enough to sweep the inside of the crucible. If the pipe inside the furnace isn't long enough, then the gas cannot be heated to the desired temperature. Or, if the flow rate of the argon is not small enough, the argon gas cannot be heated.

After a while the sweeping with argon gas was ended. Because it would be harmful when adding bismuth to the ZA-27 melt. This situation is explained in the Section 3.2.3.

When the aluminum slices inside the crucible were melted, the mica head mask was put on, and then the crucible was taken out of the furnace and put onto an isolator brick. The zinc slices were put inside the crucible using tongs. After that the crucible was again put into the furnace and waited for the melting of the zinc slices.

Meanwhile, the die in the annealing furnace was temporarily taken out of the furnace and the temperature of the die was checked whether it was reached to 300˚C or not. If the

die temperature reached to 300˚C it was left on the isolator brick. When the die temperature dropped to 290˚C, the pure ZA-27 alloy melt was taken out of the furnace and put onto the isolator brick and stirred. When the die temperature decreased to 285˚C, the ZA-27 melt was poured into the die using tongs.

The melt should be smoothly poured into the die. The pouring of the melt should be continuous. The approximate theoretical pouring flow rate per time should be similar as in the Figure 3.10.

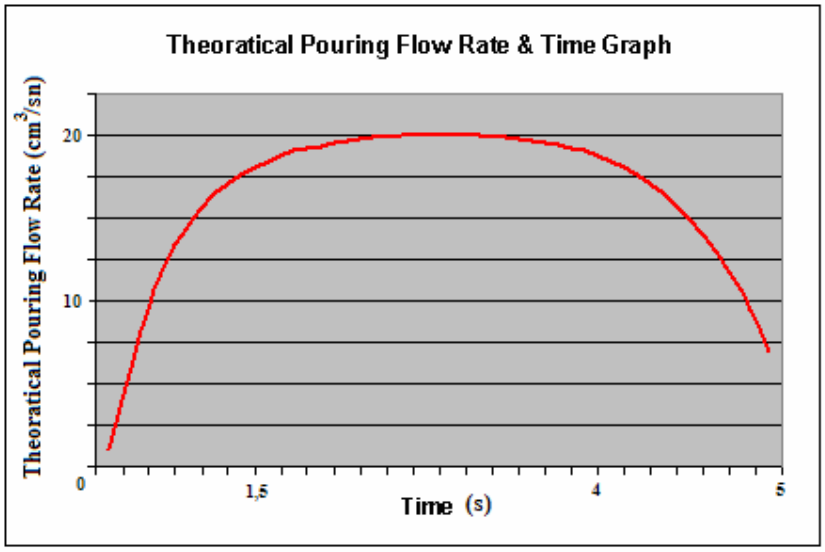

Figure 3.10. A schematic view of approximate theoretical pouring flow rate per time

The volume of the melt should be more than the cavity volume of the die. Because, when you pour melt into the die, it shrinks. The length of the cast specimen shortens because of this shrinkage. So, we have to pour more melt to compensate this shrinkage.

After this operation, the crucible was again put into the melting furnace. 2-3 minutes after, the bolts of the die was opened using an allien key. While opening the die, hand gloves were used in order not to burn the hands. After opening the die, the specimen was taken using proper tongs and it was wounded into glass wool which was 5 cm thickness. In this wool the specimen cooled slowly in order not to make any structural tension.

Note: The die was never water cooled. It would be harmful for the die and for the casting inside. Die could crack and microcracks could form inside the specimen. The cracks would reduce the life of the die. Microcracks would lead to the lower mechanical properties than the actual values. For example, the tensile properties of the specimens could be lower.

After removing the specimens the die was cleaned using a wire brush. A proper copper wire was put inside of the die and the two sides of the wire were hammered as seen in the Figure 3.7.

3.2.3. End of the Argon Gas Sweeping

Argon is an inert gas and in the casting industry it is widely used. In alloy making, after adding the bismuth to the crucible, the crucible was put into the furnace. Argon gas was sent off into the furnace to remove the air hence oxygen in it. After that, argon gas was opened to sweep the oxygen of the air. If bismuth contacts with oxygen at high temperatures like 600˚C it burns with green flame. When argon gas was used as sweeper in this experiment, I saw a greenish circle in the inner sides of the crucible. After that I didn't use argon gas and I made bismuth added castings without argon gas sweeping. And I didn't see any greenish circles inside the crucible. Also, I have never met a bismuth particle burning with green flame. So, I decided not to use argon gas. The cause of this event may be this: Argon gas is an inert gas and this gas also used to purify the molten metal. For example, in the steel industry the melt is stirred using argon gas. By this operation, the unwanted materials were removed from the steel. In my experiment, argon gas probably had a similar effect. It separated the bismuth from the ZA melt and sends it to the outside of the crucible in gas phase. When this gas circulated, it met with the oxygen of the air and it burned. (Remember that it was at a very high temperature) So, the uniform greenish circles were formed inside the crucible. The explanation above may be the cause of that greenish circles.

3.2.4. Casting of Squeezed Pure ZA-27 Alloy

Squeeze casting experiments of this thesis were done using the squeeze casting set-up which can be seen in the Figure 3.11. This set-up mainly consists of two components. One of them was the oil pump which is used to pressurize the oil to the desired value. The other component was the piston that was used to transmit the squeezing force to the specimen. Pure ZA-27 container was again taken, opened and the contents of the container were put on the table. Zinc and aluminum slices were separated. Crucible was held and inside of the crucible was cleaned using a wire brush. The crucible containing aluminum slices was put into the furnace and furnace door was closed.

Figure 3.11. The squeeze casting set-up

The die was taken and opened. The two sides of the die were cleaned using a wire brush. The bottom thermocouple was blocked with a copper wire. The die was put into the hot annealing furnace. Similarly, the punch of the die was put into the annealing furnace for heating.

When the aluminum slices inside the crucible melted, the zinc slices were put inside the same crucible as explained before. After that the crucible was again put into the furnace and waited for the melting of the zinc slices inside the aluminum melt.

Meanwhile, the die was temporarily taken out of the furnace, put onto the isolator brick that has glass wool on it. The temperature of the die was checked whether it was reached to 300˚C or not. If the die reaches to 300˚C, it was put on the glass wool. The oil pump of the press was switched on. When the die temperature dropped to 290˚C, the pure ZA-27 alloy melt was taken out of the furnace and put onto the isolator brick and stirred. Also, the punch was taken out of the furnace and put onto another isolator. This isolator brick should be close to the squeeze casting press and the suitable tongs to handle this punch should be put near punch. When die temperature was 285˚C, the ZA-27 melt was poured into the die using proper size tongs. The volume of the poured melt should be more than the cavity volume of the die. Because, when you pour melt into the die it shrinks.

Note: A glass wool was put onto the isolator brick. When you take out the die from the furnace and put it onto a brick, it cools rapidly from the bottom. Because, the heat transfer coefficient of the brick is higher than the air. So, when we measure temperature of the die at the bottom as 285˚C, at the same time the temperature of the bottom of the die will be lower than 285˚C. So, if we pour melt into this die, the bottom side of our melt will solidify early. Also, the squeezing pressure leads to fast cooling of the castings due to a good contact between the die and the melt. With these two causes, only half of the specimen was squeezed. Because, it is not possible to squeeze a solid element.

So, a piece of glass wool was put onto the isolator brick as in the Figure 3.12. This leads to the slow cooling of the bottom side of the die. When we measure 285˚C in the middle, the bottom temperature will be higher. So if we pour the melt at this condition, the bottom side of the specimen will not solidify early. Then squeezing of the every side of the specimen would be possible as seen in the Figure 3.13.

After pouring, the die was immediately put into the press using the back side of another pair of tongs. The punch was held with another pair of tongs and it was put onto the die. The lever of the squeeze casting press was immediately pulled with the other hand. Also, the chronometer was started in order to pressurize the specimen for 103 seconds. At last, the specimen started to be squeezed.

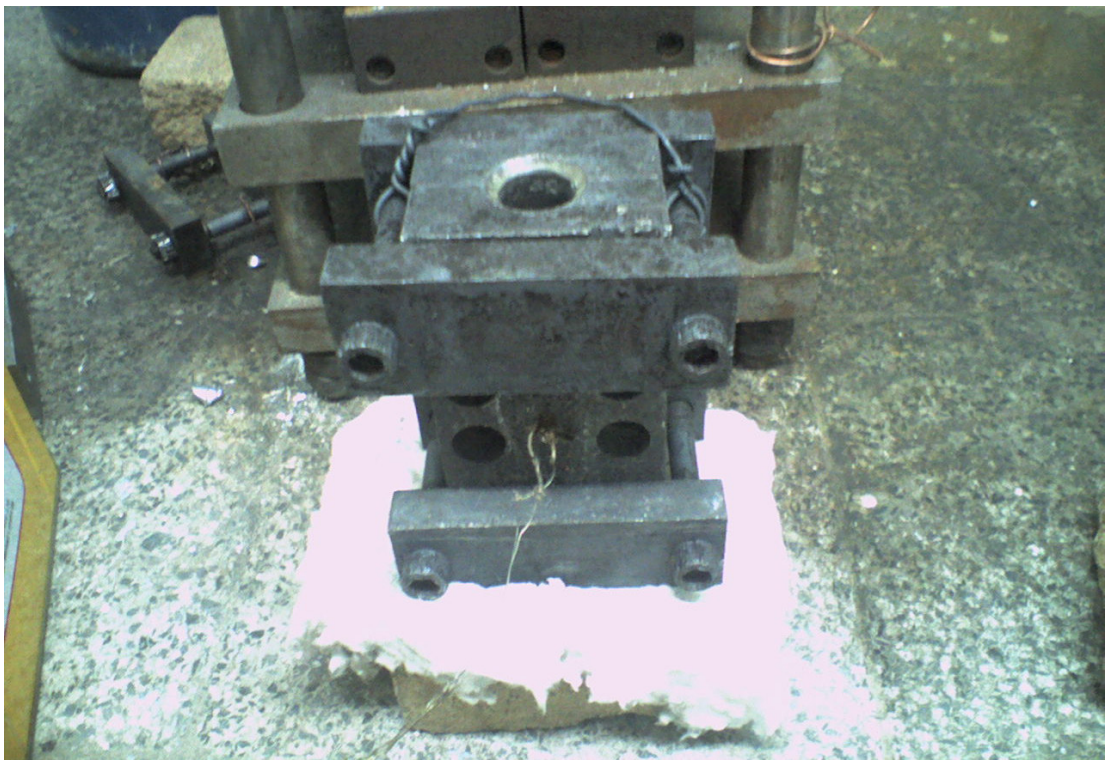

Figure 3.12. Placing a piece of glass wool between the die and the brick

If, the punch was drawn into the die too much and it touched to the die, then the squeezing operation was unsuccessful. Then, the lever was pushed, the die was taken out of the press and put onto the isolator. The bolts of the die were unscrewed and the casting was taken out of the die. This specimen was again put into the crucible which was in the furnace. The die was cleaned and reassembled. The die was put into the annealing furnace and heated again for another use.

If the punch was drawn into the die too short, this meant the squeezing operation was again unsuccessful. Then, the die was taken out of the press, the specimen was taken out of the die. This specimen was again put into the crucible which was in the furnace. The die was cleaned and reassembled. The die was put into the annealing furnace and heated again.

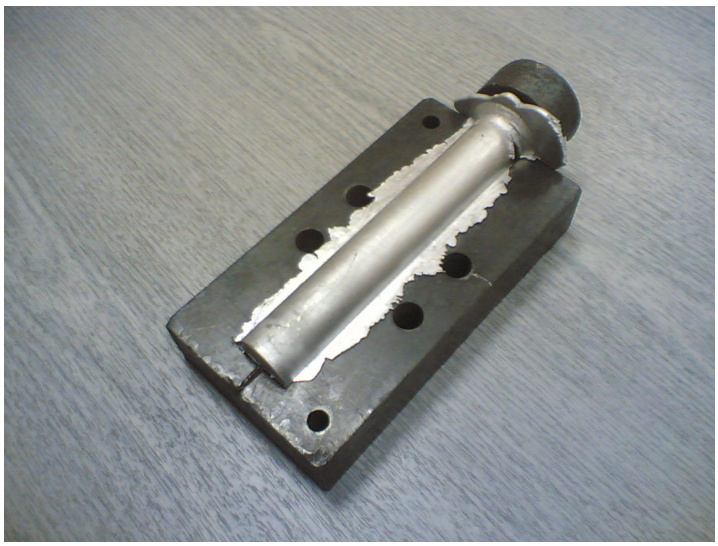

Figure 3.13 A photo of an adequately squeezed specimen

The allowable entering degree of the punch is middle. The punch should be drawn into the die until to the middle of its length. After this operation, the crucible was again put into the melting furnace. 2-3 minutes after, the bolts of the die opened and the specimen was wounded into a glass wool. After that, the die was cleaned with a wire brush. A proper copper wire was put inside the die and the die was put inside the annealing furnace for the next casting.

3.2.5. Casting of Bismuth Added ZA-27 Alloy

In this experiment, the ZA-27 container was again taken, opened and the contents of the container was put on the table. Zinc and aluminum slices were separated. Crucible was held and inside of the crucible was cleaned using a wire brush. The crucible containing aluminum slices was put into the furnace and the furnace door was closed.

The die was taken, opened, cleaned and reassembled as before. The die and its punch were put into the annealing furnace. When the aluminum slices inside the crucible was melted, the zinc slices were put inside the same crucible and melted.

Preparation of Bismuth Shots: Bismuth is a white crystalline, and a brittle metal with a pinkish tinge. Bismuth is a type of low-melting element. Its melting temperature is

271˚C. When bismuth is heated in air it burns with a blue flame, forming yellow fumes of the oxide. Bismuth expands 3.32% on solidification.

Bismuth shots we had, were generally found as small particles with an average approximate diameter was 2 mm, and length was 8-10 mm. The solubility of this volume bismuth shot is not high in a ZA-27 melt. So, when bismuth was added into the ZA melt, at that moment while stirring, bismuth shots goes to the upper side of the melt and it contacts with oxygen of the air and it burns with a bluish green flame. Because, the solubility of the bismuth shots was not enough in ZA-27 melt.

In order to prevent this, a new method was found. Bismuth shots were put between two pieces of cardboard. The both sides of this cardboard were closed to prevent the leakage of the bismuth shots. The air, in the cardboard was deflated. After that, the cardboard was hammered many times to convert bismuth shots into dust form. After that, the bismuth dust was collected; required amount of bismuth for one specimen was weighed with a sensitive balance. This dust was wrapped into an aluminum foil. This wrapped foil was put onto the table for usage.

After the zinc and aluminum slices were melted, the crucible was taken out of the furnace and it was put on the brick. (Remember that, at this time the temperature of the die should be 300˚C for not to lose time and for not to heat bismuth in the crucible too much. If you leave bismuth in the crucible too long and heat it, some of the bismuth evaporates.) The wrapped aluminum foil containing bismuth was mixed into the melt. The foil was pushed to the bottom of the crucible using the graphite sticks. This operation was continued for 5-6 seconds. After that, crucible was put into the furnace again. The crucible was heated for 5-10 minutes. After that the melt in the crucible was stirred carefully. Stirring shouldn’t be very fast.

If the die temperature was 300˚C, it was put on the glass wool. The oil pump of the press was switched on. When the die temperature dropped to 290˚C, the pure ZA-27 alloy melt was taken out of the furnace and put onto the isolator brick and stirred carefully again. Also, the punch was taken out of the furnace and put onto another isolator. When die

temperature was reached to 285˚C, the melt was stirred again carefully to prevent the sinking of the bismuth element in the molten ZA alloy. (Remember that the density of the bismuth is twice of the density of the ZA alloy). The ZA-27 melt was poured into the die using proper size tongs. The volume of the poured melt should be more than the cavity volume of the die. Because, when you pour the melt into the die, it shrinks upon cooling.

After pouring, the die was immediately put into the press using the back side of an another pair of tongs. The punch was put onto the die. The lever of the squeeze casting press was immediately pulled, the chronometer was started in order to pressurize the specimen for 103 seconds. At last, the specimen started to be squeezed.

The allowable entering degree of the punch was its middle. The punch should draw into the die until to the middle of its length. After this operation, the crucible was again put into the melting furnace. 2-3 minutes after, the bolts of the die opened and the specimen was wounded into glass wool. After that, the die was cleaned with a wire brush. A proper copper wire was put inside of the die and the die was put inside the annealing furnace for the next squeeze casting practice.

According to Papworth and Fox [32], bismuth has the effects below on aluminum alloys:

The surface oxide film is modified by the addition of bismuth as it disrupts the film's formation. In the liquid state, bismuth forms a surface covering on the liquid alloy, thus reducing the ability of aluminum and magnesium to form an oxide film. As the oxide grows, bismuth disrupts the oxide's integrity as it becomes incorporated into the oxide film.

The addition of bismuth changes the surface tension of aluminum alloys and hence their contact angles by the disruption of the oxide film. Bismuth changes the morphology of the oxide film, by being incorporated into the oxide, therefore changing the behaviour of the film and its properties. The oxide film was responsible for the high surface tension of the liquid alloy and consequently the high contact angle of the alloy. Changing the integrity of the film reduces the strength of the film, which in turn reduces the surface tension of the alloy.

The addition of bismuth disrupts the formation of oxide defects in aluminum alloys by reducing the integrity of the oxide film. Oxide defects are caused by two actions. The first is turbulent flow; the second is two advancing liquid flows coming together from different directions. Bismuth disrupts the integrity of the oxide film and reduces its strength. In turbulent flow, the film, which is much weaker, is broken up into small pieces, therefore, stopping long cracks developing within the alloy. In the case of two advancing liquid flows coming together, instead of forming an oxide barrier between the two flows, the weaker oxide breaks up due to the turbulence, allowing the two liquids to mix, therefore making an integral casting [32].

A well squeeze casting sample is seen below in the Figure 3.14 and its characteristic can be summarized as:

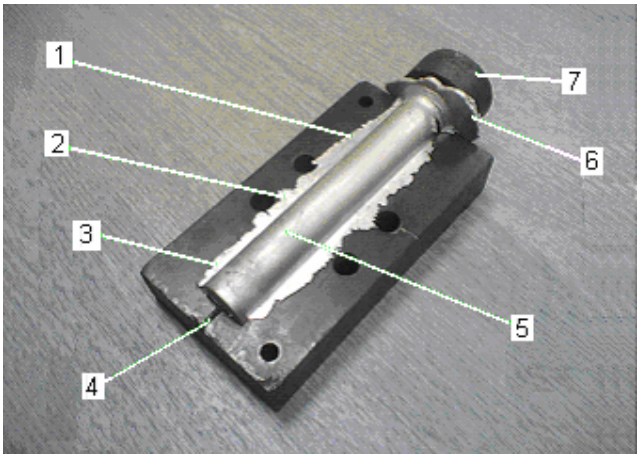

Figure 3.14. Explanation of the photo of an adequately squeezed specimen

i) This shows that this side of the specimen was squeezed well. Generally, it is easy to squeeze only the upper side of the specimen.

ii) The midpoint of the specimen was squeezed well. Squeezing this midpoint is not very easy.

iii) The bottom side of the specimen was squeezed well. Squeezing this is very hard. Putting isolator glass wool (in Section 5), excessive heating of the melt, and pressurizing the die quickly, play important role on this result.

iv) The bottom thermocouple hole is closed well. That prevents the leakage of the melt and good squeezing of the specimen.

v) There is no clear surface defect on the squeezed specimen. That is another sign of well squeezing application.

vi) The melt was poured a bit more in order to compensate shrinkage and prevented shortening of the specimen.

vii) The punch was drawn into the die as required. It was not drawn into the die very little and also it was not touching to the die.

3.3. Cooling Curve Determination

In some of the experiments, temperature values were recorded in every 30 seconds. Using these data the temperature-time curve was drawn as seen in the Figure 3.15.

Firstly, a table was prepared. In this table the columns showed the time and the temperature. The time values were written, starting from 0 second up to 5 minutes. The time interval was changing between 5 seconds and 10 seconds.

When the melt was poured, a person was started the chronometer and at every 5 or 10 seconds, asked the his friend to read temperature. It can be noted that when not squeezed, the die heats up considerably later than the squeeze casting, upon pouring of the squeeze melt into it. The die heats up quickly and cools quickly during squeeze casting. The punch surface also facilitates heat transfer. Hence, it is evident that the melt cools and freezes more quickly due to the efficient heat transfer through the die and the punch as a result of squeezing [1].

The difference in cooling rates and the modification of the solidification front during squeeze casting naturally, expected to produce a different microstructure and, hence different mechanical properties [1]. In this experiment, the solidification rate in squeeze casting was calculated as 0.6˚C/sec, whereas it was 0.514˚C/sec in gravity casting. This

17% increase can be attributed to the reduction in thermal resistance due to the prevention of an air-gap formation at the die-melt interface during squeeze casting.

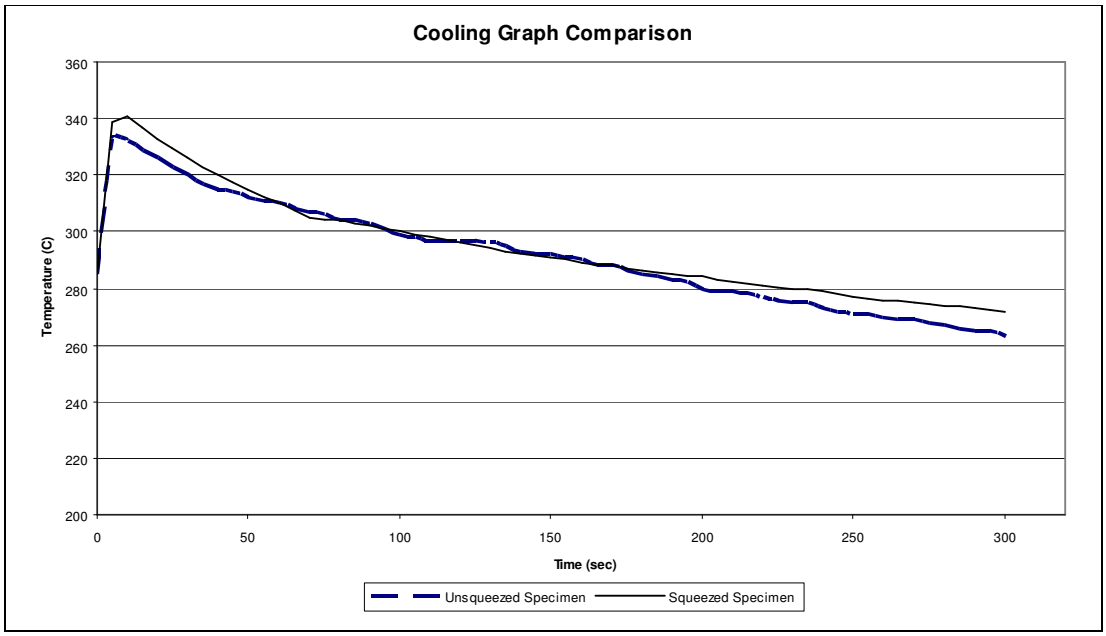

Figure 3.15. Comparison of the cooling rate of the squeezed and unsqueezed specimens

3.4. Determination of Density

In the measurement of density, the ASTM D792 Standard A method was used [33]. This standard has been employed for determination of the specific gravity and the density of solid plastics by displacement of a liquid and by following the change in weight [33].

The procedure of the measurement of density is explained below:

A sheet was prepared. The numbers, and contents were written on the sheet. The m_a, m_w, d columns were prepared in the chart for filling later. m_a means the weight of the specimen in air. m_w means the weight of the specimen in water. d means the calculated density of the specimen.

Before starting the density measurement, rough sides of the specimen was grinded and cleaned in order not to nucleate bubbles inside the specimen.

A set-up was prepared as seen in the Figure 3.17.

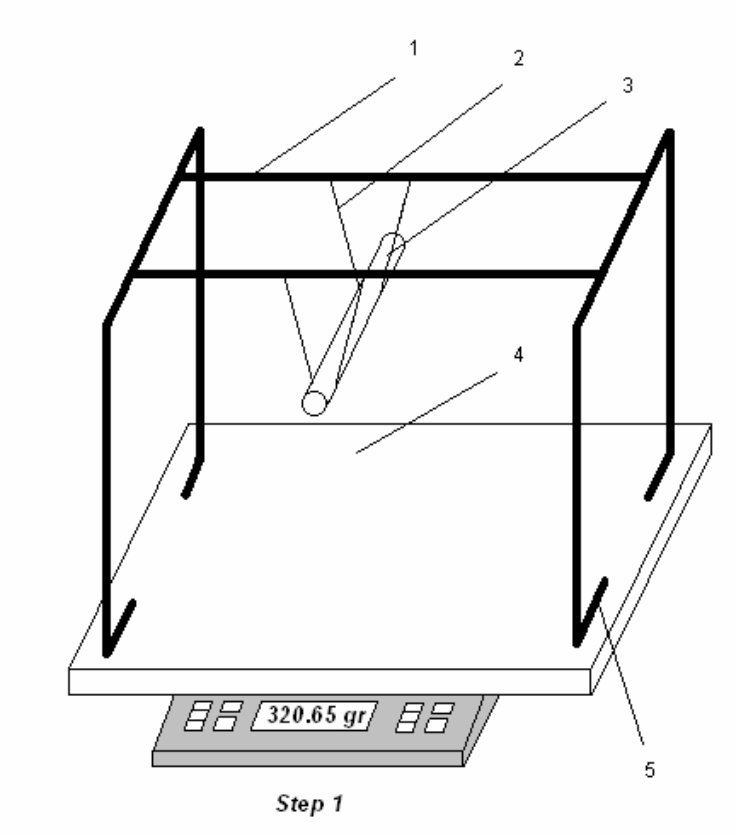

Figure 3.16. Density measurement set-up

Firstly the specimens were weighed using a sensitive electronic balance. The accuracy of the scale was 0,01gr. When the measuring value on the scale was stabilized this value noted on the chart. The specimen weighted again to be sure the weight of the specimen. Then this value was accepted the ma value of this specimen. All specimens were weighed and m_a values were noted on the table.

Some amount of distilled water was poured inside a plastic container. This container was fixed inside the density setup. Using this technique the specimens were sunk into the water and their weights were measured. While measuring, the turbulence of the water should be diminished, and the scale should show a consistent value. (Note: Don't keep the specimen in the water too much. If you see that bubbles coming from specimen, that means water is filling inside the specimen. Also, the weight value changes on the scale. This leads

to the wrong measuring of the weight. To prevent this, note the measured value and take the specimen out of the water.)

This measurement was repeated at least twice in order to prevent wrong measurements. These values are accepted as m_w value and written on the chart.

After finishing the weighting in air and in water, the density value was calculated according to the formula 3.4. below. After that the calculated density values were written on the chart.

$$\rho_0 = \frac{m_a}{m_a - m_w} \tag{3.4}$$

Explanation of the setup materials in Figure 3.17:

i) This is a steel wire that has 3 mm thickness. This wire is bended as seen above and formed the chassis of the setup.

ii) This wire is made of aluminum and the thickness was about 0.5 mm. The task of this wire was to hold the specimen. This wire was selected thin in order not to fill too much volume in the water.

iii) The specimen should be hanged on the thin wire. The specimen should be parallel to the floor.

iv) The sub plate was made of foam. The thickness of the foam was about 5 cm. Total weight of the setup was only 125 gr. (The maximum allowable working weight of the scale is 600 gr. The weight of the setup=125 gr. The max weight of the specimen was about 360 gr. Total weight =125+360=485 gr<600 gr.)

v) The end of the thick wire was bended in order to increase area of the wire. (That means in order to decrease pressure made by wire to the foam.) After that, these 4 bended tips were sticked with a tape to the foam carefully.

3.5. Chip Length Measurement

Chip length measurement is one of the main indicator of the machinability characteristics of the material. The specimens were machined in a lathe at three different cutting speeds. These speeds were 125 rpm, 250 rpm, and 500 rpm. The cutting tool was high speed steel.

Figure 3.17. A view of turning operation and collection of chips

The cutting speed was calculated by using the formula below:

$$\upsilon = \frac{\pi D n}{1000} \quad (\text{mm/min}) \tag{3.5}$$

Procedure: Firstly, a cleaning pass was applied. The outer surface of the specimen was cleaned. Using the known cutting speeds, rpm equivalents were found according to the Table 3.8.

Table 3.8. The rpm equivalents for three different cutting speeds

		RPM VALUES ACCORDING TO THE SPECIMEN DIAMETER AND CUTTING SPEED																					
πD/1000	Dia \ n	180	180	190	200	210	220	230	240	250	270	280	290	300	325	510	520	530	550	575	600	625	650
0,0785	25	14,14	14,14	14,92	15,71	16,49	17,28	18,06	18,85	19,63	21,21	21,99	22,78	23,56	25,53	40,06	40,84	41,63	43,20	45,16	47,12	49,09	51,05
0,0770	24,5	13,85	13,85	14,62	15,39	16,16	16,93	17,70	18,47	19,24	20,78	21,55	22,32	23,09	25,01	39,25	40,02	40,79	42,33	44,26	46,18	48,11	50,03
0,0754	24	13,57	13,57	14,33	15,08	15,83	16,59	17,34	18,10	18,85	20,36	21,11	21,87	22,62	24,50	38,45	39,21	39,96	41,47	43,35	45,24	47,12	49,01
0,0738	23,5	13,29	13,29	14,03	14,77	15,50	16,24	16,98	17,72	18,46	19,93	20,67	21,41	22,15	23,99	37,65	38,39	39,13	40,61	42,45	44,30	46,14	47,99
0,0723	23	13,01	13,01	13,73	14,45	15,17	15,90	16,62	17,34	18,06	19,51	20,23	20,95	21,68	23,48	36,85	37,57	38,30	39,74	41,55	43,35	45,16	46,97
0,0707	22,5	12,72	12,72	13,43	14,14	14,84	15,55	16,26	16,96	17,67	19,09	19,79	20,50	21,21	22,97	36,05	36,76	37,46	38,88	40,64	42,41	44,18	45,95
0,0691	22	12,44	12,44	13,13	13,82	14,51	15,21	15,90	16,59	17,28	18,66	19,35	20,04	20,73	22,46	35,25	35,94	36,63	38,01	39,74	41,47	43,20	44,92
0,0675	21,5	12,16	12,16	12,83	13,51	14,18	14,86	15,54	16,21	16,89	18,24	18,91	19,59	20,26	21,95	34,45	35,12	35,80	37,15	38,84	40,53	42,22	43,90
0,0660	21	11,88	11,88	12,53	13,19	13,85	14,51	15,17	15,83	16,49	17,81	18,47	19,13	19,79	21,44	33,65	34,31	34,97	36,29	37,93	39,58	41,23	42,88
0,0644	20,5	11,59	11,59	12,24	12,88	13,52	14,17	14,81	15,46	16,10	17,39	18,03	18,68	19,32	20,93	32,85	33,49	34,13	35,42	37,03	38,64	40,25	41,86
0,0628	20	11,31	11,31	11,94	12,57	13,19	13,82	14,45	15,08	15,71	16,96	17,59	18,22	18,85	20,42	32,04	32,67	33,30	34,56	36,13	37,70	39,27	40,84

The lathe was set to 125 rpm. The pass depth was set as 1 mm. The lathe was started. The chips were collected as seen in the Figure 3.18. Only 1/3 of the length of the specimen was turned for 125 rpm.

After that all chips which turned at 125 rpm was put into a nylon container and details were written on it, as seen in the Figure 3.19

Figure 3.18. Classification of the chips

The lathe was stopped and set to 250 rpm. Nothing changed except rpm. The lathe was started and continued from 1/3 to 2/3 length of the specimen. Only 1/3 of the length of

the specimen was turned for 250 rpm as before. The chips were collected and put into nylon container. The details were again written on it.

Later, the lathe was stopped and set to 500 rpm. Nothing changed except rpm. The lathe was started and continued from 2/3 to 3/3 length of the specimen. Only 1/3 of the length of the specimen was turned for 500 rpm as before. The chips were collected and put into nylon container. The details were again written on it.

The chips were measured several times to ensure a proper average value. The measured values were written on a paper for evaluation.

3.6. Surface Roughness Measurement

On the microscopic scale, surfaces exhibit waviness and roughness. The surface profile can be measured and recorded. For easier visualisation recordings are usually made with a larger gain on the vertical axis as in Figure 3.20.

This gives a distorted image with sharp peaks and steep slopes; in reality the peaks (asperities) have gentle slopes of typically 5- 20˚ inclination. The traces or more frequently, signal obtained from profilometer may be processed electronically or, after digitization in a computer to derive various values for a quantitative characterization of the surface profile. Of the various measures, the following are most frequently used:

R_t is the maximum roughness height (the height from the maximum peak to deepest trough). It is important when the roughness is to be removed, for example by polishing. Often a more meaningful figure is obtained by taking the average height difference between the 5 highest peaks and 5 deepest valleys within the sampling length. (10 point height, R_z)

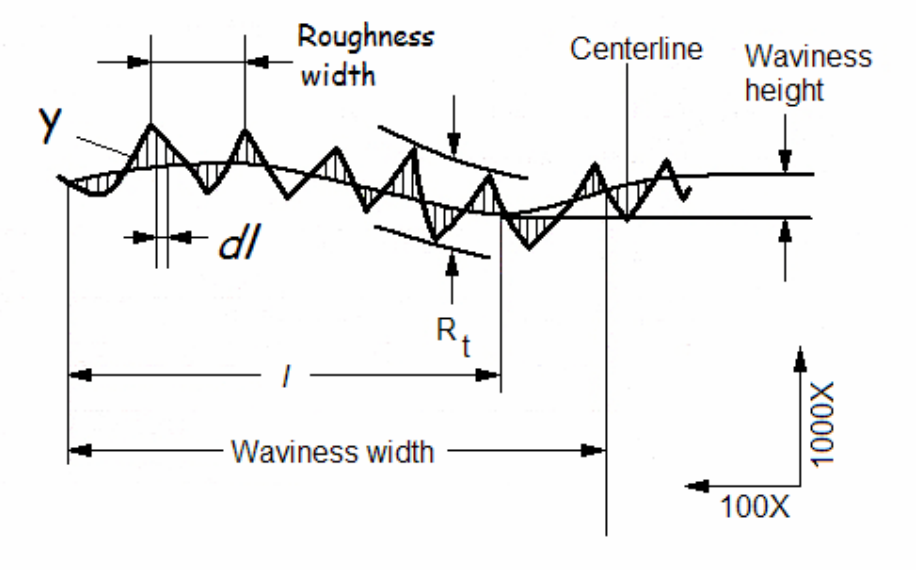

Figure 3.19. Magnification of the surface roughness of a part [19]

A line drawn in such a way that the area filled with material equals the area of unfilled portions, defines the centerline or mean surface. The average deviation from this mean surface is called centerline average (CLA) or arithmetical average (AA), denoted also as R_a,

$$R_a = \frac{1}{l}\int_0^1 |y|\, dl \quad \text{or} \quad R_a = \frac{y_1 + y_2 + y_3 + \ldots + y_n}{n} \tag{3.6}$$

The root mean square (rms) value R_q is frequently preferred in practice and also in the theory of contacting surfaces.

$$R_q = \left[\frac{1}{l}\int_0^1 y^2\, dl\right]^{1/2} \quad \text{or} \quad R_q = \left(\frac{y_1^2 + y_2^2 + y_3^2 + \ldots + y_n^2}{n}\right)^{1/2} \tag{3.7}$$

R_q is closely related to R_a(R_a=1.11R_q for a sine wave) and, for technical surfaces, the relationship between various values is fairly well defined.

Table 3.9. Approximate relationship between the surface roughness values [19]

Type of Surface	RMS / CLA	Rt / Ra
Turned	1.1	4-5
Ground	1.2	7-14
Lapped	1.4	7-14
Preferential	1.25	8

Skewness expresses the distribution of roughness heights and is a quantitative measure of the fullness of the surface. The Abbott curve shows the load bearing area available when cuts are taken at various levels from the top of the profile.

R_z is the average height of profile; roughness measurement standard (ISO 5436-1, type C,D) $0{,}1 < R_z < 20$ μm [1].

R_k is the parameters of the material ratio curve; roughness measurement standard (ISO 5436-1, Type D) [1]. Core roughness depth (R_k) is the area on the surface with the extremes filtered out. It measures how even the surface is by showing the percentage of the area on the surface between "hi's" and "lo's" [1] $0.1<R_z<20$μm.

R_{max} represents the largest peak to valley height in any of the 5 sampling lengths.

Convenient units of measurement are the micrometer (mm) or nanometer (nm) and the microinch (min).

$$1\mu in = 0.025\ \mu m \quad = 25nm = 250\ A^{\circ} \tag{3.8}$$

$$1\mu m = 40\ \mu in \tag{3.9}$$

Most common surface roughness measuring instrument is based on the principle of the record player. An arm with a reference rest is drawn across the surface, while a stylus follows the finer surface details. The surface profile can be recorded as in the figure 3.20. and various roughness characteristics computed. Portable instruments used in the plant give readout of R_q directly.

3.7. Hardness Test

The hardness tests were done in KOSGEB-IMES in İstanbul. The specimens which used for surface roughness was also used for hardness determination. Brinell method was selected to measure the hardness values. The Brinell hardness test method consists of indenting the test material with a tungsten carbide ball of either 1, 2.5, 5 or 10 mm diameter by applying a test force of between 1 and 3000 kgf. The full load is normally applied for 10 to 15 seconds in the case of iron and steel and for at least 30 seconds in the case of other metals.

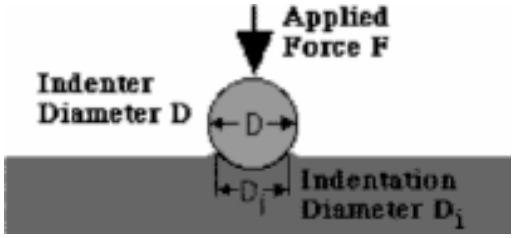

Figure 3.20. Brinell Test

The diameter of the indentation left in the test material is measured. The Brinell harness number (BHN) is calculated by dividing the load applied by the surface area of the indentations below formula.

$$BHN = \frac{F}{\frac{\pi}{2} D\left(D - \sqrt{D^2 - D_i^2}\right)} \tag{3.10}$$

The diameter of the impression is the average of two readings at right angles and the use of a Brinell hardness number table can simplify the determination of the Brinell

hardness. A well structured Brinell hardness number reveals the test conditions, for example "75 HBW 10/500/30" which means that a Brinell Hardness of 75 was obtained using a 10 mm diameter tungsten carbide ball with a 500 kgf test force for a period of 30 seconds. Compared to the other hardness test methods, the Brinell ball makes the deepest and widest indentation, so the test averages the hardness over a wider amount of material, which will more accurately account for multiple grain structures and any irregularities in the uniformity of the material. This method is the best for achieving the bulk or macro-hardness of a material, particularly those materials with heterogeneous structures.

In our experiment pressing force was 62.5 kg and the diameter of the ball was 2.5 mm. The ball was pressed on the specimen for 15 seconds. The Brinell hardness values were determined from the center and two sides of the specimens. 8 measurements were measured from the middle axis, right side and the left side of the specimens. The parts were divided into 8 zones and measurements were done. It means from one specimen, 24 hardness measurements were taken. Zone 1 means the top side and the zone 8 means down side of the specimens.

3.8. Tensile Testing

The tensile test is the most widely used test to determine the mechanical properties of materials. In this test, a piece of material is pulled until it fractures. Strain and stress graphics were drawn by the tensile testing machine. From this curve, the elastic modulus and yield strength are determined. The highest load in the tensile test gives the tensile or ultimate strength. After fracture, the final length and cross-sectional area of the specimen are used to calculate the percent elongation and percent reduction of area, respectively. These quantities indicate the ductility of the material. By using the instantaneous length and cross-sectional area, the true stress and true plastic strain are calculated from the load and elongation. Thus, from one test a large amount of information can be obtained about the mechanical properties of a material.

Tensile testing of the specimens was done in KOSGEB/IMES- Dudullu, İstanbul. Specimens were machined to a standard size for the tensile testing according to the ASTM E8 standard [34]. The standard tensile test specimen drawing can be seen in the Figure

3.22. The tensile test machine brand name was DARTEC RF-91146 Universal Tensile & Press Test Machine, 1200 kN capacity.

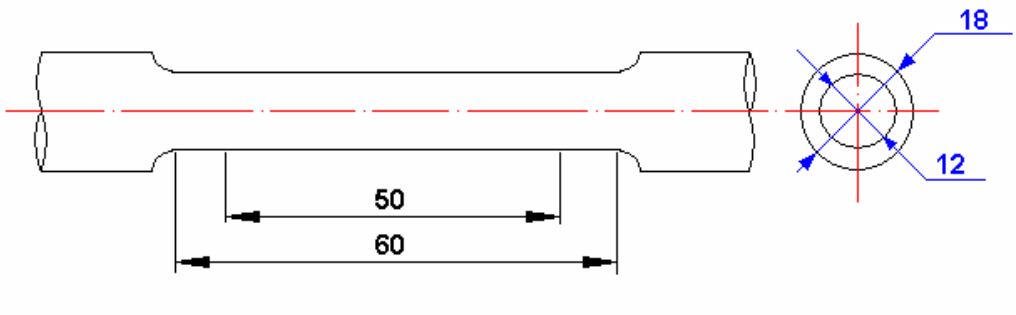

Figure 3.21. Drawing of tensile test specimen

3.8.1. Experimental Procedure

- Each specimen was machined according to the ASTM E8. It is necessary to thread the two heads which diameter is 18 mm. Because the tensile test holder was threaded. After threading, for each specimen, width w_0 and thickness t_0 values were written to the tensile test computer.

- On the straight section of the specimen two distinct pair of lines was drawn, which length was called as L_0. This will be the gage length, L_0. The gage length was measured as in Figure 3.23

- The testing machine has already been set-up and calibrated by the lab assistant.

- The specimen was screwed to the bottom grip and later it was screwed to the upper grip. While screwing the all threads weren't screwed in order to prevent tension. Approximately 80% of the threads were screwed to the grips for both upper and bottom sides.

Figure 3.22. Marking and measuring of the initial length (L_0) of the tensile test specimen

- After all controls are finished, the start button was pressed. Tensile test machine firstly eliminates the space between machine heads by giving preload.

- Machine started to stretch the specimen. After a while a cracking noise was heard and the specimen cracked. After the specimen was broken the heads were separated fast and the two components of the cracked specimen were taken out of the grips.

- The two parts of the specimen was put on the table. The final diameter (d_f) was measured using calipers and noted. The final diameter was the minimum diameter which occurred at the neck.

- The two parts of the specimen was joined and the distance between the two lines were measured. This value was noted as final length (L_f). This value is used to calculate the elongation characteristic of each specimen.

- The fractured surfaces were covered with a handkerchief and kept for the SEM photographs.

3.8.2. Analysis of Data

- A table was made which included the original and final dimensions.
- Stress strain curves were prepared and evaluated.
- For each point, the strain and stress (engineering values) values were calculated.
- The calculated values as load, elongation, stress and strain were added to the tensile test table.
- Using the load-extension curves which were drawn during tension test, tensile strength and yield strength values were calculated.
- Using the measurements of the specimen dimensions before and after the test, the percent reduction in area and the percent elongation values were calculated.
- Finally the specimen name, the elastic modulus, the yield strengths, the tensile strengths, the percent elongations and the percent reduction in areas were added to the table.

3.9. Microstructural Examination

Six different photographs of the 12 different specimens were taken under magnifications of 50X, 100X and 500X as etched and unetched conditions. Totally 144 microstructure photographs were taken. The parts are taken from the top and the bottom end of the 9 bismuth added specimens. So, effect bismuth and pressure could be understood easier. Photograph of the pure ZA-27 specimens were taken from the middle point of the specimens. Before taking photographs it is necessary to prepare metallographic parts according to a standard.

Figure 3.23. View of the Olympus microscope used for microstructural observation of the specimens

In this experiment ASTM E-3 standard was used to prepare the parts. The procedure is follows:

3.9.1. Cutting and Grinding

Cutting: While taking the sample from the part, it was selected at an admissible dimension. The dimension of the sample wasn't very small or big. Diameter was 25 mm and the height was between 5-10 mm. In normal conditions, while taking a sample from the part, it is necessary to use water cooled cutting device in order not to heat and deform the sample.

Rough Sanding: This operation is used to eliminate burned or hardened surface and to smooth the surface of the sample. For this reason emery between 60 and 120 grid was

used. In this operation cutting fluid could also be used to eliminate the structural deformations because of friction.

Putting in Bakelite: When working with small samples, and edges are important, the samples are dipped into bakelite. Using this bakelite, samples are easily handled. In our operations, our samples were big enough and so bakelite mount was not used.

Fine Sanding: This type of sanding was applied before polishing of the sample. The sample was sanded starting from low grids to high grids. Before starting every sanding operation, the scratches and lines done by previous sandpaper, should be eliminated. This elimination was done by turning the sample between 45-90˚. Wet Si-C emery was used to do that operation.

Following should be considered while elimination of scratches:

- The scratches which remained from previous work should start to transform to the new lines which made by new emery.
- The worn and old emery paper should be changed.
- While sanding, a pressure should be applied to the sample.
- The disc sanding instruments are suitable to do this work.
- Recommended emery papers for fine sanding are below:
- 180 Grid, 280 Grid, 400 Grid, 600 Grid.
- Instead of 280, 240 or 320 grids should be selected for some samples.
- Before starting the polishing, hands and samples should be washed to clean the wastes which remained from previous work.

Polishing: This operation is done in two steps as mid and final polishing. Mid polishing was done using disk polishing apparatus of 20 cm diameter. This tool turns at 550 rpm. Alumina suspension of 6-15 microns and polishing broadcloth was used for this work. However, for some metals, diamond polishing paste should be used.

For faster operation or, if the edges are important, 6 μm diamond paste is suggested.

Broadcloth should be nylon or preferably silk for above operation.

While applying above operation the pressure should be adjusted well.

Final polishing should be done using disks turning between 150 – 250 rpm. Suitable polishing broadclothes should be used to do that work. The polishing paste should be diamond paste (1 or 0.15 μm) or powder alumina (0.05 μm).While using dry powder alumina, distilled water should be poured using atomizer. After this work, if the alumina was used, the sample should be washed in flowing water. A piece of cotton should be used while washing the sample. After that, the sample should be shaken in alcohol and should be dried with dryer. If diamond was used, soapy water or alcohol should be used for separation.

After that, the sample should be washed in flowing water with rubbing, should be washed with alcohol and should be dried with dryer.

Note: In most of the materials, examination of precipitations and some similar formations, graphite structure counting and size in cast iron, are made in this stage before etching. 50X, 100X and 500X photographs were taken before and after etching.

3.9.2. Etching

Etch is achieved with suitable etcher for the material. After the etching time reached, the sample was washed in alcohol and dried. Aluminum etchants are summarized in Table 3.10.

Table 3.10. Definition of aluminum etchants

MACRO ETCHING		
Etcher	Operation	Used for
100 ml Distilled H_2O 10-20 gr NaOH	5-15 minutes, between 650-700˚C, In high concentration, in room temperature	All Al and Al Alloys
MICRO ETCHING		
2ml HF(48%), 3ml HCl (conc) 20 ml HNO_3 (Conc), 175 ml H_2O	Keep 10-30sec in the solution, wash with hot water and dry.	Pure Al, Al-Mn, Al-Si, Al-Mg, and Al-MgSi Alloys
100 ml Distilled H_2O 10-20 gr NaOH	5-10 minutes, between 60-70˚C, In high concentration, in room temperature	All Al and Al Alloys
25 ml HNO_3(conc), 75 ml H_2O	Dip 45-60 second into solution at 70˚C	Al-Cu, Al-Mg, Al-Zn Alloys

4. RESULTS AND DISCUSSION

4.1. Variation in Density

The results of the density determination are given in Table 4.1.

In the table below the measured values of the specimens are also seen.

Table 4.1. Calculated average density values of the specimens

Sp. No	Specimen Details	Weight in Air [m_a]	Weight in Air (On Setup) [m_{a2}]	Weight in Water (On Setup, In Water) [m_w]	Average ma_{av}	Average mw_{av}	Calculated Density d	Calculated Average Density d_{av}
1	% 0 Bi, 0 MPa	361,52	361,53	288,13	361,525	288,13	4,926	4,726
2	% 0 Bi, 0 MPa	356,95	356,95	279,65	356,95	279,65	4,618	
4	% 0 Bi, 0 MPa	61,33	61,335	48,1	61,3325	48,1	4,635	
5	% 0 Bi, 50 MPa	326,93	326,9	260,44	326,915	260,44	4,918	4,798
7	% 0 Bi, 50 MPa	72,377	72,38	56,905	72,3785	56,905	4,678	
8	% 0 Bi, 50 MPa	291,38	291,38	228,04	291,38	228,04	4,600	
9	% 0 Bi, 100 MPa	352,16	352,16	283,8	352,16	283,8	5,152	4,923
10	% 0 Bi, 100 MPa	337,77	337,79	269,175	337,78	269,175	4,924	
11	% 0 Bi, 100 MPa	70,54	70,55	55,5175	70,545	55,5175	4,694	
14	% 0.5 Bi, 0 MPa	365,63	365,65	290,27	365,64	290,27	4,851	4,845
15	% 0.5 Bi, 0 MPa	360,46	360,46	285,83	360,46	285,83	4,830	
16	% 0.5 Bi, 0 MPa	369,82	369,82	293,65	369,82	293,65	4,855	
18	% 0.5 Bi, 50 MPa	338,57	338,6	269,09	338,585	269,09	4,872	4,929
19	% 0.5 Bi, 50 MPa	57,72	57,725	46,05	57,7225	46,05	4,945	
21	% 0.5 Bi, 50 MPa	329,79	329,8	263,32	329,795	263,32	4,961	
22	% 0.5 Bi, 50 MPa	326,21	326,29	260,16	326,25	260,16	4,936	
23	% 0.5 Bi, 100 MPa	323,73	323,8	256,23	323,765	256,23	4,794	4,864
25	% 0.5 Bi, 100 MPa	313,13	313,17	249,5	313,15	249,5	4,920	
26	% 0.5 Bi, 100 MPa	315,75	315,79	250,17	315,77	250,17	4,814	
27	% 0.5 Bi, 100 MPa	74,045	74,04	58,8	74,0425	58,8	4,858	
28	% 1 Bi, 0 MPa	366,95	366,97	291,42	366,96	291,42	4,858	4,846
29	% 1 Bi, 0 MPa	365,99	366,02	291,01	366,005	291,01	4,880	
30	% 1 Bi, 0 MPa	373	373,02	296,92	373,01	296,92	4,902	
31	% 1 Bi, 0 MPa	363,9	363,92	289,47	363,91	289,47	4,889	
32	% 1 Bi, 0 MPa	73,22	73,23	57,65	73,225	57,65	4,701	
34	% 1 Bi, 50 MPa	327,25	327,26	261,09	327,255	261,09	4,946	4,911
35	% 1 Bi, 50 MPa	319,21	319,2	254,7	319,205	254,7	4,949	
37	% 1 Bi, 50 MPa	71,245	71,26	56,53	71,2525	56,53	4,840	
38	% 1 Bi, 100 MPa	315,99	316,02	251,53	316,005	251,53	4,901	4,939
40	% 1 Bi, 100 MPa	335,63	335,66	268,19	335,645	268,19	4,976	
41	% 1 Bi, 100 MPa	59,91	59,907	47,335	59,9085	47,335	4,765	
42	% 1.5 Bi, 0 MPa	358,29	358,29	284,65	358,29	284,65	4,865	4,851
43	% 1.5 Bi, 0 MPa	55,016	55,016	43,65	55,016	43,65	4,840	
45	% 1.5 Bi, 0 MPa	238,3	238,34	189,15	238,32	189,15	4,847	
46	% 1.5 Bi, 50 MPa	56,17	56,17	44,13	56,17	44,13	4,665	4,853
47	% 1.5 Bi, 50 MPa	310,4	310,45	246,82	310,425	246,82	4,881	
48	% 1.5 Bi, 50 MPa	327,58	327,61	261,21	327,595	261,21	4,935	
49	% 1.5 Bi, 50 MPa	55,035	55,035	43,43	55,035	43,43	4,742	
52	% 1.5 Bi, 100 MPa	316,73	316,78	252,33	316,755	252,33	4,917	4,874
53	% 1.5 Bi, 100 MPa	60,61	60,605	48,1	60,6075	48,1	4,846	
54	% 1.5 Bi, 100 MPa	297,9	297,89	236,58	297,895	236,58	4,858	
Red : Cancelled								

Firstly, the specimens were weighed in the air on the scale. This was m_{a1}, after that a second measurement was done on the set-up, in air. This was the m_{a2}. After that, if these two values were consistent, average of these values were calculated and written as mav. If these two values were not consistent, third or fourth measurements were done, until reaching a consistent value. After reaching a consistent value for each specimen in air and in water, density values were calculated for each specimen. After that, average of specimen densities were found and accepted as average density (d_{av}).

In the table below the density table of the 0% Bi specimens are listed.

Table 4.2. The density table of the specimens containing 0% Bi

Sp. No	Specimen Details	Weight in Air [m_a]	Weight in Air (On Setup) [m_{a2}]	Weight in Water (On Setup, In Water) [m_w]	Average ma_{av}	Average mw_{av}	Calculated Density d	Calculated Average Density d_{av}
1	% 0 Bi, 0 MPa	361,52	361,53	288,13	361,525	288,13	4,926	4,726
2	% 0 Bi, 0 MPa	356,95	356,95	279,65	356,95	279,65	4,618	
4	% 0 Bi, 0 MPa	61,33	61,335	48,1	61,3325	48,1	4,635	
5	% 0 Bi, 50 MPa	326,93	326,9	260,44	326,915	260,44	4,918	4,798
7	% 0 Bi, 50 MPa	72,377	72,38	56,905	72,3785	56,905	4,678	
8	% 0 Bi, 50 MPa	291,38	291,38	228,04	291,38	228,04	4,600	
9	% 0 Bi, 100 MPa	352,16	352,16	283,8	352,16	283,8	5,152	4,923
10	% 0 Bi, 100 MPa	337,77	337,79	269,175	337,78	269,175	4,924	
11	% 0 Bi, 100 MPa	70,54	70,55	55,5175	70,545	55,5175	4,694	
Red : Cancelled								

According to this table, the average density of the %0 Bi, not squeezed (0 MPa) was 4.726 gr/cm^3. With the increase of pressure, density value increases. That means the applying squeezing pressure has a beneficial effect on the density and removing porosity. According to M.S. Yong and A.J. Clegg [35], the pressure applied in squeeze casting promotes rapid solidification and a refined cell structure. An applied pressure of 60 MPa was sufficient to eliminate all traces of shrinkage and gas porosity within the casting. Metallographic examination of the castings revealed that the cell size reduced from 127 to 21µm when the applied pressure was increased from 0.1 to 60 MPa.

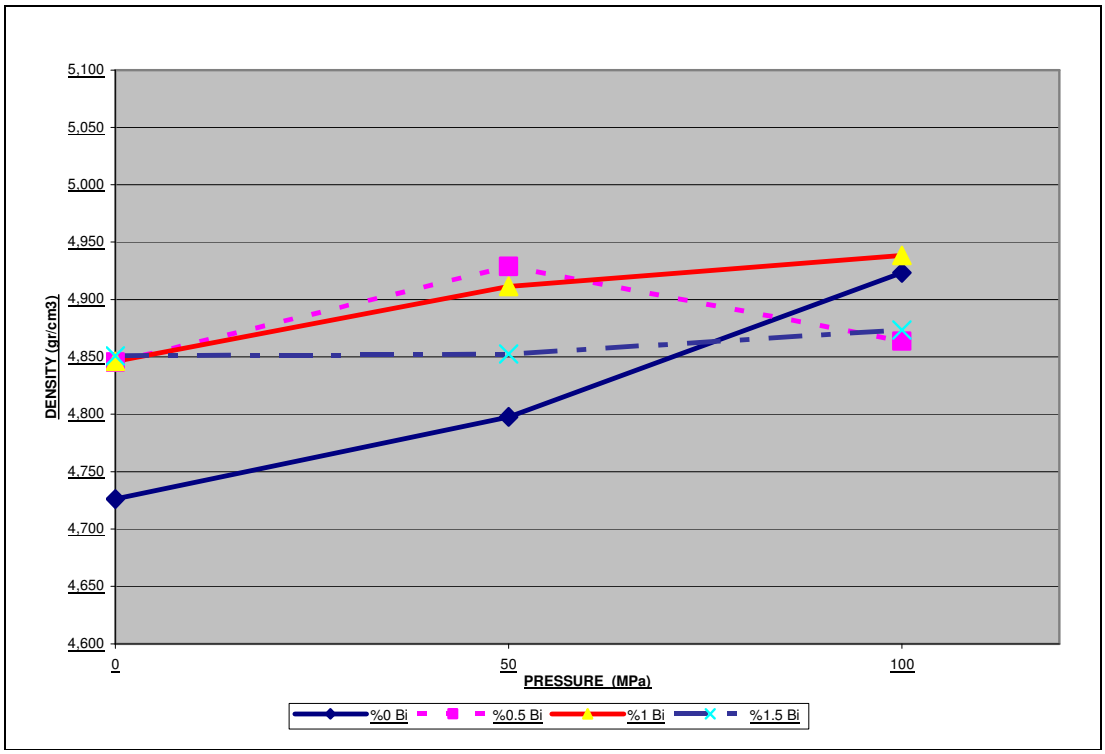

Figure 4.1. Average density vs squeeze casting pressure plot as a function of bismuth addition

In the Figure 4.1. on the vertical axis, increasing pressure values were written. On the vertical axis the calculated average density values can be seen. According to the graph, the densities of the specimens increase with the increasing pressure. As mentioned before, this is the result of squeezing pressure. Also, if we look at the figure we can see that, when the bismuth content was higher, the average density value was found higher almost for all pressure types.

This is in agreement with studies carried out by Akyuz [36] who investigated the mechanical properties and machinability of Al-Mg casting alloys. He found that the squeeze casting leads to an increase in the density of the Al-10%Mg alloy by 2.8% and 0.6% increase in the density of Al-5%Mg alloy.

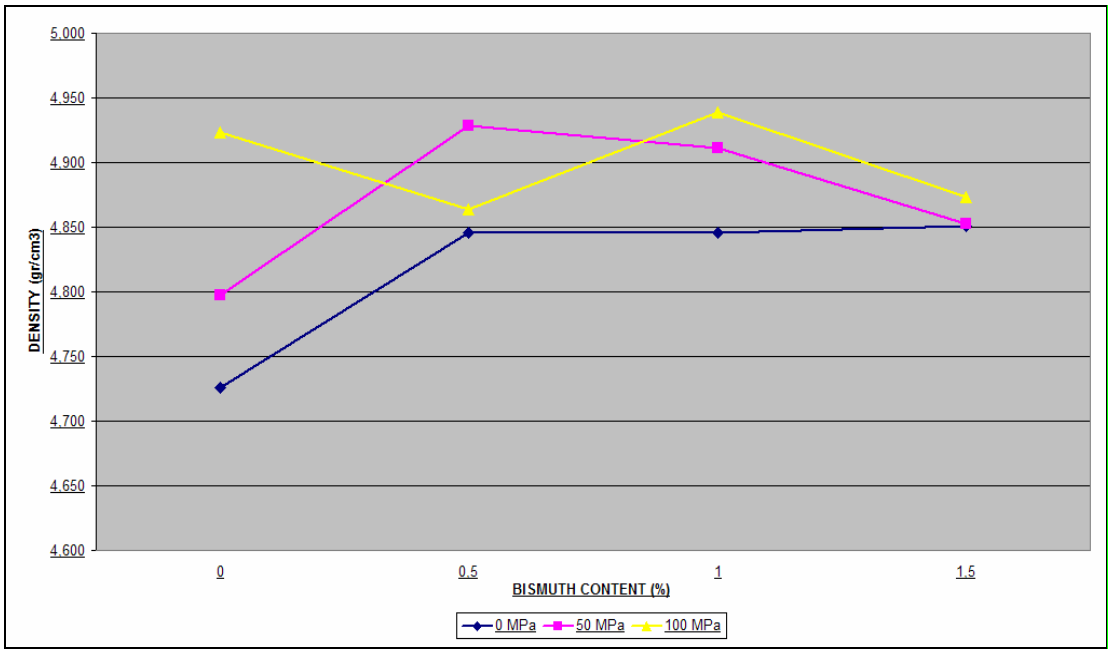

Figure 4.2. Average density vs bismuth concentration (%) plot as a function of squeeze casting pressure

In Figure 4.2. above, on horizontal axis, bismuth contents were written. On the vertical axis the calculated average density values were written. According to the graph, if we ignore the pressure effect, the density of the specimens increase with the increasing bismuth content. This result should be true because, bismuth's density is 2 times of the pure ZA-27.

4.2. Variation in Chip Length

In order to understand that the bismuth addition and squeezing had an effect on the machinability characteristic of the specimen, operations below were done. Specimens were taken from every type of bismuth addition and every type of squeezing pressure. One of the best and easy way to understand the machinability characteristics of a material, is applying turning operation on it. 12 types of specimens were taken and turning operation was applied. Firstly, a cleaning pass was done, after that the specimens were turned under three different rpm's. After that the chips were collected and their lengths were measured as below.

Table 4.3. Chip lengths of the specimens at three different cutting speeds

Average Chip Length	Content	υ (mm/min)	Chip Length Measurement Results																			
55,9	% 0.25 Bi, 0 MPa	14,49	86,0	37,0	37,0	59,0	70,0	60,0	42,0													
31,8		20,41	42,0	27,0	25,0	33,0																
34,8		40,82	39,0	20,0	33,0	47,0	35,0															
269,7	4) % 0 Bi, 0 MPa	14,49	487,0	173,0	149,0																	
227,8		20,41	253,0	178,0	248,0	232,0																
148,4		40,82	130,0	164,0	151,0	128,0	169,0															
156,1	7) % 0 Bi, 50 MPa	14,49	181,0	186,0	125,0	183,0	136,0	154,0	128,0													
156,0		20,41	250,0	108,0	143,0	144,0	133,0	140,0	218,0	112,0												
91,9		40,82	92,0	88,0	108,0	86,0	85,0	91,0	93,0													
207,0	11) % 0 Bi, 100 MPa	14,49	160,0	206,0	285,0	177,0																
216,8		20,41	219,0	193,0	216,0	239,0																
102,0		40,82	113,0	88,0	112,0	95,0																
3,7	13) % 0.5 Bi, 0 MPa	14,49	3,7	3,6	3,7	4,0	3,8	3,4	3,7													
3,3		20,41	2,7	3,0	4,2	3,5	3,4	3,0	3,3													
2,8		40,82	3,4	3,0	2,6	2,9	2,7	2,8	2,6	2,6												
16,3	19) % 0.5 Bi, 50 MPa	14,49	13,0	10,5	15,2	14,0	14,0	17,5	22,0	26,0	16,5	20,0	18,0	20,0	17,5	8,5	13,0	16,0	15,5	13,2	18,5	
7,8		20,41	5,8	7,6	7,5	8,7	10,6	7,9	5,9	7,0	8,0	9,7	6,0	9,0	6,2	6,2	8,5	6,5	11,5			
6,0		40,82	6,0	5,9	7,6	5,9	6,6	5,3	5,8	5,1	5,9	8,0	5,4	5,8	6,2	5,3	4,9	4,8	6,8			
27,3	27) % 0.5 Bi, 100 MPa	14,49	17,0	36,0	15,0	23,0	17,0	41,0	24,0	32,0	28,0	35,5	21,0	20,5	37,0	32,5	27,5	32,0	30,5	29,5	24,0	23,0
5,6		20,41	5,5	5,2	5,7	6,0	7,0	5,6	5,5	6,3	5,5	5,9	6,0	5,9	5,2	5,0	5,0	4,9	5,9	5,4	4,7	6,0
3,9		40,82	4,0	3,6	3,3	5,5	4,0	4,5	3,2	3,6	5,2	5,0	3,6	3,0	4,8	2,5	3,8	3,7	3,6	3,2		
3,9	32) % 1 Bi, 0 MPa	14,49	4,0	4,0	4,2	3,5	3,7	4,3	3,3	3,8												
2,9		20,41	3,0	2,5	3,0	3,1	2,9	2,9	2,8	3,0												
2,4		40,82	3,0	2,6	3,0	3,0	2,4	2,4	2,0	2,0	2,0	1,7	2,5	2,6								
4,7	37) % 1 Bi, 50 MPa	14,49	4,8	3,8	4,7	5,0	5,2	5,0	4,2	4,5	5,0											
4,5		20,41	3,6	3,5	5,0	5,0	4,5	4,5	4,2	5,0	5,2											
2,7		40,82	2,0	2,2	3,1	3,0	2,8	2,5	3,2													
10,4	41) % 1 Bi, 100 MPa	14,49	10,9	10,5	8,0	7,5	12,0	12,2	12,2	12,7	7,3	9,3	9,3	13,0	8,8	8,3	9,5	12,8	13,0			
5,3		20,41	4,0	4,2	4,4	4,2	5,9	4,9	4,4	5,6	7,5	7,2	7,0	5,5	4,0	6,5	4,8	4,5	5,3	4,6		
3,0		40,82	3,0	2,9	3,0	3,0	3,8	2,9	3,7	2,8	3,7	2,2	2,9	2,4	2,5	2,7	2,4	3,6				
2,3	43) % 1.5 Bi, 0 MPa	14,49	1,9	2,4	2,8	2,0	2,2	2,4	2,5													
2,6		20,41	2,3	2,3	2,8	3,5	2,6	2,8	2,6	2,0	2,4	2,3										
1,8		40,82	1,9	1,8	1,7	1,4	1,7	1,8	2,0	1,6	2,0											
6,5	46) % 1.5 Bi, 50 MPa	14,49	5,8	6,6	6,0	5,8	7,3	8,3	5,7	5,9	6,3	6,0	6,0	7,7	7,2	7,5	6,6	6,3	6,0			
3,2		20,41	3,7	3,3	2,6	2,9	3,3	2,6	4,0	3,7	2,5											
1,8		40,82	2,0	1,7	1,9	1,8	2,0	1,6														
5,6	49) % 1.5 Bi, 50 MPa	14,49	6,2	4,4	5,4	5,6	5,0	7,0	7,0	4,6	4,7	6,0										
2,2		20,41	2,2	2,0	2,3	1,9	2,5	2,2														
1,6		40,82	1,8	1,6	1,6	1,6	1,5	1,4														
3,0	53) % 1.5 Bi, 100 MPa	14,49	2,7	2,8	3,2	3,3	3,0	3,0														
1,8		20,41	2,2	1,2	1,4	1,4	1,9	2,6														
2,3		40,82	3,0	2,2	2,3	2,2	2,4	2,5	2,2	1,5	2,2											

For shorter chips 20 measurements were enough, however for longer chips three measurements were enough. 13 parts were evaluated from 12 different types. These parts

were cast under three different pressures and four different bismuth contents. So, we got 12 different types of parts.

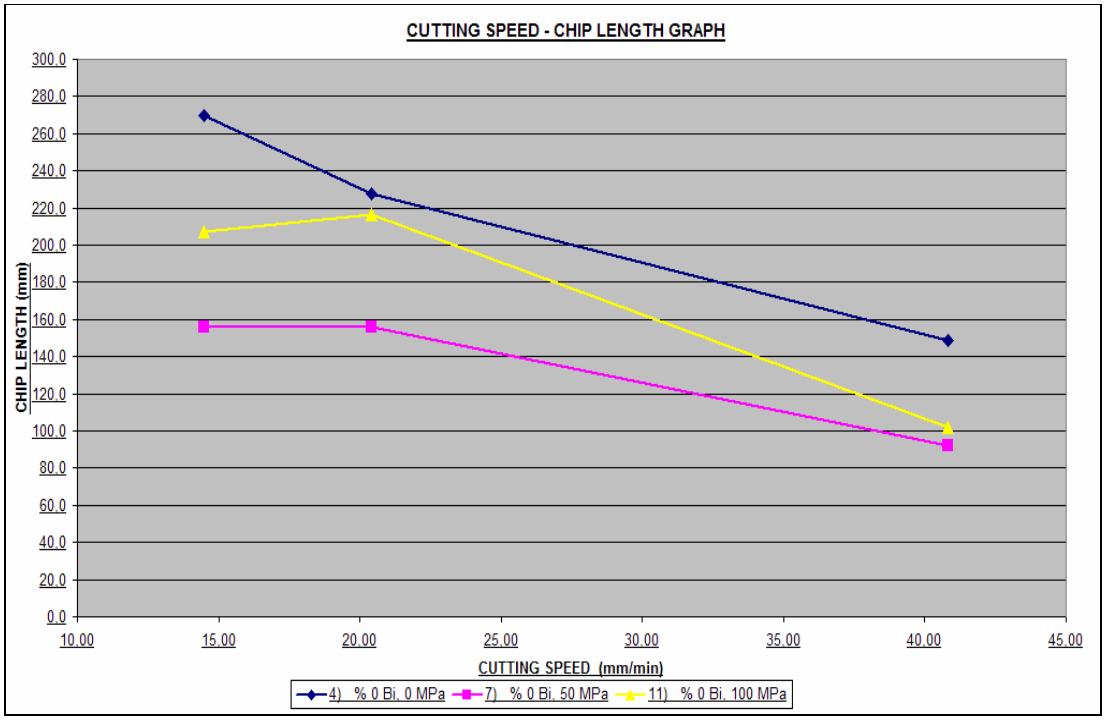

Figure 4.3. Chip length results for three different cutting speeds for 0% Bi Content

In the above graph, calculated chip lengths of the specimens which were measured at three different speeds were shown. All of the specimens in the graph contained 0% Bi. If we look at the results which were cast under 0 MPa, we see that chip lengths were 269,7 mm at 14,49 mm/min, 227,8 mm at 20,41 mm/min and 148,4 mm at 40,82 mm/min cutting speeds. Other specimen's chip lengths were generally decreased with increasing cutting speed. According to that graph, it is obvious that as the cutting speed increases, chip length decreases. So, we can say that if we increase cutting speed to an allowable value we increase the machinability for ZA-27 alloys.

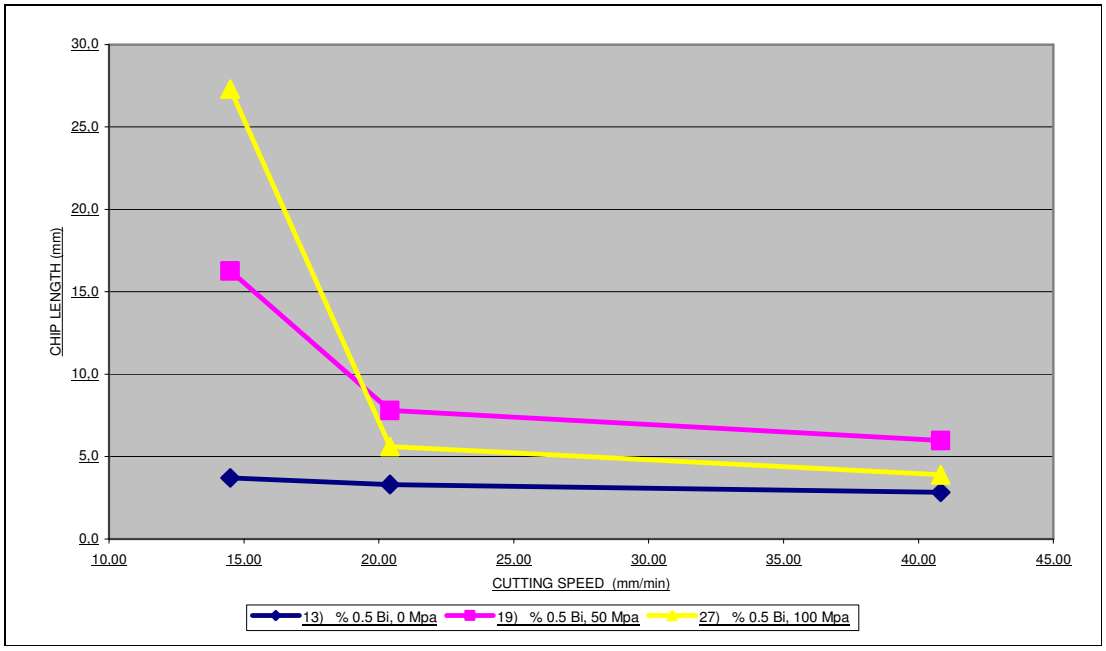

Figure 4.4. Chip length vs cutting speed plot as a function of squeezing pressure of 0.5% Bi specimens

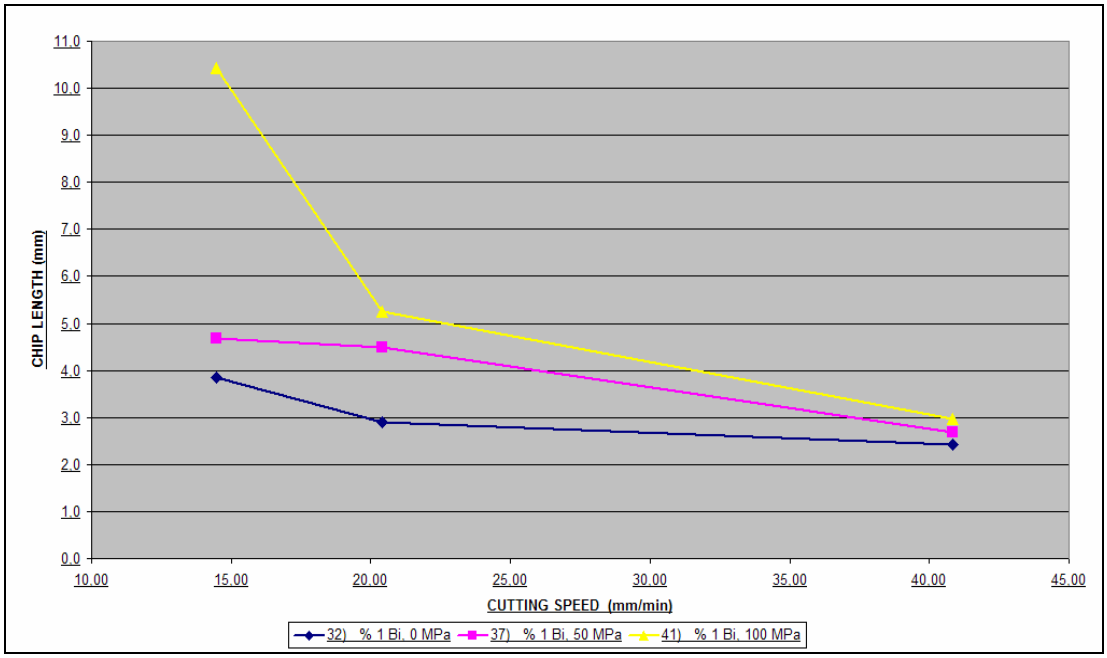

Figure 4.5. Chip length vs cutting speed plot as a function of pressure in 1% Bi specimens

According to the Figure 4.4. for 0,5% Bi content, chip length decreases considerably with increasing cutting speed. For lower speeds like 14 mm/min, chip lengths were long for all specimens. As the cutting speed was increased to 20,5 mm/min, chip lengths were decreased from 27,3 mm to 5,6 mm for specimen no 27. Increasing cutting speed from 20,41 to 40,82 mm/min didn't have too much effect on the chip length. So, we can conclude that for 0,5% Bi specimens the ideal cutting speed is around 20,5 mm/min.

In the Figure 4.5 chip length results for 1% Bi specimens are seen. According to this graph, chip lengths decreased with increasing cutting speed as before.

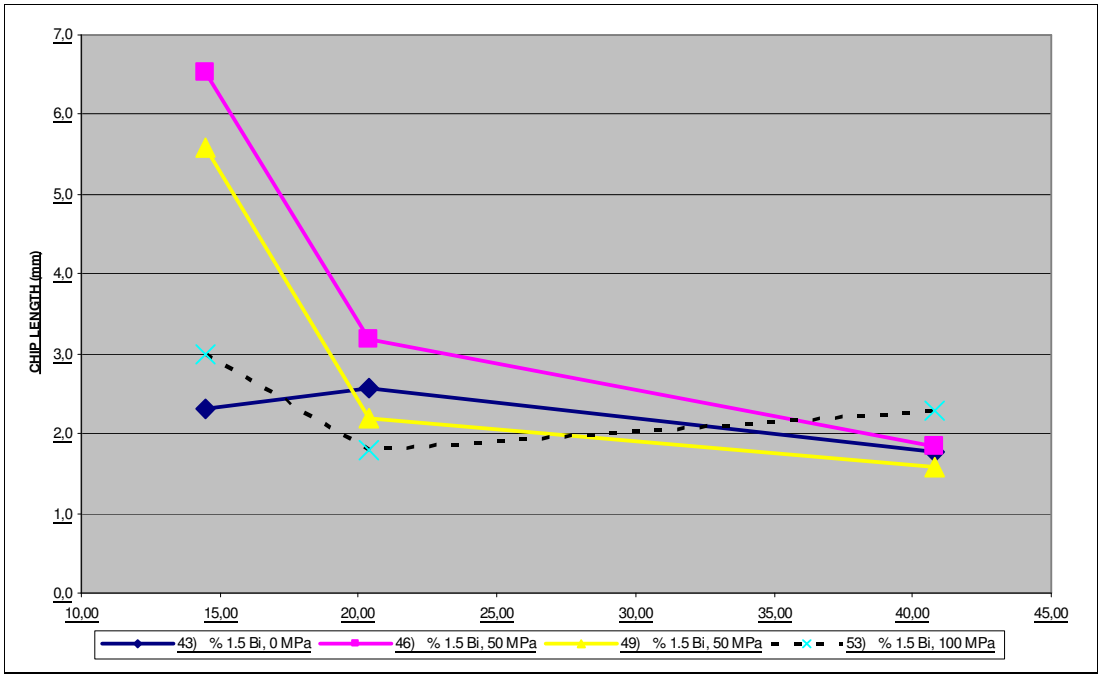

Figure 4.6. Chip length vs cutting speed plot as a function of squeezing pressure in 1.5% Bi specimens

According to the Figure 4.6. for 1,5%Bi content specimens chip lengths generally decreased with increasing cutting speed as observed before.

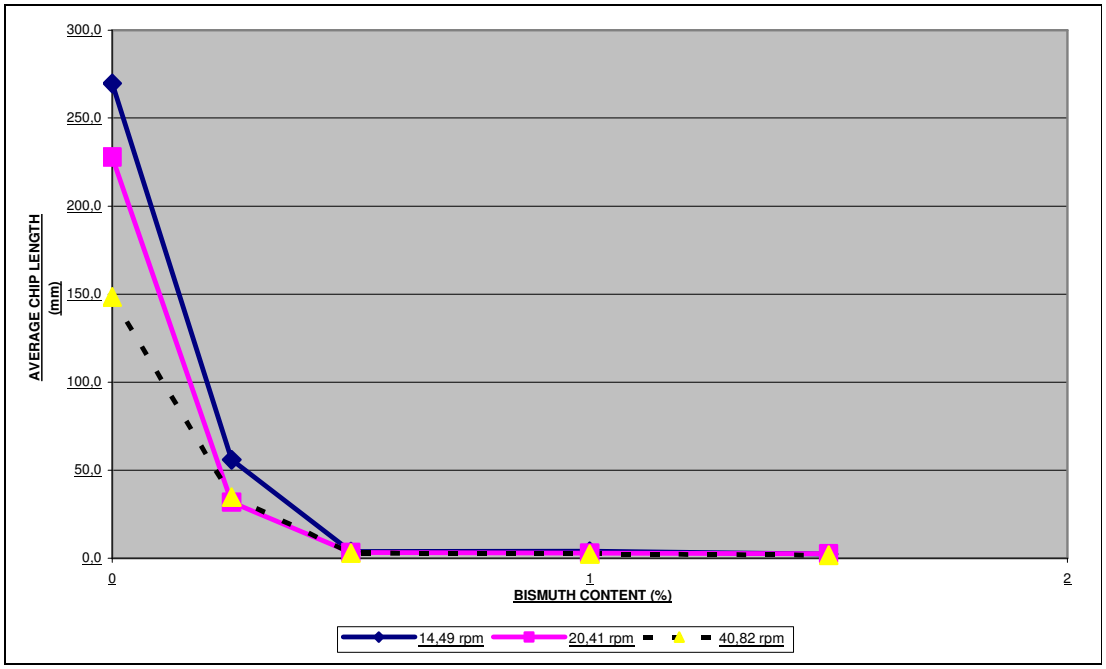

Figure 4.7. Chip length vs bismuth content (%) plot as a function of cutting speed in unsqueezed ZA-27

We learned that with increasing bismuth content chip length decreases and machinability increases. However, as seen in the above graph, one of the main factors affecting the machinability was the bismuth content. For pure ZA-27 alloy the average chip length for unsqueezed ZA-27, changes between 148 and 269 mm. When a small amount of bismuth (0.25%) added, the chip lengths were dropped to 34 -56 mm levels. That means adding bismuth is beneficial on the machinability characteristics.

Increasing bismuth a bit more, like 1%Bi, decreased chip length more but, these lengths were too small and didn't useful in terms of increasing machinability. As the bismuth content raised, chips become smaller than elemental chips or even in the powder form that was certainly not desired. Because when the powder chips form machining gets harder. The chips were stuck to the cutting tool and the turning operation became harder.

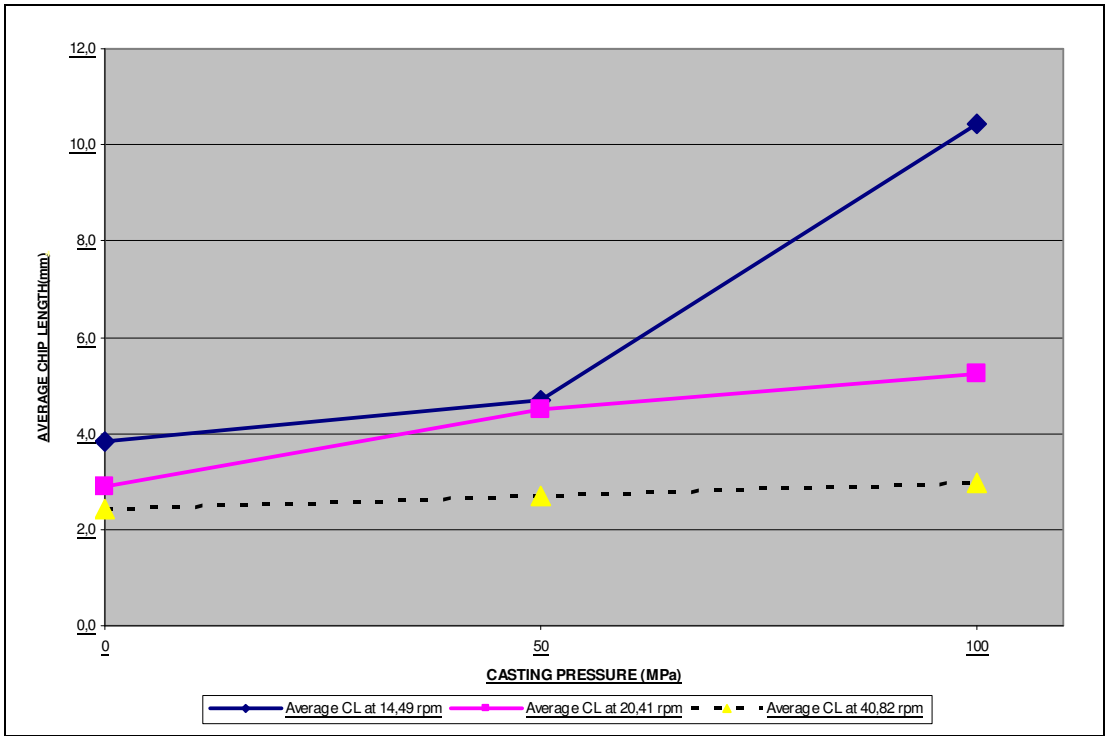

Figure 4.8. Chip length vs casting pressure plot as a function of cutting speed of 1% Bi specimens

In the above plot, the average chip length values of the 1% Bi specimens are investigated. All these parts were machined from different bismuth contents. The two parameters were the cutting speed and the casting pressure. So, drawing a graph which shows average chip lengths at different casting pressures was possible. According to this graph; as the casting pressure was increased the chip length was also increased.

However M.A.Savas found that addition of bismuth into zinc and following this, squeeze casting were most beneficial in terms of chip disposal, i.e. reduction in chip length during turning [3]. Also Erturan, is in the same opinion with Savas [2].

4.3. Variation in Surface Roughness

The results of the surface roughness of specimens can be seen in the table below.

Table 4.4. Surface roughness results of the specimens

SPECIMEN NUMBER	SURFACE ROUGHNESS RESULTS (µ)				
	R_a	R_z	R_{max}	R_q	R_t
16	**1,45 – 1,57**	**7,5 – 8,2**	**9,2 – 10,2**	**1,90 – 1,97**	**11,8 – 12,2**
48	**1,27 – 1,30**	**8,6 – 9,2**	**10,7 – 12,1**	**1,67 – 1,77**	**13,0 – 13,3**
29	**1,60 – 1,67**	**8,7 – 10,9**	**11,8 – 14,1**	**2,02 – 2,07**	**12,7 – 13,9**
2	**1,02 – 1,10**	**7,0 – 8,2**	**8,8 – 9,0**	**1,35 – 1,37**	**9,5 – 9,7**
5	**1,30 – 1,38**	**9,8**	**10,5 – 10,9**	**1,80 – 1,87**	**10,9 – 11,0**
10	**1,92 – 2,2**	**11,7 – 12,3**	**15,5 – 16,2**	**2,75 – 2,79**	**14,9 – 15,3**
26	**2,07 – 2,40**	**11,6 – 13,3**	**15,0 – 16,4**	**3,1 – 3,3**	**16,5 – 19,7**
34	**1,65 – 1,80**	**10,1 – 11,7**	**13,1 – 15,1**	**2,47 – 2,7**	**14,2 – 15,5**
38	**1,5 – 1,77**	**9,9 – 12,9**	**11,3 – 13,3**	**1,95 – 2,1**	**13,8 – 16,0**
21	**1,75 – 1,82**	**10,7 – 11,8**	**12,7 – 13,8**	**2,2 – 2,27**	**13,5 – 16,7**
45	**1,32 – 1,5**	**7,4 – 8,2**	**8,4 – 9,6**	**1,55 – 1,62**	**8,9 – 9,8**
54	**1,57 – 1,62**	**7,9 – 9,5**	**10,8 – 11,3**	**1,9 – 1,92**	**11,8 – 12,7**

SPECIMEN NUMBER	*SURFACE ROUGHNESS RESULTS (μ)*																								
	Ra		$R_{a_{avg}}$	B_{iarg}%	R_{aGA}	Rz		$R_{z_{avg}}$	B_{iarg}%	R_{zGA}	Rmax		$R_{max_{avg}}$	B_{iarg}%	R_{maxGA}	Rq		$R_{q_{avg}}$	B_{iarg}%	R_{qGA}	Rt		$R_{t_{avg}}$	B_{iarg}%	R_{tGA}
2) % 0 Bi, 0 MPa	1,02	1,1	1,06	1,487	1,606	7	8,2	7,6	9,800	9,871	8,8	9	8,9	11,817	12,075	1,35	1,37	1,36	1,988	2,100	9,5	9,7	9,6	11,883	13,221
5) % 0 Bi, 50 MPa	1,3	1,38	1,34			9,8	9,8	9,8			10,5	10,9	10,7			1,8	1,87	1,835			10,9	11	10,95		
10) % 0 Bi, 100 MPa	1,92	2,2	2,06			11,7	12,3	12			15,5	16,2	15,85			2,75	2,79	2,77			14,9	15,3	15,1		
16) % 0.5 Bi, 0 MPa	1,45	1,57	1,51	1,843		7,5	8,2	7,85	10,517		9,2	10,2	9,7	12,883		1,9	1,97	1,935	2,457		11,8	12,2	12	15,067	
21) % 0.5 Bi, 50 MPa	1,75	1,82	1,785			10,7	11,8	11,25			12,7	13,8	13,25			2,2	2,27	2,235			13,5	16,7	15,1		
26) % 0.5 Bi, 100 MPa	2,07	2,4	2,235			11,6	13,3	12,45			15	16,4	15,7			3,1	3,3	3,2			16,5	19,7	18,1		
29) % 1 Bi, 0 MPa	1,6	1,67	1,635	1,665		8,7	10,9	9,8	10,700		11,8	14,1	12,95	13,117		2,02	2,07	2,045	2,218		12,7	13,9	13,3	14,350	
34) % 1 Bi, 50 MPa	1,65	1,8	1,725			10,1	11,7	10,9			13,1	15,1	14,1			2,47	2,7	2,585			14,2	15,5	14,85		
38) % 1 Bi, 100 MPa	1,5	1,77	1,635			9,9	12,9	11,4			11,3	13,3	12,3			1,95	2,1	2,025			13,8	16	14,9		
45) % 1.5 Bi, 0 MPa	1,32	1,5	1,41	1,430		7,4	8,2	7,8	8,467		8,4	9,6	9	10,483		1,55	1,62	1,585	1,738		8,9	9,8	9,35	11,583	
48) % 1.5 Bi, 50 MPa	1,27	1,3	1,285			8,6	9,2	8,9			10,7	12,1	11,4			1,67	1,77	1,72			13	13,3	13,15		
54) % 1.5 Bi, 100 MPa	1,57	1,62	1,595			7,9	9,5	8,7			10,8	11,3	11,05			1,9	1,92	1,91			11,8	12,7	12,25		
0 MPa General Average	1,348	1,460	1,404	1,606		7,650	8,875	8,263	9,871		9,550	10,725	10,138	12,075		1,705	1,758	1,731	2,100		10,725	11,400	11,063	13,221	
50 MPa General Average	1,493	1,575	1,534			9,800	10,625	10,213			11,750	12,975	12,363			2,035	2,153	2,094			12,900	14,125	13,513		
100 MPa General Average	1,765	1,998	1,881			10,275	12,000	11,138			13,150	14,300	13,725			2,425	2,528	2,476			14,250	15,925	15,088		

Table 4.5. Surface roughness results of the all specimens

The effect of cutting speed on surface roughness was investigated using a constant cutting speed (approximately 47 mm/min).

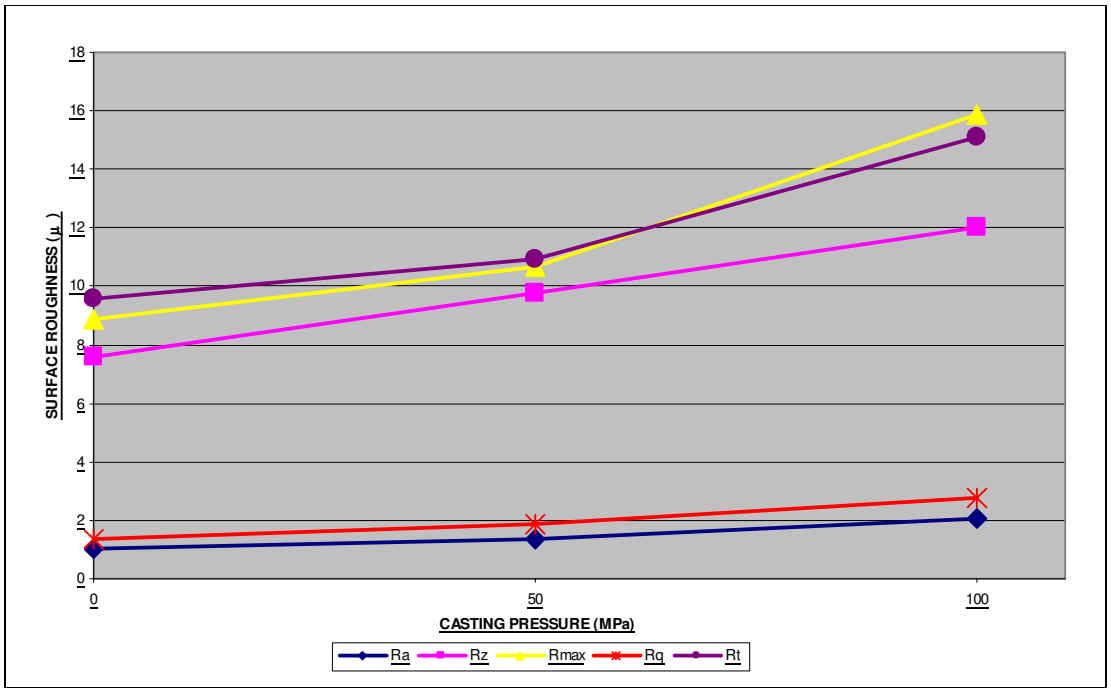

Figure 4.9. Surface roughness vs casting pressure plot under different casting pressures for 0% Bi

According to the above graph, for 0% Bi content the surface roughness results for all types increase considerably with increasing casting pressure. For 0 MPa, the surface roughness value increased to 1,93 µ for 0.5Bi%. This value was 1,36 µ for pure ZA-27. Adding small amounts of bismuth increased roughness 42% for 0.5Bi% specimen with respect to 0Bi% specimen. The average height of profile (Rz) value for 0MPa is 7,85. For 50 MPa this value increased suddenly to 11,25. And for 100MPa, Rz value is 12,45. That means, applying small amount of pressure increased the surface roughness suddenly about 43%. Increasing pressure more results in less increase in surface roughness. The resultant increase in the surface roughness of the 100 MPa specimen was about 11% with respect to 50 MPa specimen.

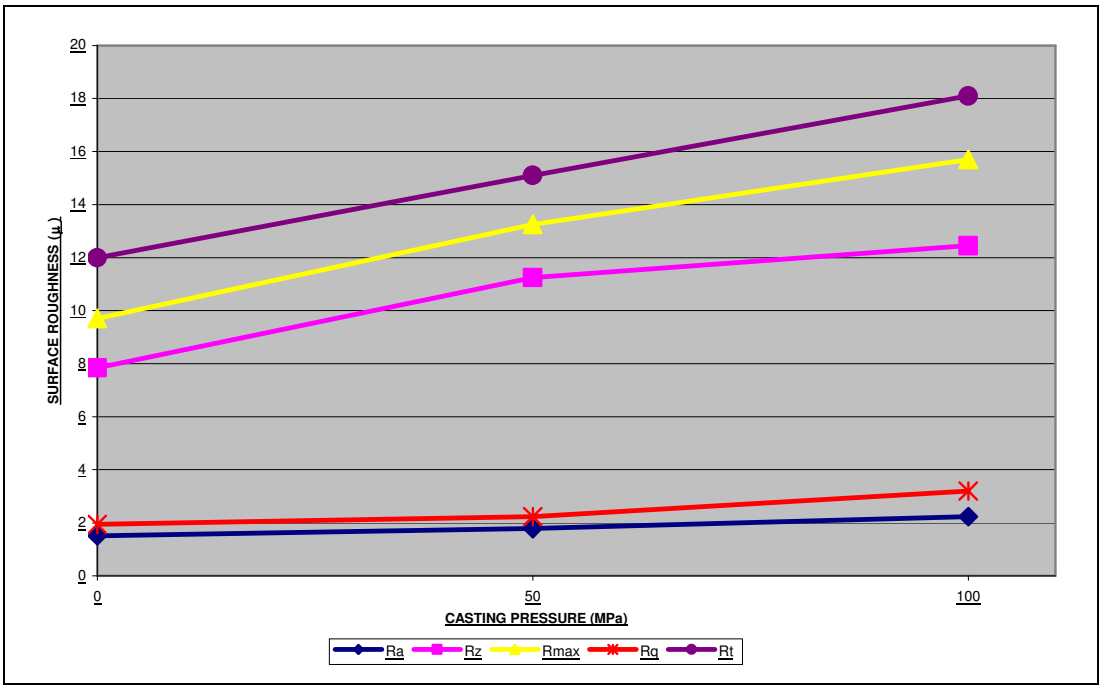

Figure 4.10. Surface roughness vs casting pressure plot for 0.5% Bi

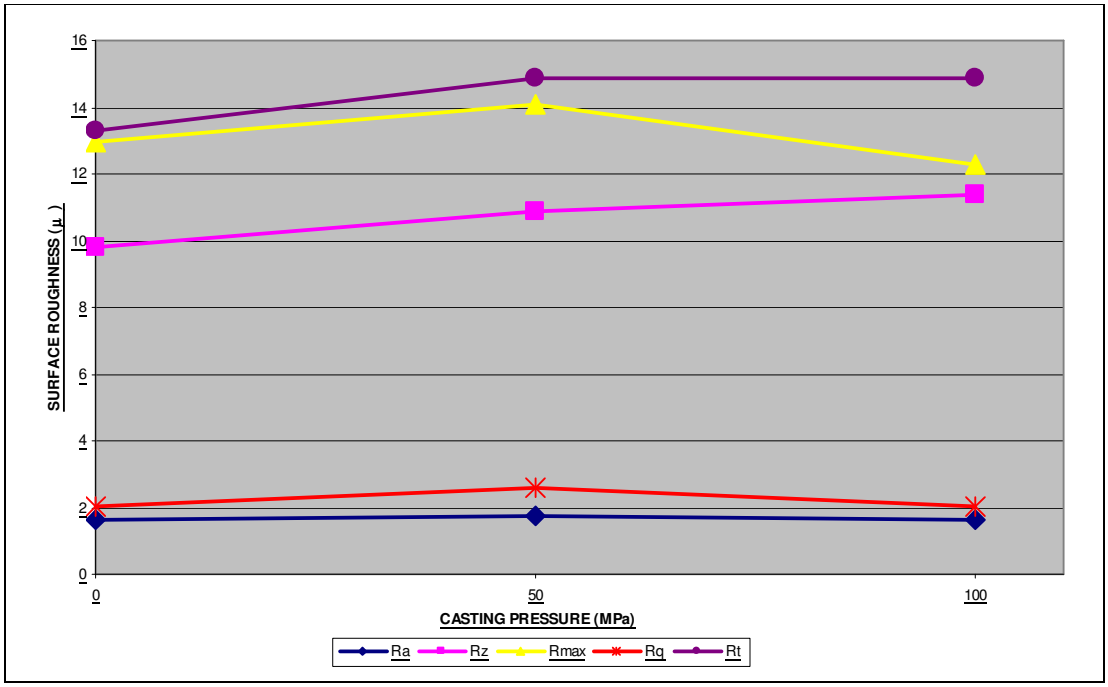

Figure 4.11. Surface roughness vs casting pressure plot for 1% Bi

If we increase the bismuth content from 0Bi% to 0,5Bi% the result don't change. According to Figure 4.10., for 0% Bi content, surface roughness results for all types

increase considerably with increasing casting pressure. Note that the cutting speed was constant and approximately 47 mm/min (600 rpm lathe speed) for all specimens. For example, the Rq value of the specimens are 1,36 – 1,83 - 2,77 regarding the three type of casting pressures 0-50 and 100 MPa, respectively. As the casting pressure increased, surface roughness values also increased in a constant trend.

If we look at Figure 4.11, we can see that average height of profile increases with increasing pressure. For example; these values were 9,8 - 10,9 - 11,4 µm for the pressures 0-50-100 MPa respectively. But contrary to that, Ra value firstly increases at 50MPa, later decreases a bit at 100 MPa. This result may be because of the wrong measuring the 100 MPa value. These values are so small and misreadings may occur while measuring the surface roughness values.

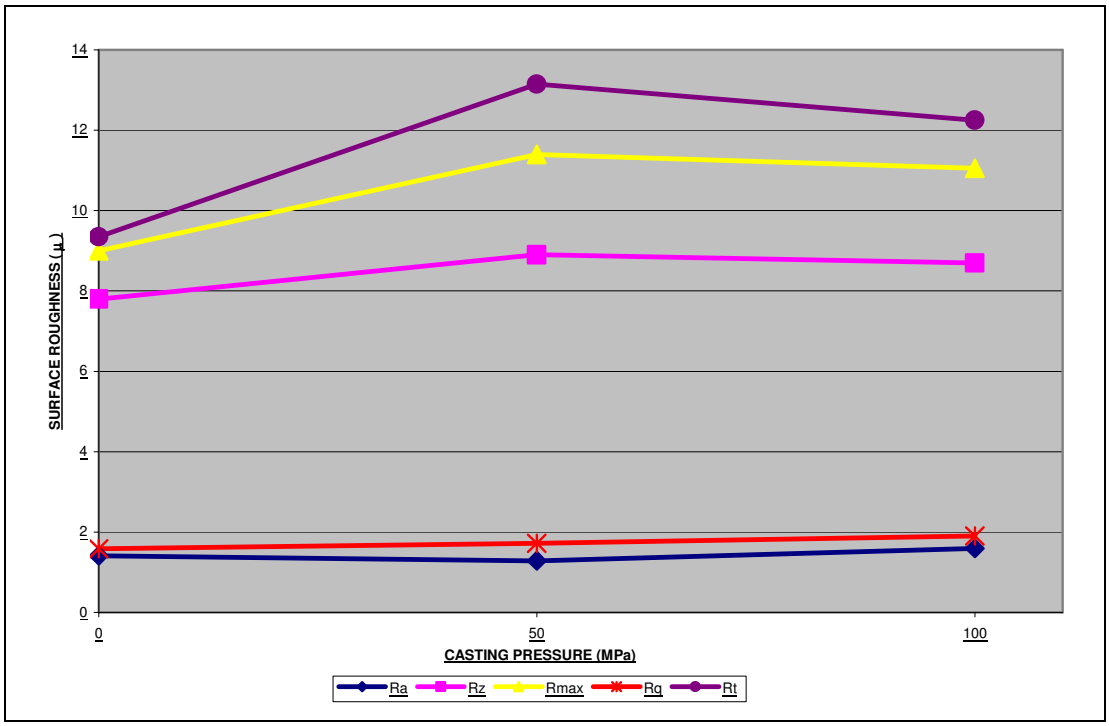

Figure 4.12. Surface roughness vs casting pressure plot for 1.5% Bi

In Figure 4.12, the average height difference between 5 highest peaks and 5 deepest valleys (R_t) of the 50 MPa value (13,15µ) is higher the 50 MPa value (8,9). The 50 MPa value is a bit higher than the 100 MPa value (8,7). As a result, if we consider centerline average, the surface roughness value of the 100 MPa is higher than 50 MPa value. The

roughness values are 1,58 – 1,72 and 1,91 μm at the related pressures of 0-50-100 MPa, respectively. So, we conclude that the part which was cast under 50 MPa pressure, may have some local increase in roughness values. But, according to the R_q value, we can say that when the casting pressure increases the surface roughness value increases, too.

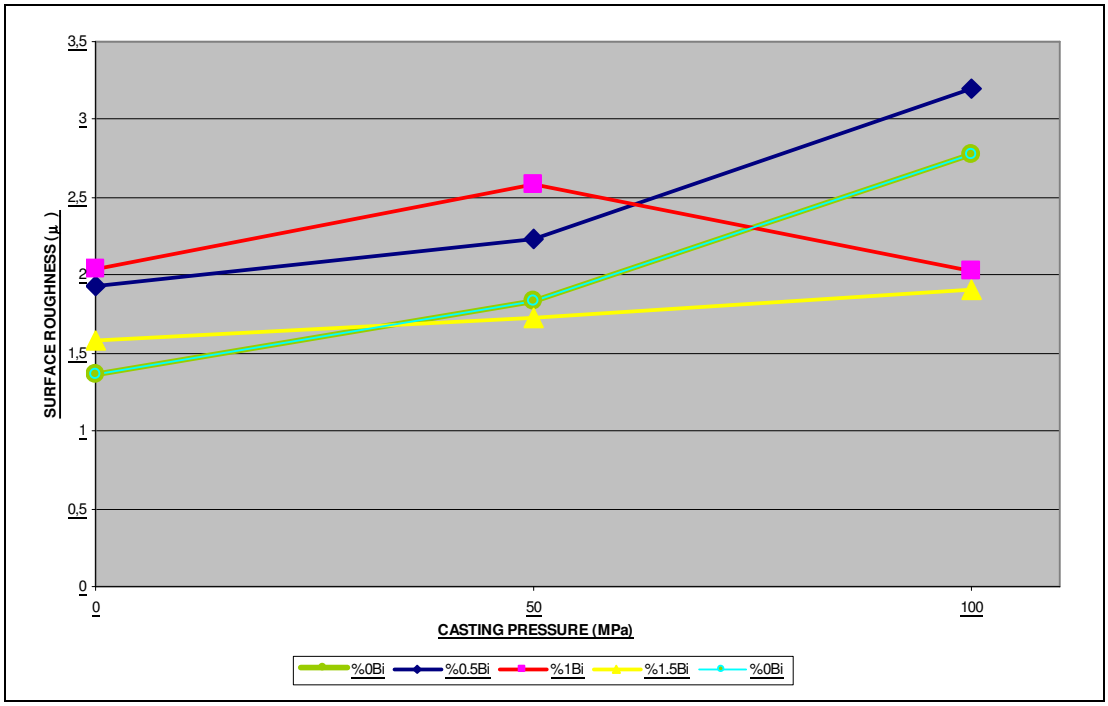

Figure 4.13. Average surface roughness vs casting pressure plot in Rq measures for all Bi added specimens

In the above graph, the average of the surface roughness values were found for all parts which were cast under 0 MPa, 50 MPa and 100 MPa, respectively. Using these average roughness values Figure 4.13 was generated. According to this figure, we can easily see that surface roughness values increase for most types with increasing pressure. But, contrary to that the Rq value of 1%Bi firstly increases at 50 MPa, later decreases at 100 MPa. This result may be because of wrong measuring the 100 MPa value. These values are too small and misreadings may occur while measuring the Rq value. As consequence, we can say that average increment according to the casting pressure is almost linear.

When a small amount of bismuth was added discontinuous chips were formed and because of discontinuity in chip formation surface roughness values were increased. But,

when bismuth content increased to 1.5 Bi% the chips were returned to powder form and also this situation leads to the decrease in surface roughness values. As a result, one way of increasing surface quality in ZA alloys, is adding 1.5 Bi%wt into the alloy. This result is similar with the result found by Baskaya [1]. Baskaya reported that as the Bi concentration was increased, smaller surface roughness values were obtained.

4.4. Variation in Hardness

The specimens which were used for surface roughness were also used for hardness determination. While determining the hardness the Brinell method was used. The force was 62.5 kg and the diameter of the ball was 2.5 mm. The ball was pressed on the specimen for 15 seconds.

The Brinell hardness values were determined from the center and from the two sides of the specimens. 8 measurements were done from the middle axis of the 12 specimens.

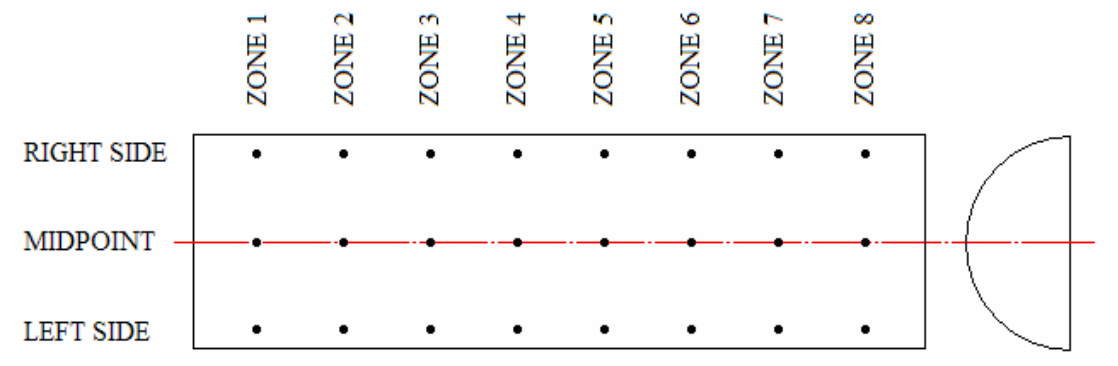

Figure 4.14. Schematic explanation of the zones that Brinell hardness test was applied.

The middle point hardness results are shown the table below.

Table 4.6. Brinell hardness results of the 12 specimens

	NO	ZONE 1	ZONE 2	ZONE 3	ZONE 4	ZONE 5	ZONE 6	ZONE 7	ZONE 8
Right Side	**2**	90,7	90,7	86,8	77,9	88,7	88,7	88,7	81,3
Midpoint	***2***	*88,7*	*86,8*	*68,8*	*64,9*	*68,8*	*76,3*	*74,7*	*84,9*
Left Side	**2**	90,7	88,7	88,7	74,7	90,7	88,7	88,7	77,9
% 0 Bi, 0 MPa	**2 (Avg)**	90,0	88,7	81,4	72,5	82,7	84,6	84,0	81,4
Right Side	**5**	84,9	76,3	77,9	84,9	86,8	81,3	74,7	77,9
Midpoint	**5**	83,0	81,3	74,7	68,8	74,7	70,2	84,9	88,7
Left Side	**5**	73,2	83,0	84,9	77,9	79,5	79,5	79,5	79,5
% 0 Bi, 50 MPa	**5 (Avg)**	80,4	80,2	79,2	77,2	80,3	77,0	79,7	82,0
Right Side	**10**	97,9	92,8	88,7	84,9	84,9	90,7	90,7	83,0
Midpoint	***10***	*95,0*	*77,9*	*73,2*	*66,2*	*62,4*	*68,8*	*84,9*	*84,9*
Left Side	**10**	92,8	92,8	95,0	76,3	88,7	90,7	90,7	83,0
% 0 Bi, 100 MPa	**10 (Avg)**	95,2	87,8	85,6	75,8	78,7	83,4	88,8	83,6
Right Side	**16**	86,8	83,0	86,8	76,3	76,3	83,0	83,0	79,5
Midpoint	**16**	84,9	74,7	71,7	70,2	74,7	74,7	76,3	79,5
Left Side	**16**	88,7	86,8	88,7	60,1	81,3	81,3	83,0	77,9
% 0.5 Bi, 0 MPa	**16 (Avg)**	86,8	81,5	82,4	68,9	77,4	79,7	80,8	79,0
Right Side	**21**	74,7	83,0	77,9	68,8	77,9	92,8	84,9	83,0
Midpoint	***21***	*77,9*	*81,3*	*79,5*	*79,5*	*86,8*	*84,9*	*90,7*	*88,7*
Left Side	**21**	84,9	79,5	81,3	76,3	88,7	86,8	84,9	76,3
% 0.5 Bi, 50 MPa	**21 (Avg)**	79,2	81,3	79,6	74,9	84,5	88,2	86,8	82,7
Right Side	**26**	97,2	95,0	84,9	83,0	84,9	84,9	84,9	84,9
Midpoint	**26**	99,5	92,8	88,7	86,8	84,9	70,2	77,9	76,3
Left Side	**26**	99,5	97,2	81,3	81,3	83,9	84,9	84,9	76,3
% 0.5 Bi, 100 MPa	**26 (Avg)**	98,7	95,0	85,0	83,7	84,6	80,0	82,6	79,2

Table 4.7. Brinell hardness results of the 12 specimens (continued)

	NO	ZONE 1	ZONE 2	ZONE 3	ZONE 4	ZONE 5	ZONE 6	ZONE 7	ZONE 8
Right Side	**29**	77,9	77,9	83,0	77,9	79,5	86,8	88,7	97,2
Midpoint	**29**	84,9	84,9	79,5	81,3	88,7	86,8	88,7	95,0
Left Side	**29**	83,9	81,3	76,3	79,5	88,7	88,7	86,8	81,3
% 1 Bi, 0 MPa	**29 (Avg)**	82,2	81,4	79,6	79,6	85,6	87,4	88,1	91,2
Right Side	**34**	83,0	83,0	84,9	83,0	84,9	77,9	84,9	79,5
Midpoint	**34**	95,9	90,7	83,9	83,0	77,9	88,7	74,7	79,5
Left Side	**34**	86,8	86,8	86,8	77,9	77,9	76,3	71,7	74,7
% 1 Bi, 50 MPa	**34 (Avg)**	88,6	86,8	85,2	81,3	80,2	81,0	77,1	77,9
Right Side	**38**	86,8	86,8	86,8	77,9	74,7	81,3	83,9	83,0
Midpoint	**38**	83,0	84,9	74,7	74,7	74,7	74,7	73,2	77,9
Left Side	**38**	83,0	83,0	83,0	83,0	79,5	77,9	77,9	76,3
% 1 Bi, 100 MPa	**38 (Avg)**	84,3	84,9	81,5	78,5	76,3	78,0	78,3	79,1
Right Side	**45**	63,6	73,2	79,5	76,3	71,7	74,7	74,7	74,7
Midpoint	**45**	60,1	56,8	63,6	64,9	66,2	71,7	73,2	76,3
Left Side	**45**	77,9	77,9	77,9	73,2	76,3	74,7	70,2	71,7
% 1.5 Bi, 0 MPa	**45 (Avg)**	67,2	69,3	73,7	71,5	71,4	73,7	72,7	74,2
Right Side	**48**	95,0	83,0	77,9	76,3	76,3	76,3	76,3	76,3
Midpoint	**48**	88,7	81,3	79,5	77,9	76,3	76,3	74,7	77,9
Left Side	**48**	84,9	77,9	77,9	76,3	76,3	76,3	77,9	76,3
% 1.5 Bi, 50 MPa	**48 (Avg)**	89,5	80,7	78,4	76,8	76,3	76,3	76,3	76,8
Right Side	**54**	79,5	81,3	77,9	81,3	92,8	92,8	90,7	88,7
Midpoint	**54**	83,0	79,5	79,5	84,9	88,7	83,0	97,2	97,2
Left Side	**54**	70,2	79,5	77,9	76,3	95,0	95,0	84,9	83,0
% 1.5 Bi, 100 MPa	**54 (Avg)**	77,6	80,1	78,4	80,8	92,2	90,3	90,9	89,6

The values above were measured from the middle axis, right side and the left side of the specimens. The parts were divided into 8 zones and measurements were done. Zone 1 means the top side and the zone 8 means the bottom side of the specimens.

The graph of the hardness measurement results of all 12 specimens are shown below.

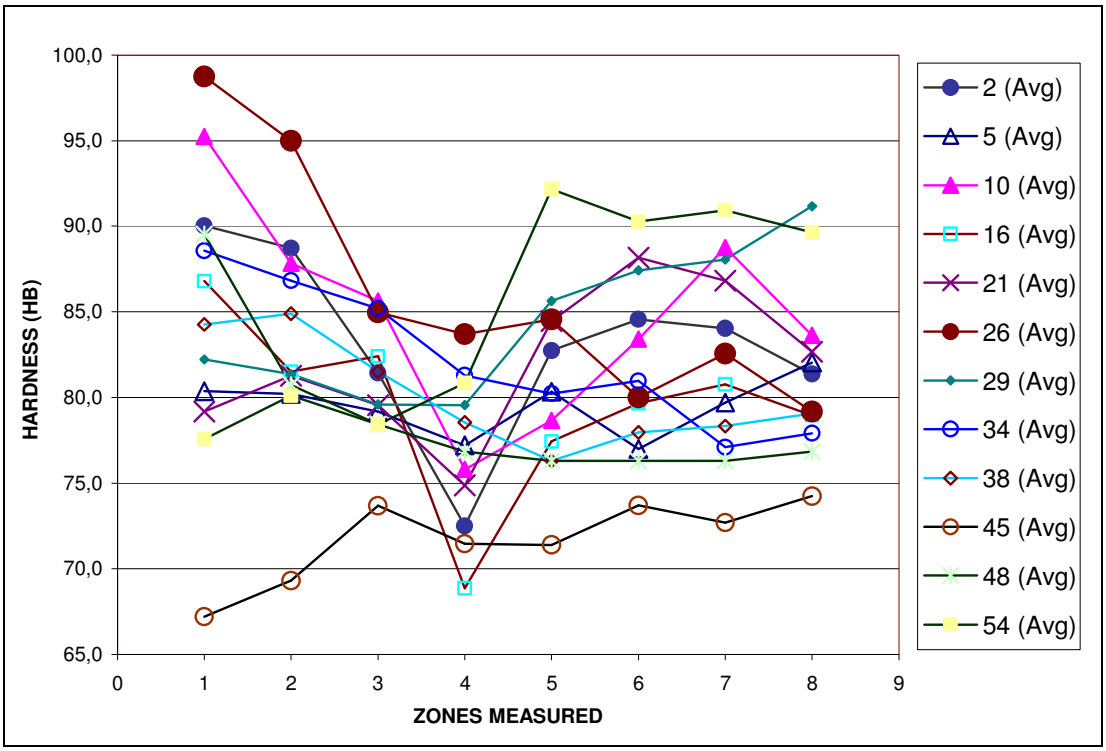

Figure 4.15. Average Brinell hardness vs zones of the 12 specimens

As seen in the figure, almost in all parts the top and the bottom hardness values are high. In most squeeze casting applications, generally the upper side's hardness was higher than the bottom side. This was because of the lack of squeezing of the bottom side. But, in these experiments an isolator was put between die and the brick (See Figure 3.12.) and the heat transfer rate was decreased. So, the bottom part of the specimen was squeezed as the upper part.

It was found that bismuth was concentrated at the fracture surface as expected since solidified last. Zinc concentration also increased since it solidified after aluminum rich dendrites. As a result, the hardness values of the middle zone were decreased as expected.

This is in agreement with studies carried out by Saçlı [37] who made the numerical and quantitative analysis of Al-Si alloy. He founded that the mid height regions of the squeeze cast specimens suffers more porosity. This fact was observed by a decrease in Rockwell Hardness values in middle regions.

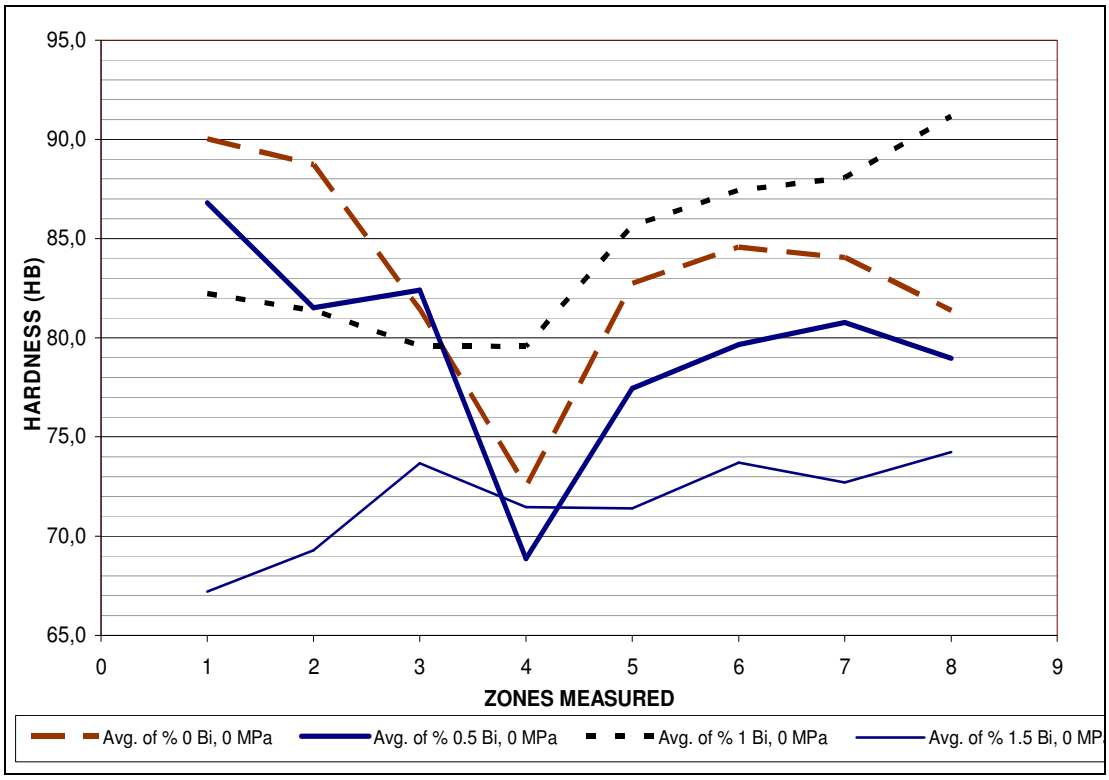

Figure 4.16. Average Brinell hardness of unsqueezed specimens vs zones plot as a function of %Bi

In Figure 4.16, the average hardness values of the unsqueezed specimens as a function of different bismuth contents were shown. The average hardness values of the 1.5% Bi content specimen was lower than the %0 Bi specimen, the 1% specimen's hardness was higher than the 0 %Bi specimen. These values are not logical. So, according to the measured results the bismuth has no effect on the hardness values of the ZA alloy. Note that bismuth content that was added in this experiment was up to 1.5%. So, excessive bismuth content (i.e. 3.5%) may have effect on the hardness of the ZA-27 alloy.

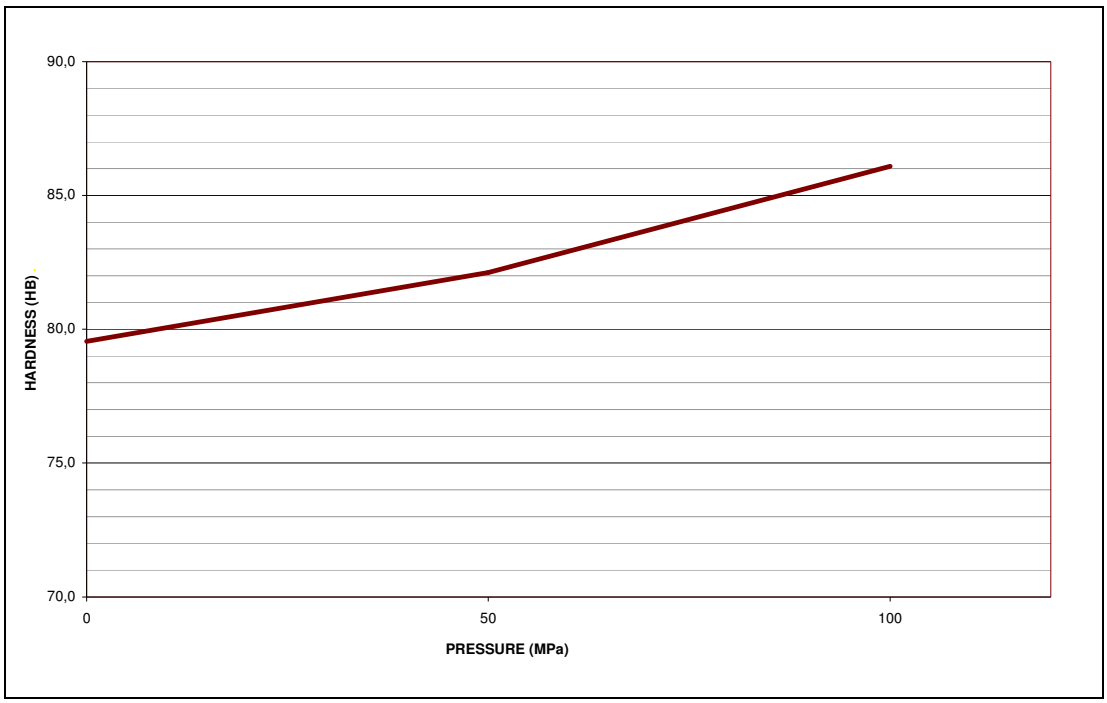

Figure 4.17. Average Brinell hardness vs pressure for plot as a function of squeezing 0.5% Bi

It is seen that if the squeezing pressure increases the hardness values also increase. The maximum average hardness value of the 100 MPa specimens was increased up to 86 HB, whereas 50 MPa specimen's maximum average hardness value was about 82 HB. Maximum measured average hardness value of the unsqueezed specimen was only about 80 HB. It is obvious from the results that with the increasing squeezing pressure the hardness of the ZA-27 alloys increase whether it contains bismuth or not. Squeezed specimens have small grains and small precipitates because of rapid solidification as a result of squeezing pressure. Cay and Kurnaz reached same results that Brinell hardness of the squeeze cast alloys were obtained at higher values than gravity castings in their research [38].

4.5. Variation in Tensile Properties

Three sets of specimens were fractured for tensile tests. Every set includes approximately 12 specimens. The three sets of fractured specimens' tables are listed below.

These tables include almost every detail including initial diameter, final diameter, initial area, fracture area, reduction in area, initial length, final length, elongation, yield strength and tensile strength values.

Table 4.8. Tensile test results of the specimens SET 1

No	Contents	Initial Diameter (mm)	Final Diameter (mm)	Area (mm^2)	Area 2 (mm^2)	Reduction in Area (%)	Initial Lenght, L_0 (mm)	Final Lenght, L_f (mm)	Elongation (%)	Yield Load (N)	Yield Strength (N/mm^2)	Tensile Load (N)	Tensile Strength (N/mm^2)
3	% 0 Bi, 0 MPa	12,5	12,4	122,72	120,76	1,59%	50	51	1,96%	17.426	142	20.510	167
6	% 0 Bi, 50 MPa	12,5	12,2	122,72	116,90	4,74%	50	51,2	2,34%	21.476	175	29.890	244
12	% 0 Bi, 100 MPa	12,5	12,3	122,72	118,82	3,17%	50	52	3,85%	21.353	174	24.860	203
17	% 0.5 Bi, 0 MPa	12,5	12,4	122,72	120,76	1,59%	50	51,5	2,91%	23.317	190	26.370	215
20	% 0.5 Bi, 50 MPa	12,5		122,72	0,00	100,00%	50	50,1	0,20%	26.016	212	29.480	240
24	% 0.5 Bi, 100 MPa	12,5	12,3	122,72	118,82	3,17%	50	51,4	2,72%	25.894	211	31.820	259
33	% 1 Bi, 0 MPa	12,5	12,2	122,72	116,90	4,74%	50	50,5	0,99%	17.917	146	20.650	168
36	% 1 Bi, 50 MPa	12,5	12,3	122,72	118,82	3,17%	50	50,9	1,77%	19.144	156	28.200	230
39	% 1 Bi, 100 MPa	12,5	12,4	122,72	120,76	1,59%	50	50,9	1,77%	24.421	199	31.130	254
50	% 1.5 Bi, 50 MPa	12,5	12,4	122,72	120,76	1,59%	50	50,8	1,57%	22.703	185	26.960	220
51	% 1.5 Bi, 100 MPa	12,5	12,3	122,72	118,82	3,17%	50	51,6	3,10%	29.698	242	33.740	275

As seen in the Table 4.8. as the applied pressure increase, the tensile stress and yield stress increases, Also with the increasing pressure elongation and reduction in area values increase.

As seen in the Table 4.9 as the applied pressure increase the tensile strength and yield strength, elongation and reduction in area values also increase.

Table 4.9. Tensile test results of the specimens SET 2

No	Contents	Initial Diameter (mm)	Final Diameter (mm)	Area (mm^2)	Area 2 (mm^2)	Reduction in Area (%)	Initial Lenght, L_0 (mm)	Final Lenght, L_f (mm)	Elongation (%)	Yield Load (N)	Yield Strength (N/mm^2)	Tensile Load (N)	Tensile Strength (N/mm^2)
4	% 0 Bi, 0 MPa	12,5	12,4	122,72	120,76	1,59%	50	50,4	0,79%	17.058	139	18.400	150
7	% 0 Bi, 50 MPa	12,5	12,4	122,72	120,76	1,59%	50	50,2	0,40%	30.925	252	31.540	257
11	% 0 Bi, 100 MPa	12,5	12	122,72	113,10	7,84%	50	51,4	2,72%	29.943	244	33.560	273
13	% 0.5 Bi, 0 MPa	12,5	12,4	122,72	120,76	1,59%	50	50,3	0,60%	20.985	171	22.800	186
19	% 0.5 Bi, 50 MPa	12,5	12,3	122,72	118,82	3,17%	50	51	1,96%	17.794	145	26.550	216
27	% 0.5 Bi, 100 MPa	12,5	12,4	122,72	120,76	1,59%	50	50,9	1,77%	26.753	218	31.860	260
32	% 1 Bi, 0 MPa	12,5	12,5	122,72	122,72	0,00%	50	50,1	0,20%	0		20.780	169
37	% 1 Bi, 50 MPa	12,5	12,2	122,72	116,90	4,74%	50	50,6	1,19%	17.426	142	25.590	209
41	% 1 Bi, 100 MPa	12,5	12,4	122,72	120,76	1,59%	50	50,5	0,99%	28.225	230	30.580	249
43	% 1.5 Bi, 0 MPa	12,5	12,3	122,72	118,82	3,17%	50	50,3	0,60%	23.685	193	24.770	202
46	% 1.5 Bi, 50 MPa	12,5	12,4	122,72	120,76	1,59%	50	50,8	1,57%	26.998	220	30.810	251
49	% 1.5 Bi, 50 MPa	12,5	12,4	122,72	120,76	1,59%	50	50,1	0,20%	0		32.000	261
53	% 1.5 Bi, 100 MPa	12,5	12,4	122,72	120,76	1,59%	50	50,2	0,40%	31.416	256	32.640	266

Table 4.10. Tensile test results of the specimens SET 3

No	Contents	Initial Diameter (mm)	Final Diameter (mm)	Area (mm^2)	Area 2 (mm^2)	Reduction in Area (%)	Initial Lenght, L_0 (mm)	Final Lenght, L_f (mm)	Elongation (%)	Yield Load (N)	Yield Strength (N/mm^2)	Tensile Load (N)	Tensile Strength (N/mm^2)
1	% 0 Bi, 0 MPa	12,5	12,2	122,72	116,90	4,74%	50	52	3,85%	22.948	187	26.550	216
8	% 0 Bi, 50 MPa	12,5	12,3	122,72	118,82	3,17%	50	51,2	2,34%	28.348	231	31.040	253
9	% 0 Bi, 100 MPa	12,5	12,3	122,72	118,82	3,17%	50	52	3,85%	22.089	180	26.230	214
15	% 0.5 Bi, 0 MPa	12,5	12,5	122,72	122,72	0,00%	50	50	0,00%	0		2.610	21
18	% 0.5 Bi, 50 MPa	12,5	12,2	122,72	116,90	4,74%	50	50,9	1,77%	23.562	192	26.180	213
25	% 0.5 Bi, 100 MPa	12,5	12,4	122,72	120,76	1,59%	50	51	1,96%	30.066	245	32.230	263
31	% 1 Bi, 0 MPa	12,5	12,4	122,72	120,76	1,59%	50	50,7	1,38%	24.912	203	29.160	238
35	% 1 Bi, 50 MPa	12,5	12,4	122,72	120,76	1,59%	50	50,4	0,79%	0		20.650	168
40	% 1 Bi, 100 MPa	12,4	12,3	120,76	118,82	1,61%	50	50,7	1,38%	0		30.030	249
42	% 1.5 Bi, 0 MPa	12,5	12,4	122,72	120,76	1,59%	50	50,9	1,77%	19.267	157	23.350	190
47	% 1.5 Bi, 50 MPa	12,5	12,4	122,72	120,76	1,59%	50	51,2	2,34%	26.998	220	31.040	253
52	% 1.5 Bi, 100 MPa	12,5	12,5	122,72	122,72	0,00%	50	50	0,00%	0		31.820	259

The bismuth effect on the specimens will be evaluated with graphical representation. But, from this table it is easy to say that when the applied pressure increases the tensile stress and yield stress increase, elongation and reduction in area values also increase.

Table 4.11. Tensile test results of the all of the specimens

SET	No	Contents	Initial Diameter (mm)	Final Diameter (mm)	Area (mm^2)	Area 2 (mm^2)	Reduction in Area (%)	Initial Lenght, L_0 (mm)	Final Lenght, L_f (mm)	Elongation (%)	Yield Load (N)	Yield Strength (N/mm^2)	Tensile Load (N)	Tensile Strength (N/mm^2)
III	1	% 0 Bi, 0 MPa	12,5	12,2	122,72	116,90	4,74%	50	52	3,85%	22.948	187	26.550	216
I	3	% 0 Bi, 0 MPa	12,5	12,4	122,72	120,76	1,59%	50	51	1,96%	17.426	142	20.510	167
II	4	% 0 Bi, 0 MPa	12,5	12,4	122,72	120,76	1,59%	50	50,4	0,79%	17.058	139	18.400	150
I	6	% 0 Bi, 50 MPa	12,5	12,2	122,72	116,90	4,74%	50	51,2	2,34%	21.476	175	29.890	244
II	7	% 0 Bi, 50 MPa	12,5	12,4	122,72	120,76	1,59%	50	50,2	0,40%	30.925	252	31.540	257
III	8	% 0 Bi, 50 MPa	12,5	12,3	122,72	118,82	3,17%	50	51,2	2,34%	28.348	231	31.040	253
III	9	% 0 Bi, 100 MPa	12,5	12,3	122,72	118,82	3,17%	50	52	3,85%	22.089	180	26.230	214
II	11	% 0 Bi, 100 MPa	12,5	12	122,72	113,10	7,84%	50	51,4	2,72%	29.943	244	33.560	273
I	12	% 0 Bi, 100 MPa	12,5	12,3	122,72	118,82	3,17%	50	52	3,85%	21.353	174	24.860	203
II	13	% 0.5 Bi, 0 MPa	12,5	12,4	122,72	120,76	1,59%	50	50,3	0,60%	20.985	171	22.800	186
III	15	% 0.5 Bi, 0 MPa	12,5	12,5	122,72	122,72	0,00%	50	50	0,00%	0		2.610	
I	17	% 0.5 Bi, 0 MPa	12,5	12,4	122,72	120,76	1,59%	50	51,5	2,91%	23.317	190	26.370	215
III	18	% 0.5 Bi, 50 MPa	12,5	12,2	122,72	116,90	4,74%	50	50,9	1,77%	23.562	192	26.180	213
II	19	% 0.5 Bi, 50 MPa	12,5	12,3	122,72	118,82	3,17%	50	51	1,96%	0		26.550	216
I	20	% 0.5 Bi, 50 MPa	12,5		122,72	0,00	100,00%	50	50,1	0,20%	26.016	212	29.480	
I	24	% 0.5 Bi, 100 MPa	12,5	12,3	122,72	118,82	3,17%	50	51,4	2,72%	25.894	211	31.820	259
III	25	% 0.5 Bi, 100 MPa	12,5	12,4	122,72	120,76	1,59%	50	51	1,96%	30.066	245	32.230	263
II	27	% 0.5 Bi, 100 MPa	12,5	12,4	122,72	120,76	1,59%	50	50,9	1,77%	26.753	218	31.860	260
III	31	% 1 Bi, 0 MPa	12,5	12,4	122,72	120,76	1,59%	50	50,7	1,38%	24.912	203	29.160	
II	32	% 1 Bi, 0 MPa	12,5	12,5	122,72	122,72	0,00%	50	50,1	0,20%	0		20.780	169
I	33	% 1 Bi, 0 MPa	12,5	12,2	122,72	116,90	4,74%	50	50,5	0,99%	17.917	146	20.650	168
III	35	% 1 Bi, 50 MPa	12,5	12,4	122,72	120,76	1,59%	50	50,4	0,79%	0		20.650	
I	36	% 1 Bi, 50 MPa	12,5	12,3	122,72	118,82	3,17%	50	50,9	1,77%	19.144	156	28.200	230
II	37	% 1 Bi, 50 MPa	12,5	12,2	122,72	116,90	4,74%	50	50,6	1,19%	17.426	142	25.590	209
I	39	% 1 Bi, 100 MPa	12,5	12,4	122,72	120,76	1,59%	50	50,9	1,77%	24.421	199	31.130	254
III	40	% 1 Bi, 100 MPa	12,4	12,3	120,76	118,82	1,61%	50	50,7	1,38%	0		30.030	249
II	41	% 1 Bi, 100 MPa	12,5	12,4	122,72	120,76	1,59%	50	50,5	0,99%	28.225	230	30.580	249
III	42	% 1.5 Bi, 0 MPa	12,5	12,4	122,72	120,76	1,59%	50	50,9	1,77%	19.267	157	23.350	190
II	43	% 1.5 Bi, 0 MPa	12,5	12,3	122,72	118,82	3,17%	50	50,3	0,60%	23.685	193	24.770	202
II	46	% 1.5 Bi, 50 MPa	12,5	12,4	122,72	120,76	1,59%	50	50,8	1,57%	26.998	220	30.810	251
III	47	% 1.5 Bi, 50 MPa	12,5	12,4	122,72	120,76	1,59%	50	51,2	2,34%	26.998	220	31.040	253
II	49	% 1.5 Bi, 50 MPa	12,5	12,4	122,72	120,76	1,59%	50	50,1	0,20%	0		32.000	261
I	50	% 1.5 Bi, 50 MPa	12,5	12,4	122,72	120,76	1,59%	50	50,8	1,57%	22.703	185	26.960	220
I	51	% 1.5 Bi, 100 MPa	12,5	12,3	122,72	118,82	3,17%	50	51,6	3,10%	29.698	242	33.740	275
III	52	% 1.5 Bi, 100 MPa	12,5	12,5	122,72	122,72	0,00%	50	50	0,00%	0		31.820	259
II	53	% 1.5 Bi, 100 MPa	12,5	12,4	122,72	120,76	1,59%	50	50,2	0,40%	31.416	256	32.640	266

Red : Cancelled

Tensile test results of the fractured specimens are given in Table 4.11. The table contains initial and fracture diameters, surface area before fracture and after fracture, the

reduction in area, initial length, final length, elongation, yield load, yield strength, tensile load and tensile strength values. In calculating the yield strength (σ_{ys}), 0,2% offset method was used.

In the Table 4.12 the average values of the whole tensile test results are listed.

Table 4.12. Average values of all tensile test results

Contents	Final Diameter (mm)	Area 2 (mm^2)	Reduction in Area (%)	Final Lenght, L_f (mm)	Elongation (%)	Yield Load (N)	Yield Strength (N/mm^2)	Tensile Load (N)	Tensile Strength (N/mm^2)
% 0 Bi, 0 MPa	12,33	119,47	2,64%	51,13	2,20%	19144	156	21820	178
% 0 Bi, 50 MPa	12,30	118,83	3,17%	50,87	1,70%	26916	219	30823	251
% 0 Bi, 100 MPa	12,20	116,91	4,73%	51,80	3,47%	24462	199	28217	230
% 0.5 Bi, 0 MPa	12,40	120,76	1,59%	50,90	1,75%	22151	181	24585	200
% 0.5 Bi, 50 MPa	12,25	117,86	3,96%	50,67	1,31%	16526	202	27403	215
% 0.5 Bi, 100 MPa	12,37	120,12	2,12%	51,10	2,15%	27571	225	31970	261
% 1 Bi, 0 MPa	12,37	120,13	2,11%	50,43	0,86%	21414	175	23530	169
% 1 Bi, 50 MPa	12,30	118,83	3,17%	50,63	1,25%	18285	149	24813	219
% 1 Bi, 100 MPa	12,37	120,12	1,60%	50,70	1,38%	26323	215	30580	251
% 1.5 Bi, 0 MPa	12,35	119,79	2,38%	50,60	1,18%	21476	175	24060	196
% 1.5 Bi, 50 MPa	12,40	120,76	1,59%	50,73	1,42%	25566	208	30203	246
% 1.5 Bi, 100 MPa	12,40	120,77	1,59%	50,60	1,17%	30557	249	32733	267

According to the average values of the tensile test results graphical representations were drawn. In the Figure 4.18. the average values of the 0%Bi specimens were evaluated. According to these results, 50 MPa and 100 MPa results of tensile stress, yield stress, elongation and reduction in area results are higher than the 0 MPa values. The deviation in the 50 MPa values may be the result of a mistake while casting.

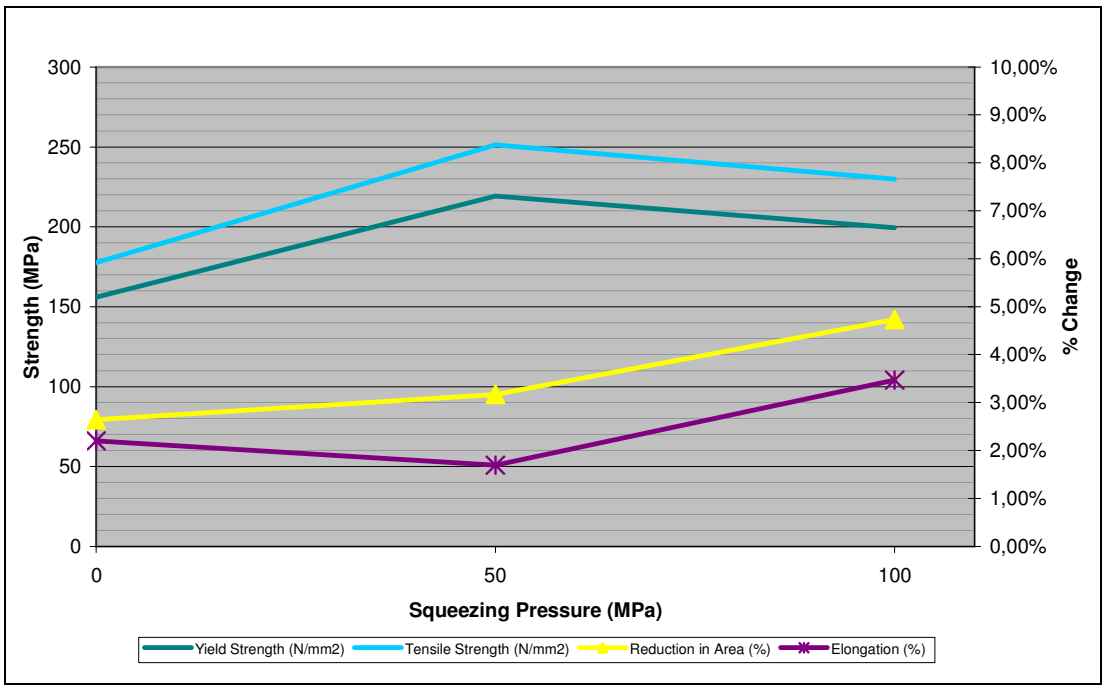

Figure 4.18. Variation of yield strength, tensile strength, reduction of area and elongation as a function of squeeze casting pressure in ZA-27 containing no bismuth

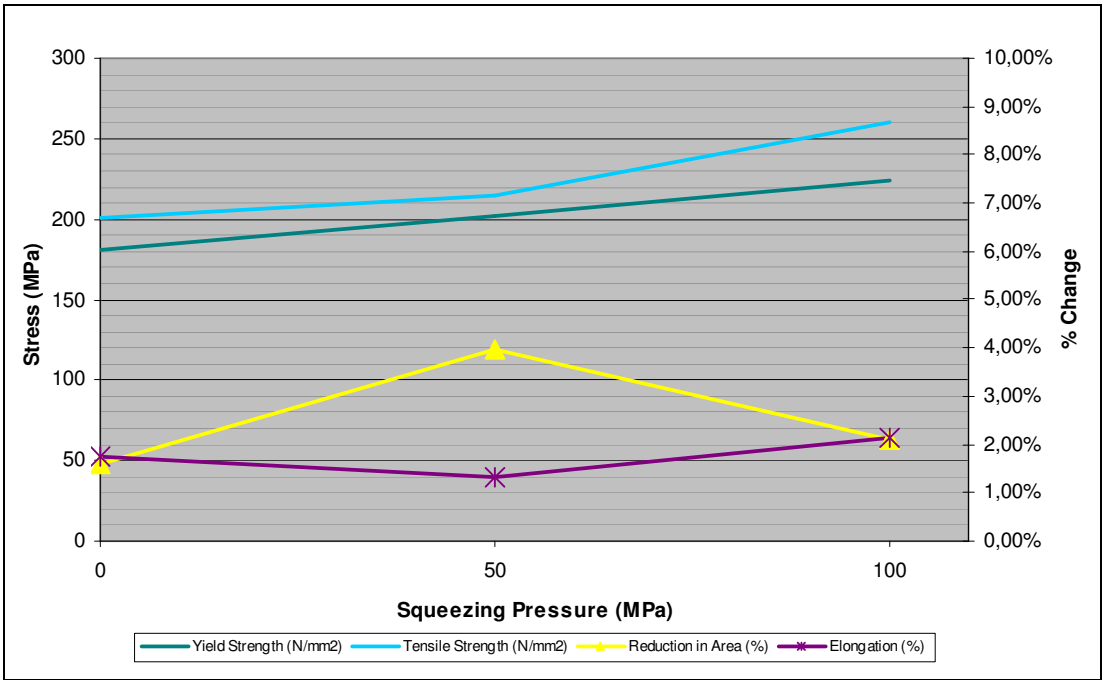

Figure 4.19. Variation of yield strength, tensile strength, reduction of area and elongation as a function of squeeze casting pressure in ZA-27 containing %0.5 Bi

In the figure 4.19 the average values of the 0.5% Bi specimens were drawn. According to this figure the tensile stress and yield stress values increase with the increasing pressure. So, it can be concluded that pressure has positive effects on the tensile and yield properties of the ZA 27 alloy.

In Figure 4.20 the average values of the 1% Bi specimens were plotted. According to this figure the tensile stress, yield stress and elongation values increase with the increasing pressure for 1%Bi+ZA-27 alloy.

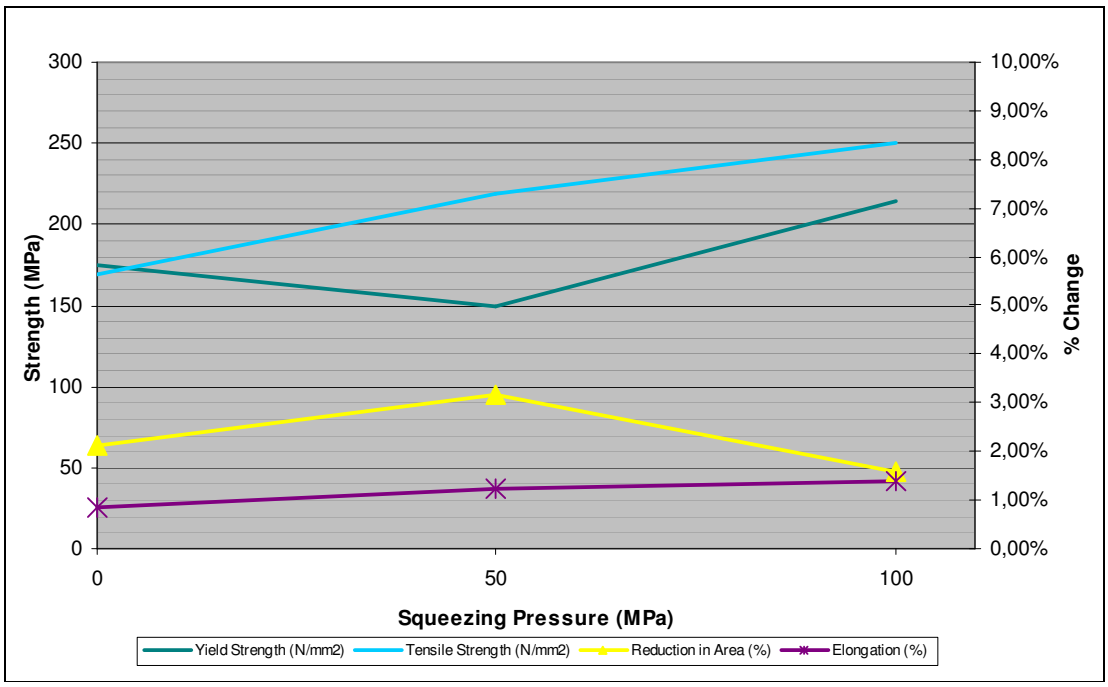

Figure 4.20. Variation of yield strength, tensile strength, reduction of area and elongation as a function of squeeze casting pressure in ZA-27 containing %1 Bi

In Figure 4.21 the average values of the 1.5% Bi specimens were drawn. According to this figure the tensile stress, yield stress values increase with increasing pressure. Also, because of high bismuth content and its negative effects on the elongation, the reduction in area and elongation values didn't change much.

According to M.A.Savas, it seems clear that the squeeze casting practice offered remarkable improvements, particularly in terms of tensile properties. This is achieved via a

reduction of porosity and refinement of the second phase. In same research, it was found that the porosity levels could be reduced to less than 1% under squeezing pressure up to 150 MPa [39].

This agrees well with the studies carried out by Chen [40] who investigated the effects of processing parameters on the tensile properties and hardness of thixoformed ZA27 alloy. They founded that the thixoforming process significantly improved both ultimate tensile strength and elongation of the alloy because of obvious reduction of porosities compared with the semi-solid die-cast no modified ZA27 alloy.

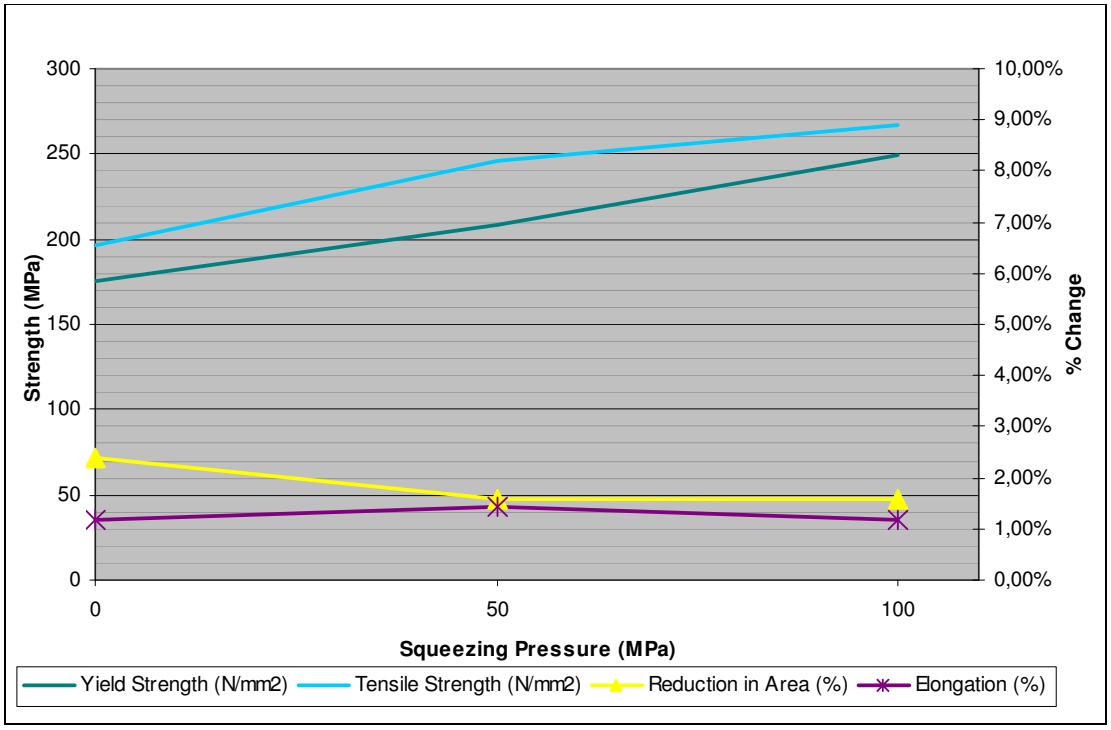

Figure 4.21. Variation of yield strength, tensile strength, reduction of area and elongation as a function of squeeze casting pressure in ZA-27 containing %1.5 Bi

In Figure 4.22 the average values of the 0 MPa specimens were drawn. According to this figure the reduction in area and elongation values decrease with increasing bismuth content for pure ZA-27. In terms of tensile and yield strength, the most suitable bismuth concentration is 0.5%. Beyond this value, the bismuth addition has no important effect on the tensile and yield properties of the unsqueezed ZA-27 alloy.

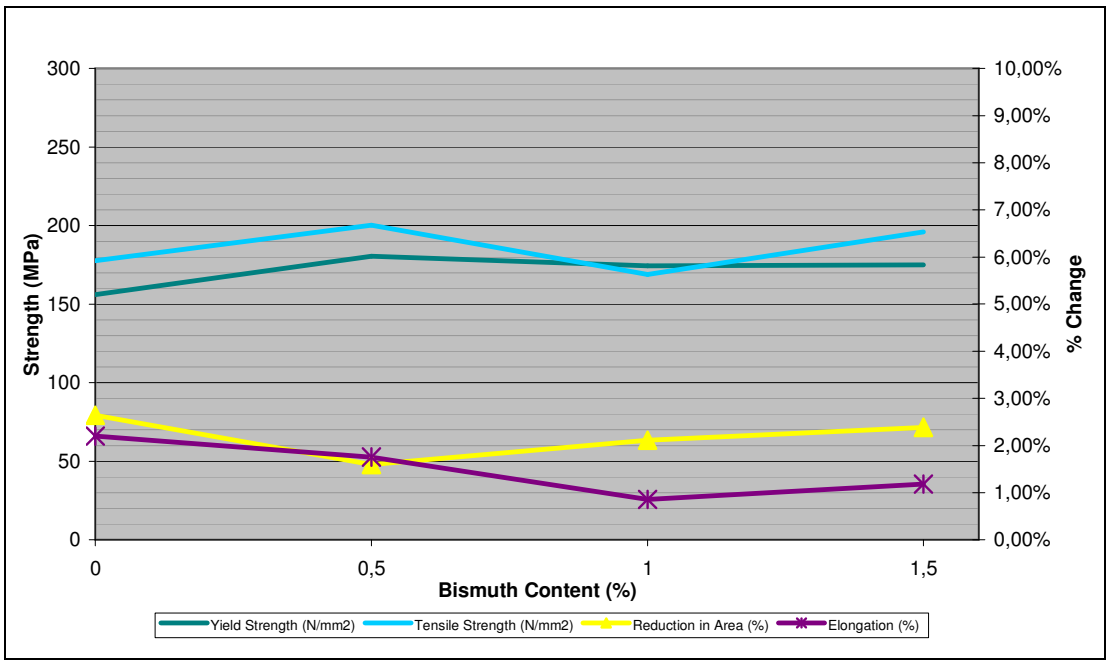

Figure 4.22. Variation of yield strength, tensile strength, reduction of area and elongation as a function of %Bi content in unsqueezed ZA-27

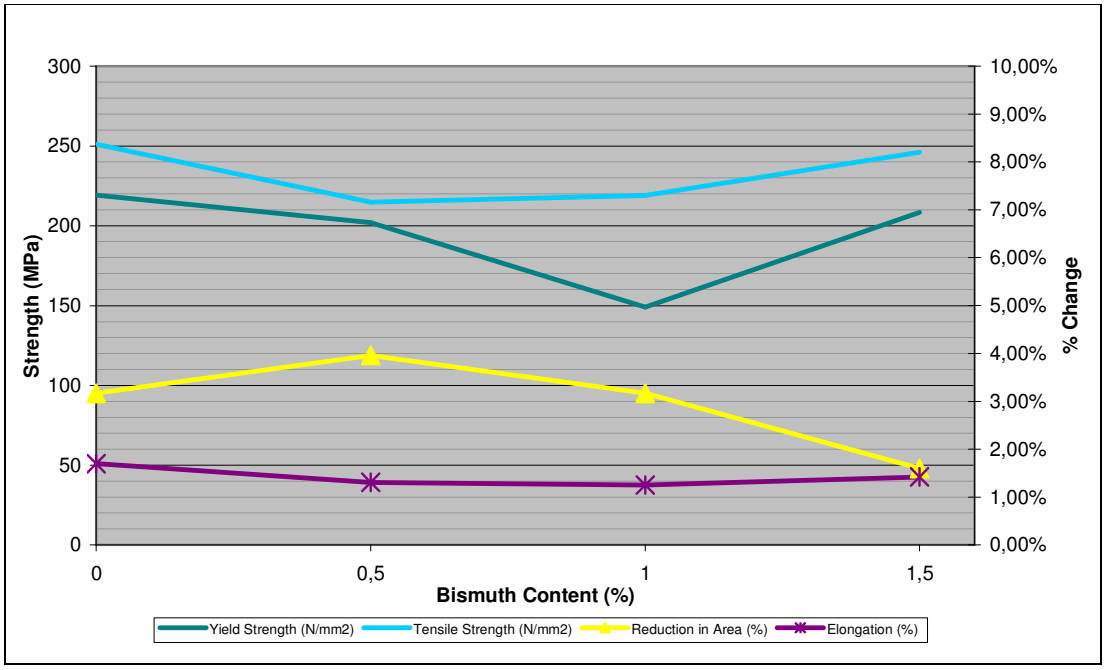

Figure 4.23. Variation of yield strength, tensile strength, reduction of area and elongation as a function of %Bi content in ZA-27 squeezed at 50 MPa

Considering the Figure 4.23, tensile and yield stresses drops up to 1% Bi content. After 1% bismuth content, tensile and yield stresses increase a bit. However, all these values are lower than the pure ZA-27 alloy's. Considering the reduction in area, for 0.5% Bi the area reduction increases. However, after 0.5% reduction in area value decreases, clearly. With increasing the bismuth content for 50 MPa specimens elongation values reduce because of brittleness of bismuth.

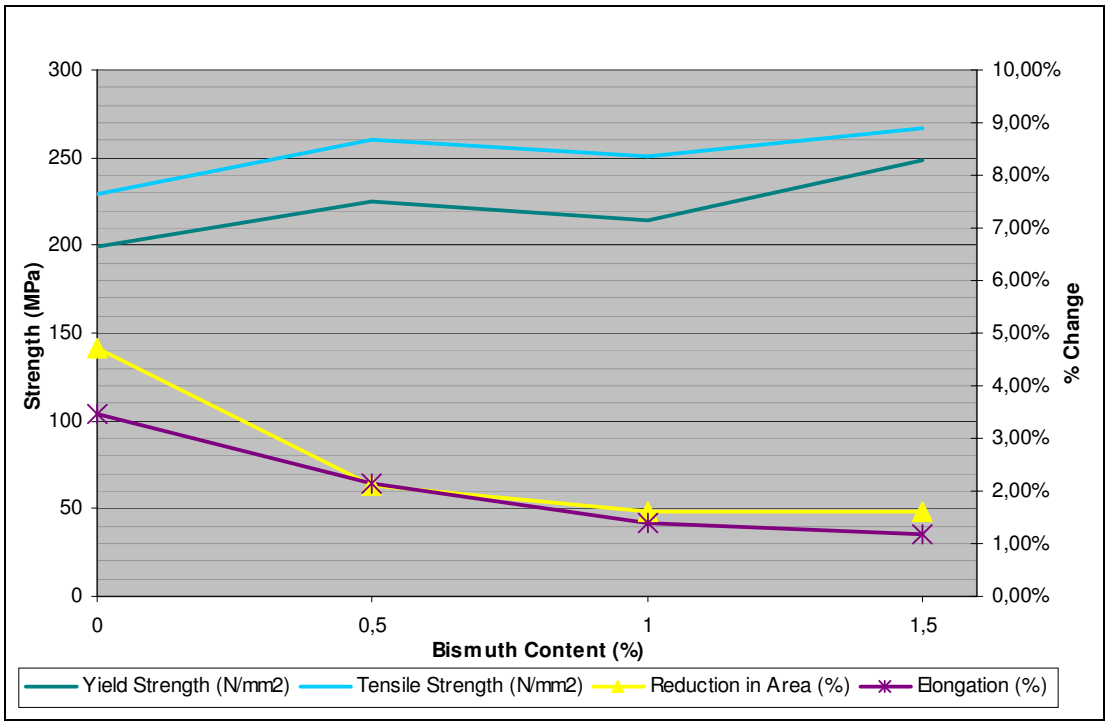

Figure 4.24. Variation of yield strength, tensile strength, reduction of area and elongation as a function of %Bi content in ZA-27 squeezed at 100 MPa

Considering the Figure 4.24, it is clear that with increasing the bismuth content the reduction in area and elongation values decrease.

4.6. Microstructure

Unsqueezed samples indicate no application of squeezing pressure, i.e., P_{ex} = 0 MPa.

The advantage of unetched samples under the microscope can be summarized as below:

The solid and porous regions are easily differentiated from each other. For instance, the top sections which solidified last, contain more black regions than the bottom sections of the same casting. These big amorphous black areas show porosities in the microstructure seen in Figure 4.25. That means there is more porosity on the top area of the specimen than the bottom side of the same specimen. The micrometer scale in the centre of the micrograph is 0.1mm in 100X magnification. Hence, the size of the bismuth particles and pores can be estimated.

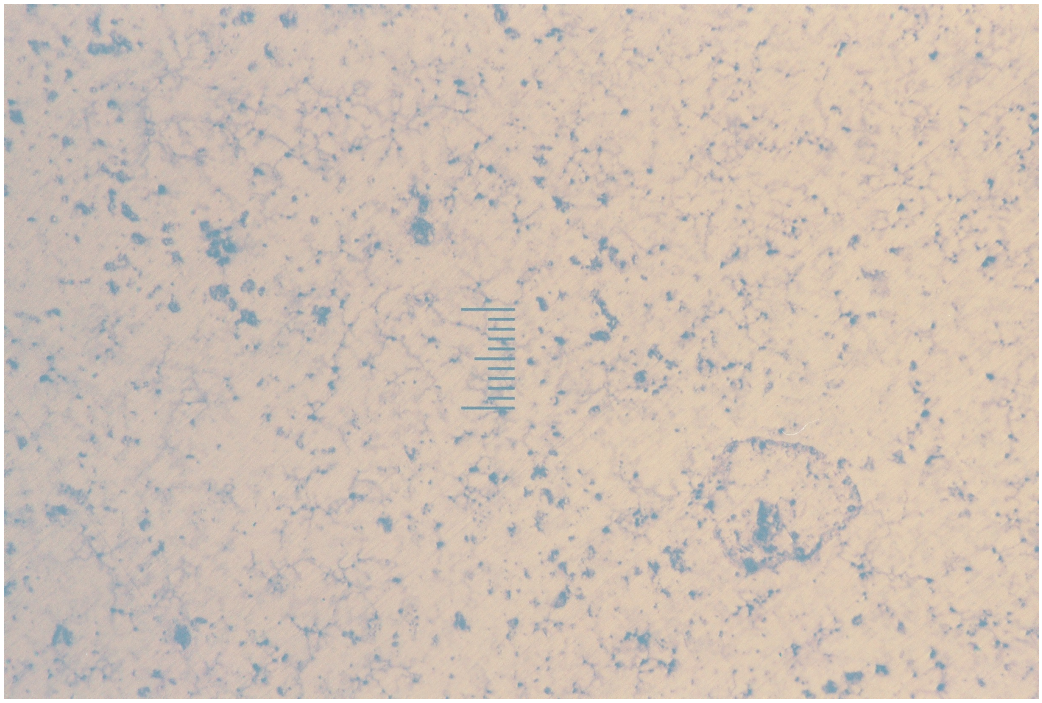

Figure 4.25. The microstructure of the top section of specimen 1 seen under the light microscope

The bismuth phase is also noticed easily in the unetched samples. Particularly, in the bottom sections which are relatively free of porosity, the bismuth particles can be seen in the white zinc matrix.

The advantage of etched samples is that it reveals concentration variations in the matrix phase such as coring as seen in the Figure 4.26.

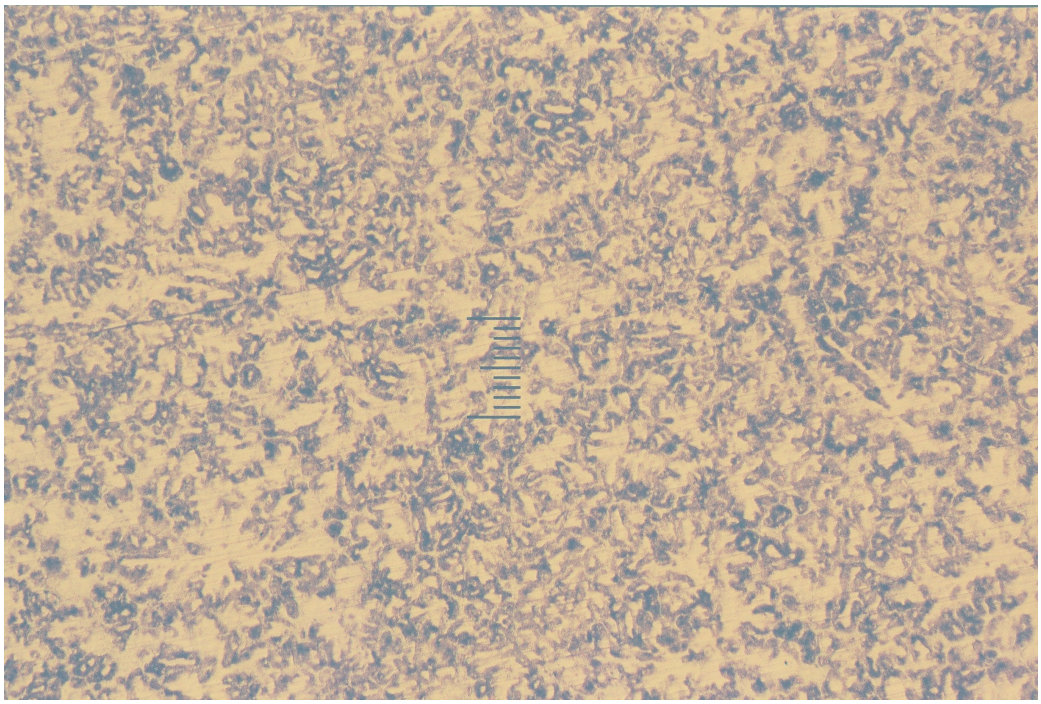

Figure 4.26. The microstructure photograph of the bottom section of specimen 18

Sample 17: Pex=100 MPa, 1.5%Bi , Top Section.

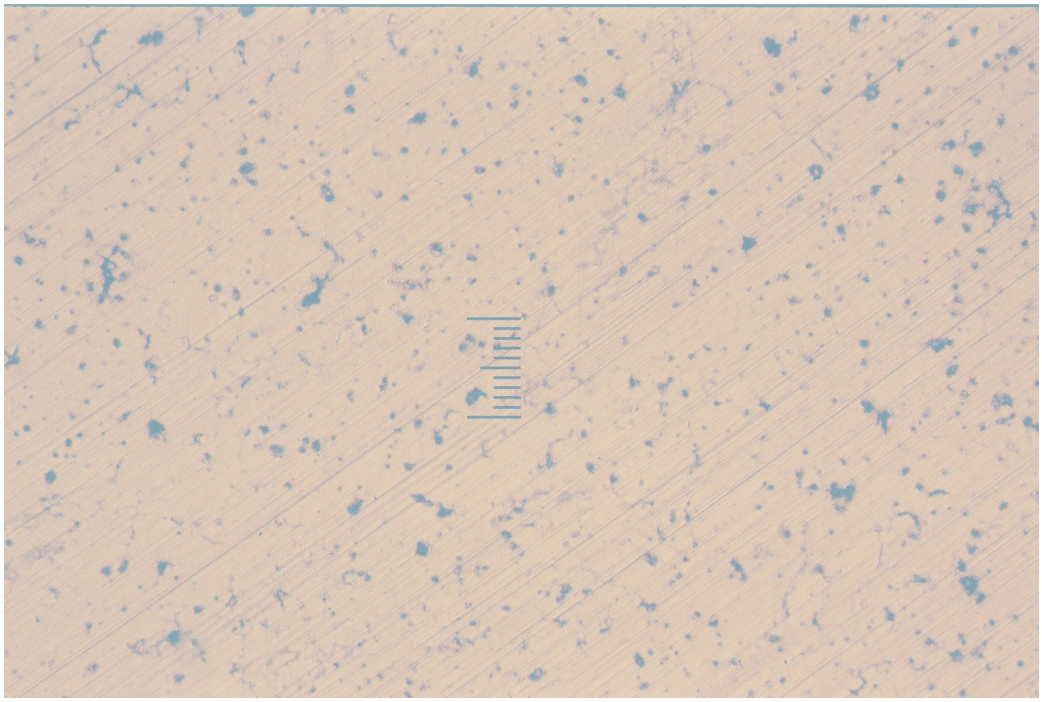

Figure 4.27. The microstructure photograph of the top section of specimen 17

The porosity is eliminated completely in Figure 4.27. The dark (black) particles are the bismuth phase formed during monotectic reaction. They are uniformly distributed in the alloy matrix and have an average size distribution varying between 5 μm to 20 μm.

Sample 18: 1.5%Bi, Bottom Section Etched

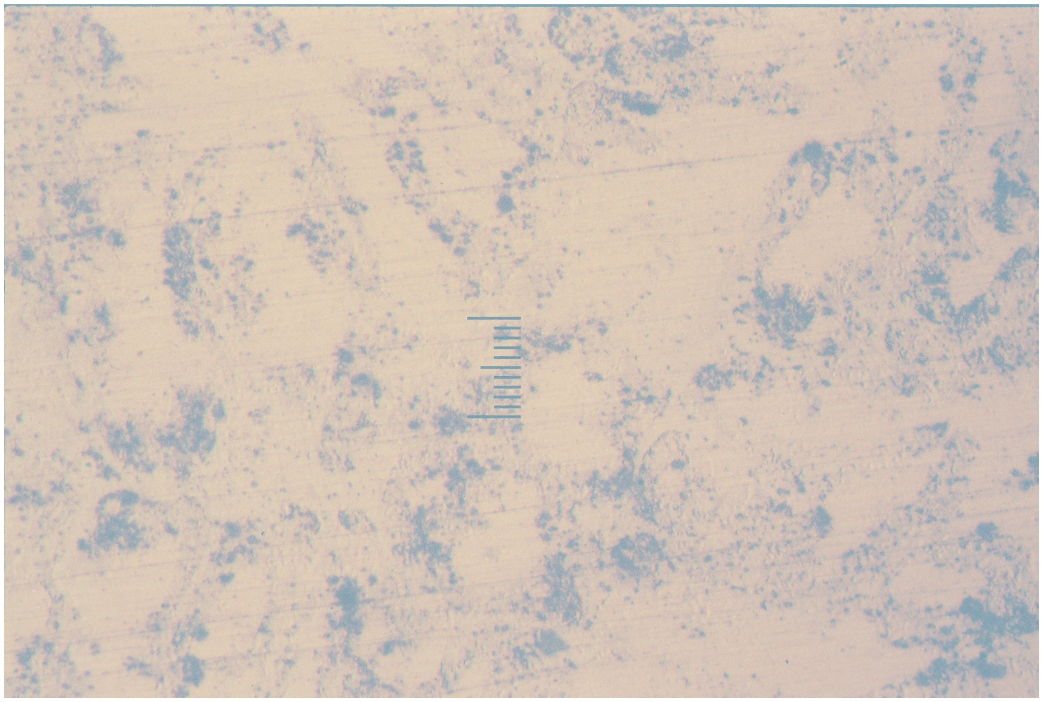

Figure 4.28. The microstructure photograph of the bottom section of specimen 18

Variation in concentration, i.e. coring effect, in the alloy matrix is readily observed. The average size of bismuth phase particles appeared to be the same as those found in the top section.

4.7. SEM Investigation

Figures from 4.30 to 4.35 show the fracture surfaces of the specimens broken in the tension test.

The fracture surface of the ZA-27 alloy containing no bismuth and squeeze cast under 100 MPa is seen in Figure 4.29. The dendrites of nonfaceted nature are seen.

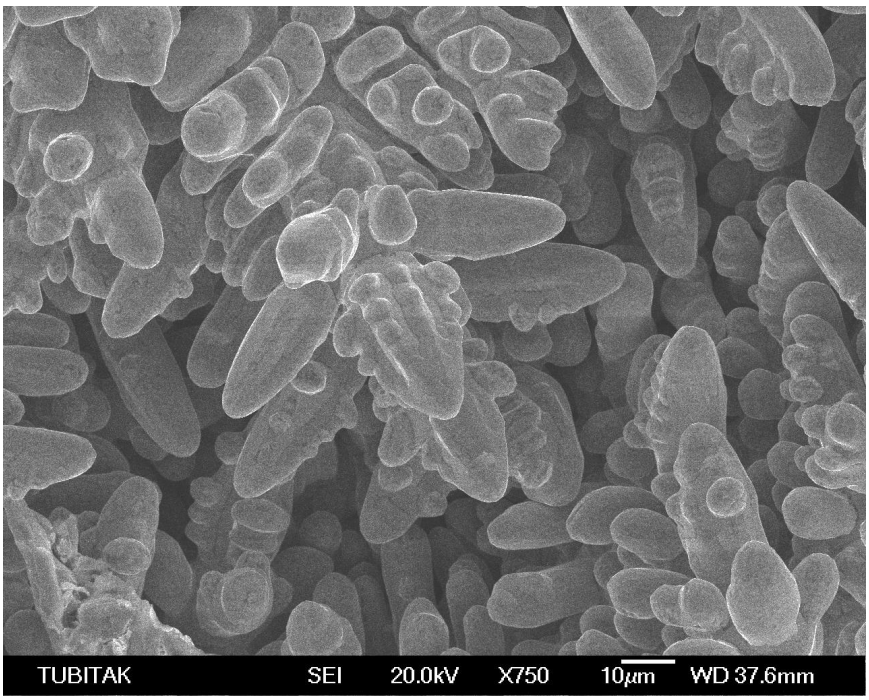

Figure 4.29. The SEM photograph of the fracture surface of 1%Bi, specimen squeeze cast under 100 MPa

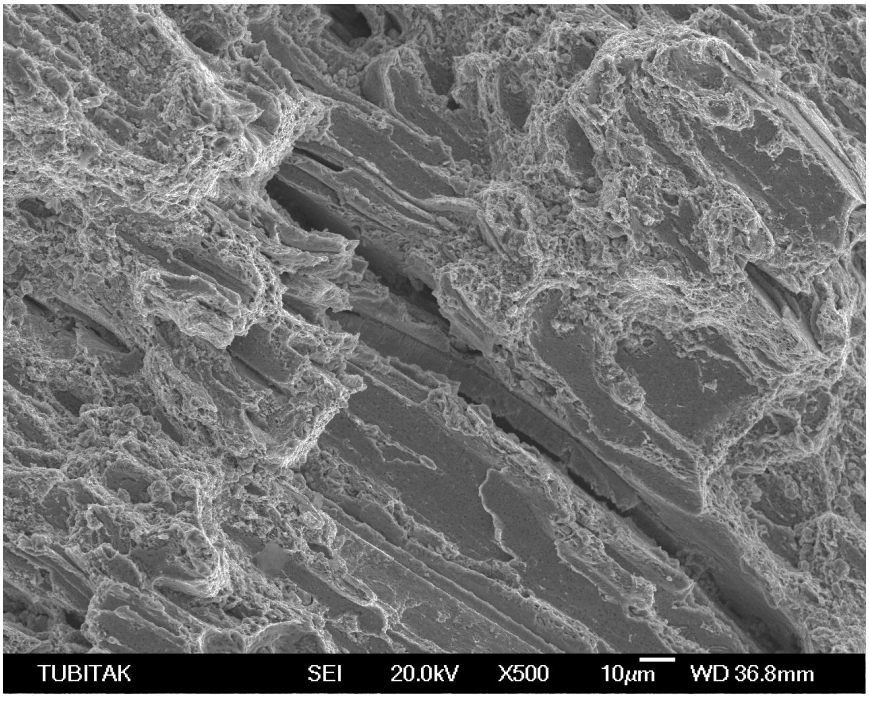

Figure 4.30. The SEM photograph of the fracture surface of 0.5% Bi, specimen squeeze cast under 50 MPa

The fracture surface of the ZA-27 alloy containing 0.5% Bi and squeeze cast under 50 MPa is given in Figure 4.30. It's seen that bismuth induces brittle fracture.

The fracture surface of the ZA-27 alloy containing 0.5% Bi and squeeze cast under 50 MPa is given in Figure 4.31. According to this photograph the bismuth particles embedded on the cleavage planes are seen clearly. The average diameter of the bismuth particles seen to be between 0.5μm to 1μm.

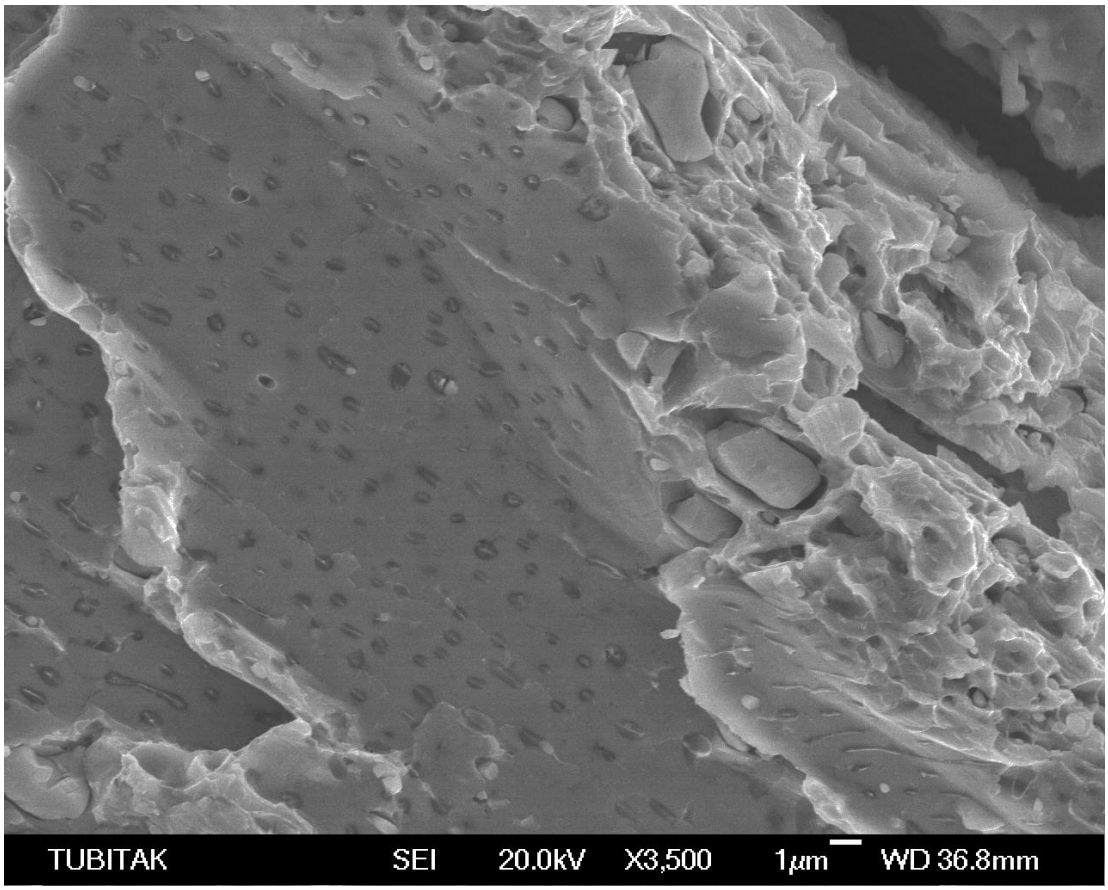

Figure 4.31. The SEM photograph of the fracture surface of 0.5%Bi, 50 MPa specimen

The fracture surface of the ZA-27 alloy containing 0.5%Bi and also not squeezed is seen in Figure 4.32. The dendrite surfaces are not clean as compared to the bismuth free ZA-27 alloy. It is possible that the dendrite surfaces are covered with the worm-like bismuth particles which solidified last as a thin film on the previously formed dendrites.

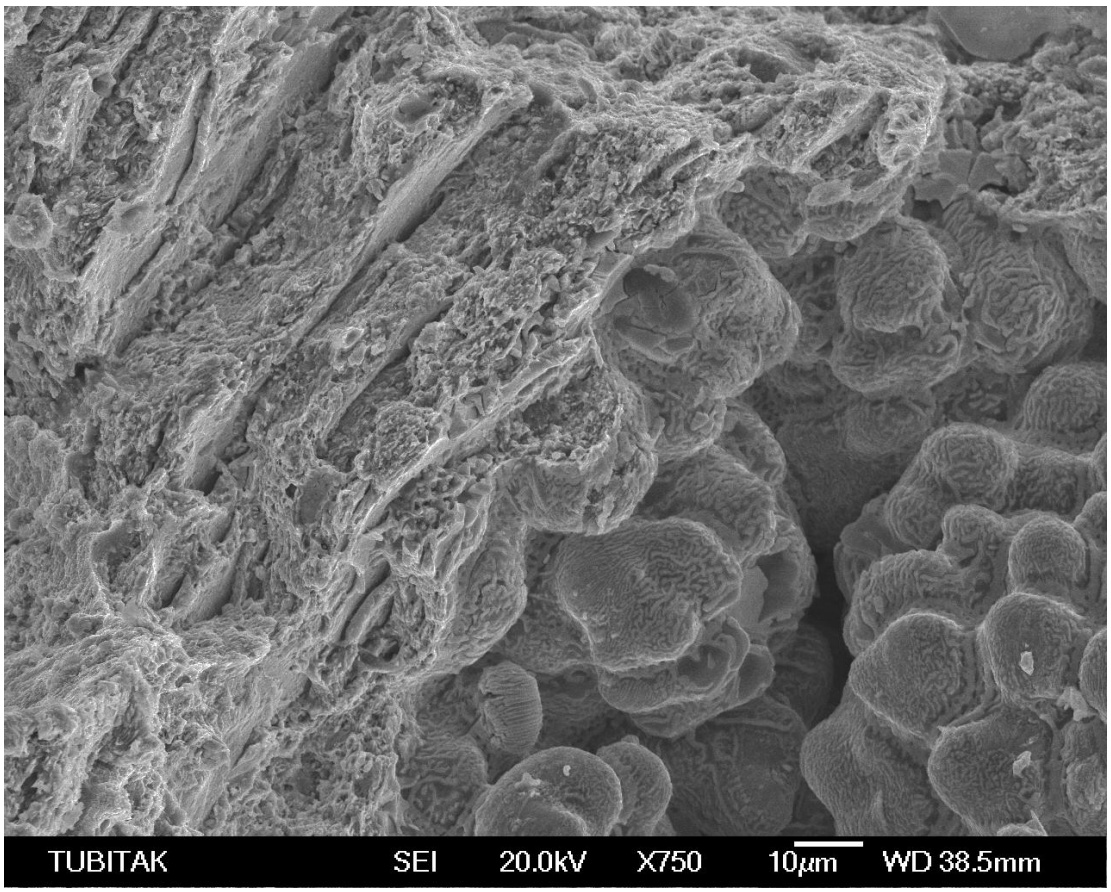

Figure 4.32. The SEM photograph of the fracture surface of 1%Bi, 0 MPa specimen

The remaining SEM micrographs of the fracture surfaces can be seen in the Appendix section.

Figure 4.33 shows the point chemical analysis of the sample containing 0.5%Bi and squeeze cast under 50 MPa. It is found that bismuth was concentrated at the fracture surface up to 1.4% Bi as expected since solidified last. Zinc concentration also increased since it solidified after the aluminum rich dendrites.

Table 4.13. Point chemical analysis of the specimen 19

Element	Weight%	Atomic%
Al K	16.98	33.40
Zn K	81.58	66.24
Bi M	1.44	0.37
Totals	100.00	

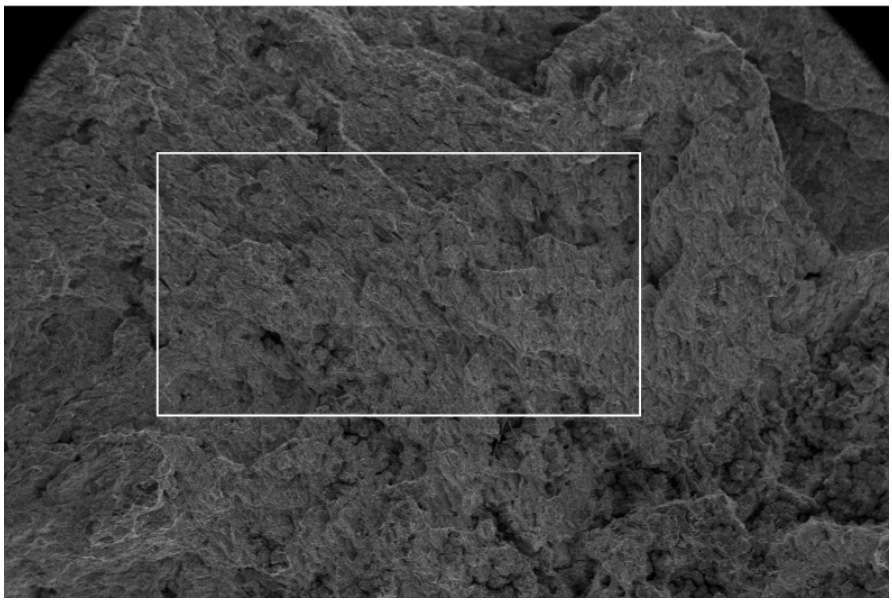

Figure 4.33. Point chemical analysis area of the specimen 19

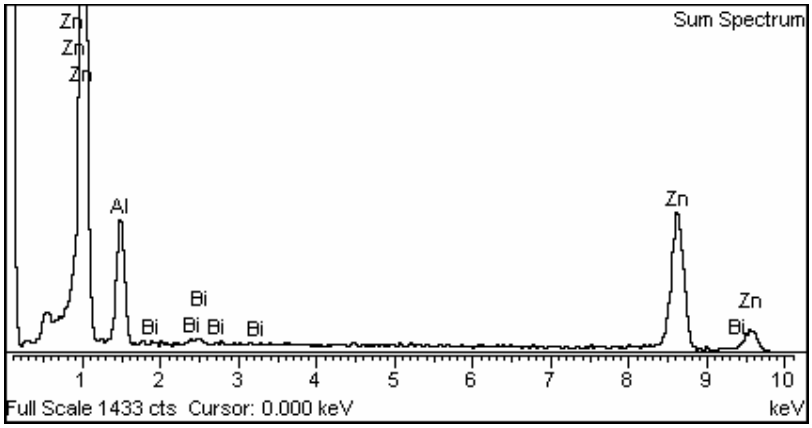

Figure 4.34. Point chemical analysis of the specimen 19

5. CONCLUSIONS AND RECOMMENDATIONS FOR FUTURE WORK

In the present study, the mechanical properties and the machinability characteristics of the ZA-27 alloy were examined. The general aim in the current work was to increase the machinability of the popular ZA-27 alloy without harming its mechanical properties. The highlights derived from this study can be summarized as follows:

Porosity levels decreased as a result of squeeze casting.

When the bismuth concentration was increased the machinability characteristics were increased, too. However, if the bismuth concentration exceeded the monotectic composition level, machinability characteristics were decreased because of the too short chips, i.e. dust.

Pure ZA-27 alloys provided the best surface roughness values as compared to their squeezed counterparts. Adding a small amount of bismuth increased surface roughness. When the squeezing pressure applied, surface roughness values increased, too.

Chip lengths were related to the squeezing pressure. As the specimens squeezed, the average chip lengths increased.

Bismuth was found to be beneficial on the machinability characteristics. When small amount of bismuth were added the average chip lengths were decreased.

With increasing the squeezing pressure the tensile strength and yield strength values increased. Reduction in area and elongation values were increased, too. So, squeezing was found beneficial on the mechanical properties of the ZA-27 alloy.

From the cooling curves, it was clear that fast cooling was observable for the squeezed ZA-27. The slopes of the curves were -0.6˚C/sec after squeezing,

and -0.514˚C/sec in gravity casting. This 17% increase can be attributed to the reduction in thermal resistance due to the prevention of an air-gap formation at the die-melt interface.

The solid and porous regions are easily differentiated from each other under the optical microscope. For instance, the top sections which solidified last contain more black regions than the bottom sections of the same casting. Hence, more porosity was found on the top area of the unsqueezed specimens than the bottom side of the same specimen.

To produce the castings directly for tension test a novel die design can be desired to eliminate the machining effects on tensile testing.

Using more thermocouples and an electronic recording unit the change of temperature at every side of the die and the specimen can be read. Using this technique, the evaluation of the heat transfer coefficient can be possible. A pyrometer can be used to learn the temperature an the die more precisely, in order to start the squeezing operation in time.

A new crucible design can be made by adding a stainless steel pipe inserted on the bottom of it. Using this pipe, argon gas can be fed into the crucible directly, in order to mix the melt using argon gas. This would eliminate the undesirable effects of air while mixing the melt with stick.

The simulation of the squeeze casting operation can be made in order to understand the heat transfer and cooling details of the die and the specimen easily.

REFERENCES

1. Baskaya, Ö., "The Mechanical Properties and Machinability of ZA-27 Casting Alloys" *MS Thesis, Boğaziçi University*, 2004.

2. Erturan H., "Squeeze Casting of Zn-Bi Monotectic Alloy", *MS Thesis, Boğaziçi University*, 1994.

3. Savas M.A., H. Erturan, and S. Altintas, "Effects of squeeze casting on the properties of Zn-Bi monotectic alloy", *Metallurgical and Materials Transactions*, Vol 28A, pp.1509-1515, 1997.

4. Scescape, "Bismuth", http://www.scescape.net/~woods/elements/bismuth.html, 2003.

5. Yang L.J., "The effect of casting temperature on the properties of squeeze cast aluminum and zinc alloys", *Journal of Materials Processing Technology 140, Singapore*, pp. 391–396, 2003.

6. Ghomashchi M.R., and A. Vikhrov, "Squeeze Casting: An Overview", *Journal of Materials Processing Technology*, Vol 1±9, pp.101, 2000.

7. Seah K. H. W., S.C. Sharma, and B.M. Girish, "Mechanical properties of as-cast and heat-treated ZA-27/graphite particulate composites", *Composites Part A 28A*, pp.251-256, 1997.

8. Schwam D., J.F. Wallace, Q. Chang, and Y. Zhu, "Optimization of the squeeze casting process for aluminum alloy parts-Final Report", *U.S. Department of Energy Assistant Secretary for Energy Efficiency and Renewable Energy*, Washington D.C., 2002.

9. Postek E.W., R.W. Lewis, D.T. Gethin, and R.S. Ransing, “Influence of initial stresses on the cast behaviour during squeeze forming processes”, *Journal of Materials Processing Technology 159*, pp.338–346, 2005.

10. Dynacast, “Zn Alloy”, http://www.dynacast.com/pdfcontent/en.znalloy.pdf, 2002.

11. Britnell D.J., and K. Neailey, “Macrosegregation in thin walled castings produced via the direct squeeze casting process”, *Journal of Materials Processing Technology 138*, pp. 306–310, 2003.

12. Ultracast, “ZA Advantages”, http://pages.infinit.net/ldsw/ucframes/productbot .html, 2006.

13. Epanchistov O.G., ``Structure and properties of metals solidified under high pressure", *Russian Casting Prod.*, pp.34-37, 1972.

14. Gervais E., H. Levert, and M. Bess, *Trans. AFS 68*, pp.183– 194, 1980.

15. Apelian D., M. Paliwal, and D.C. Herrschaft, *J. Met. 33*, pp.12– 20, 1981.

16. Abou El-khaira M.T., A. Daouda, and A. Ismail, “Effect of different Al contents on the microstructure, tensile and wear properties of Zn-based alloy”, *Materials Letters 58*, pp.1754–1760, 2004.

17. Eastern Alloys, Inc., “Material Properties”, http://www.eazall.com/ materialproperties .aspx, 2004.

18. Eastern Alloys, Inc., “FAQ”, www.eazall.com, faq.htm, 2004.

19. Schey, John A., *Introduction To Manufacturing Processes*, pp. 445-455, McGraw-Hill, 1987.

20. Climax Tools, “The Basics of Chip Formation”, www.cpmt.com/newsletter_related _docs/Part%203%20-%20Basics%20of%20Metal%20Chip%20Formation.pdf, 2006.

21. Lee J.I., Y.S. Han, H.I. Lee, and M.I. Kim, "Microstructures and mechanical properties of squeeze cast Al-Si-Cu-Mg alloy", *J. Korean Inst. Met. Mater. 32 (10)*, pp.1259-1268, 1994

22. Yen C.M. and W.J. Evans, "Aluminium Casting Alloy", *European Patent No. EP0 485 068*, 1991.

23. Chadwick G.A., "Squeeze casting of magnesium alloys and magnesium based metal matrix composites", *Conference on Magnesium Technology*, London, 1986.

24. Suresh K.R., H.B. Niranjan, P. Martin Jebaraj, and M.P. Chowdiah, "Tensile and wear properties of aluminum composites", *Wear 255*, pp.638–642, 2003.

25. Gross D.K., "Zinc Die Castings —The Importance of Alloy Chemistry", *Teck Cominco Metals Ltd.*, Toronto, Canada, 2006.

26. Aashuri H., A. Razavimanesh, A. Kolahi, and M. Mohiedin, "Impact and tensile behaviour of fractional melting processed ZA-27 alloy", *Materials Science and Engineering A333*, pp.115–122, 2002.

27. Chadwick G.A. and T.M. Yue, "Principles and applications of squeeze castings", *Met.Mater. 5 (1)*, pp.6-12, 1989.

28. Franklin J.R. and A.A. Das, *Br. Foundryman 77 (3)*, pp.150, 1984.

29. Gethin D.T., R.W. Lewis, and M.R. Tadayon, "Finite element approach for modelling metal flow and pressured solidification in the squeeze casting process", *Int. J. Numer. Meth. Eng. 35 (4)*, 1992.

30. Balan P., R.M. Pillai, K.G. Satyanarayana, and B.C. Pai, "The structure and properties of squeeze-cast eutectic Al-Si plates", *Int. J. Cast Metals Res. 6 (3)*, pp.131-136, 1993.

31. Omega Engineering, "Thermocouples - An Introduction", http://www.omega.com /thermocouples.html, 2006.

32. Papworth A., and P. Fox, "The disruption of oxide defects within aluminium alloy castings by the addition of bismuth", *Materials Letters 35*, pp.202–206, 1998.

33. ASTM, "D792 Density Measurement Standard", *ASTM D792 Standard*, www.astm. org, 2006.

34. ASTM, "E8-04 Standard Test Methods for Tension Testing of Metallic Materials", *ASTM E8 Standard,* www.astm.org, 2006.

35. Yong M.S., and A.J. Clegg, "Process optimisation for a squeeze cast magnesium alloy", *Journal of Materials Processing Technology 145*, pp.134–141, 2004.

36. Akyuz M., "Mechanical properties and machinability of Al-Mg casting alloys", *MS Thesis, Boğaziçi University*, 1988.

37. Saçlı O., "A numerical and quantitative analysis of an aluminum-silicon alloy", *MS Thesis, Boğaziçi University*, pp 63, 1999.

38. Cay F., and S.Can Kurnaz, "Hot tensile and fatigue behaviour of zinc–aluminum alloys produced by gravity and squeeze casting", *Materials and Design 26*, pp.479-485, Sakarya University-Turkey, 2005.

39. Savas M.A. and S. Altintas, "Effects of squeeze casting on the wide freezing range binary alloys" , *Materials science and engineering, Vol A173*, pp.227-231, 1993.

40. Chen T.J., Y. Hao, J. Sun, and Y.D. Li, "Effects of processing parameters on tensile properties and hardness of thixoformed ZA-27 alloy", *Materials Science and Engineering A 382*, pp.90–103, 2004.

APPENDIX A: SEM MICROGRAPHS OF THE FRACTURED SURFACES OF THE TENSION TEST SAMPLES

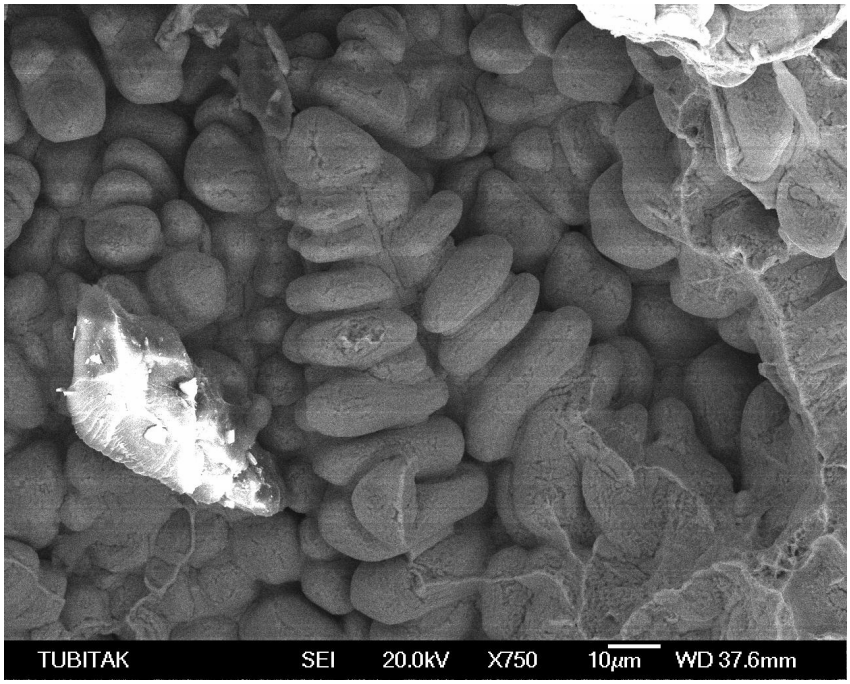

Figure A.1. The SEM micrograph of the fracture surface of 0%Bi, 100 MPa specimen

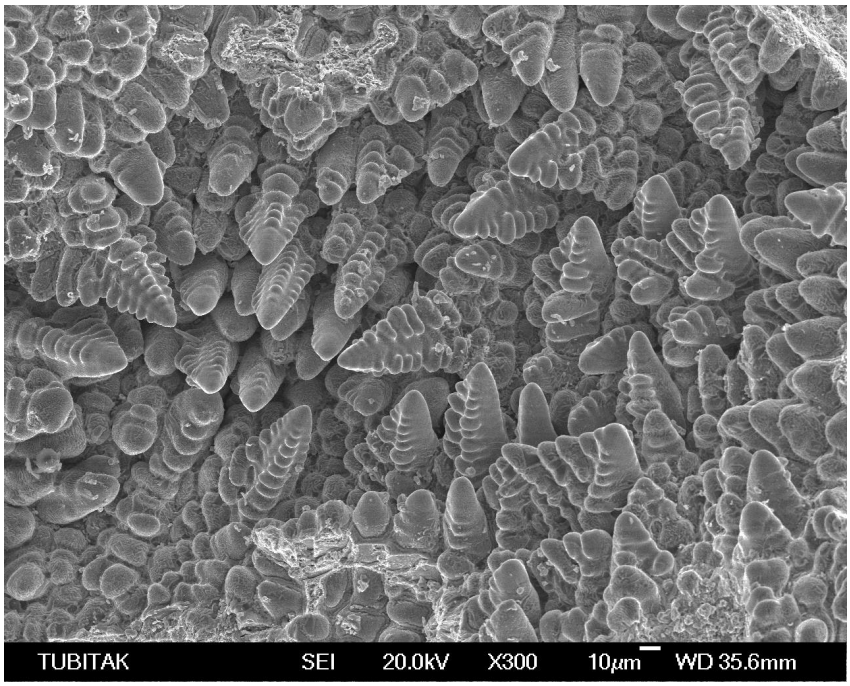

Figure A.2. The SEM micrograph of the fracture surface of 0.5%Bi, 0 MPa specimen

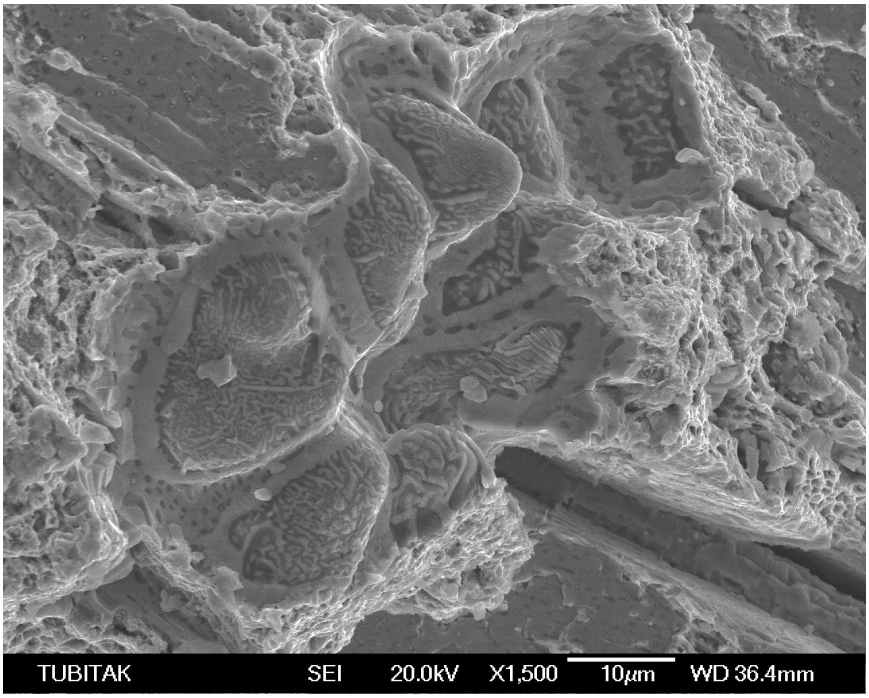

Figure A.3. The SEM micrograph of the fracture surface of 0.5%Bi, 50 MPa specimen

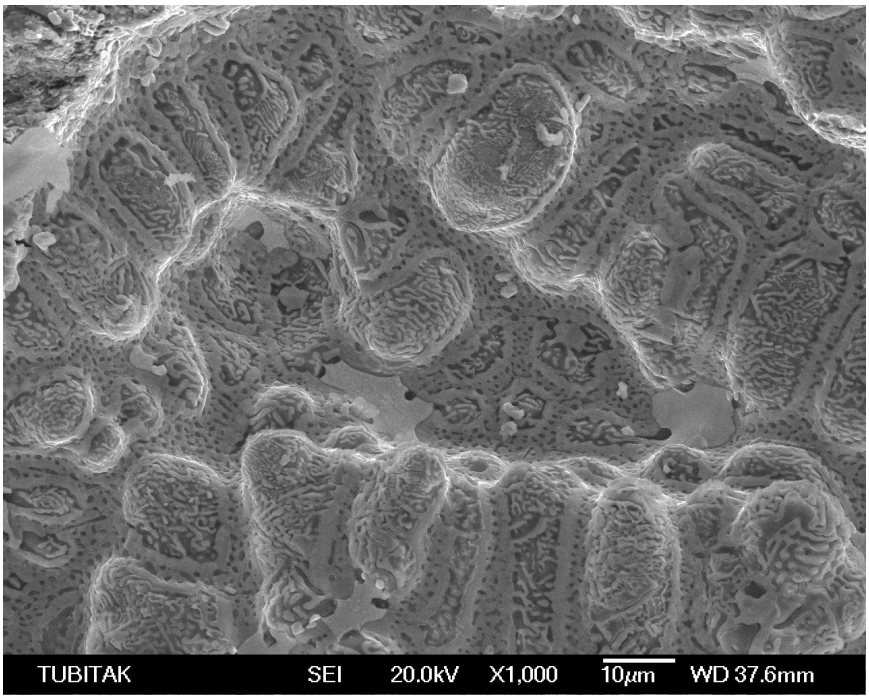

Figure A.4. The SEM micrograph of the fracture surface of 1%Bi, 100 MPa specimen

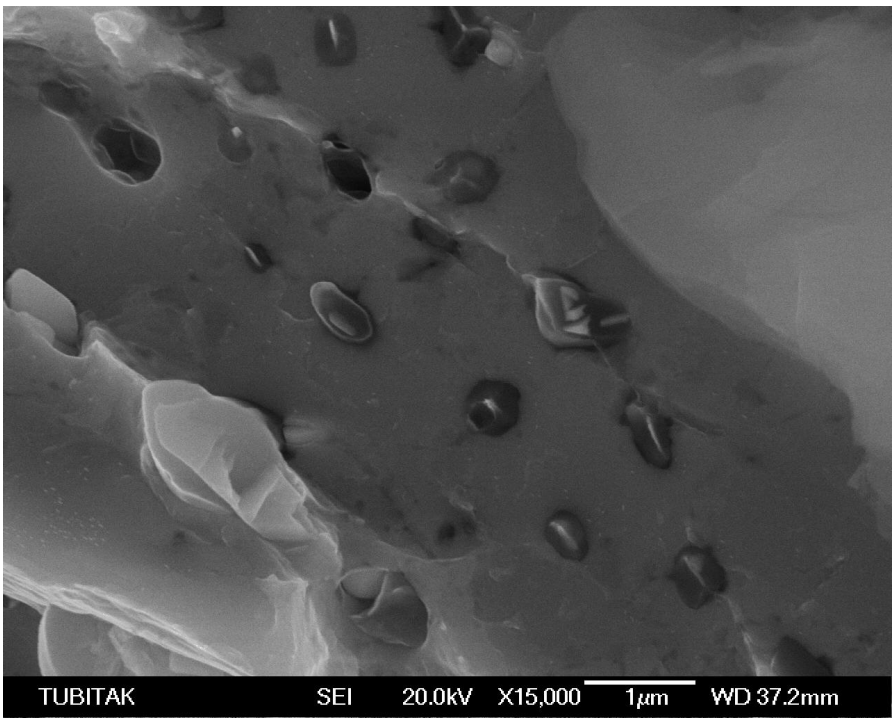

Figure A.5. The SEM micrograph of the fracture surface of 1.5%Bi, 100 MPa specimen

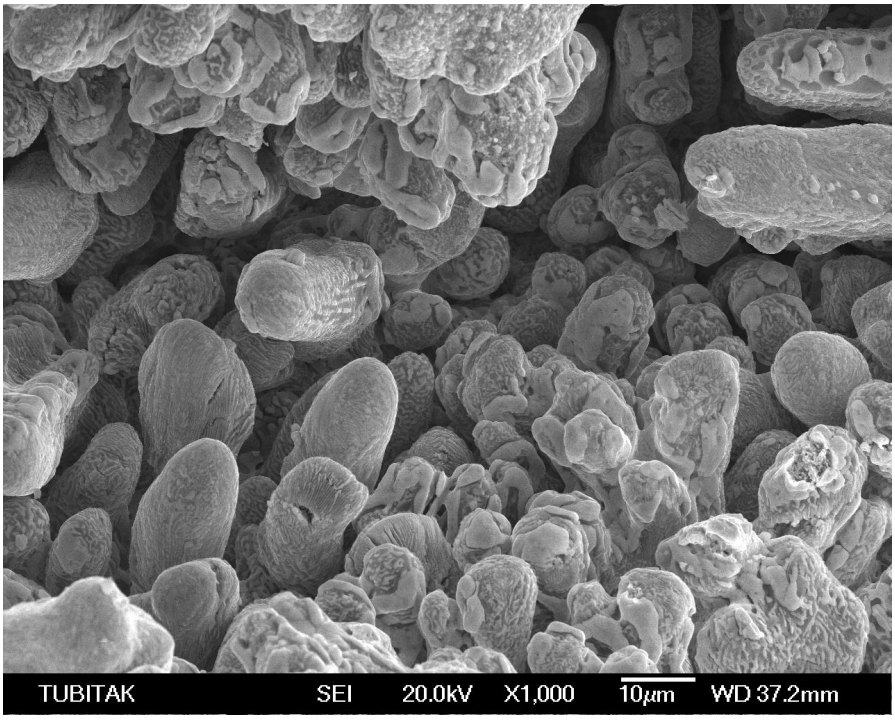

Figure A.6. The SEM micrograph of the fracture surface of 1.5%Bi, 100 MPa specimen

APPENDIX B: TECHNICAL DRAWINGS OF THE SQUEEZE CASTING DIE

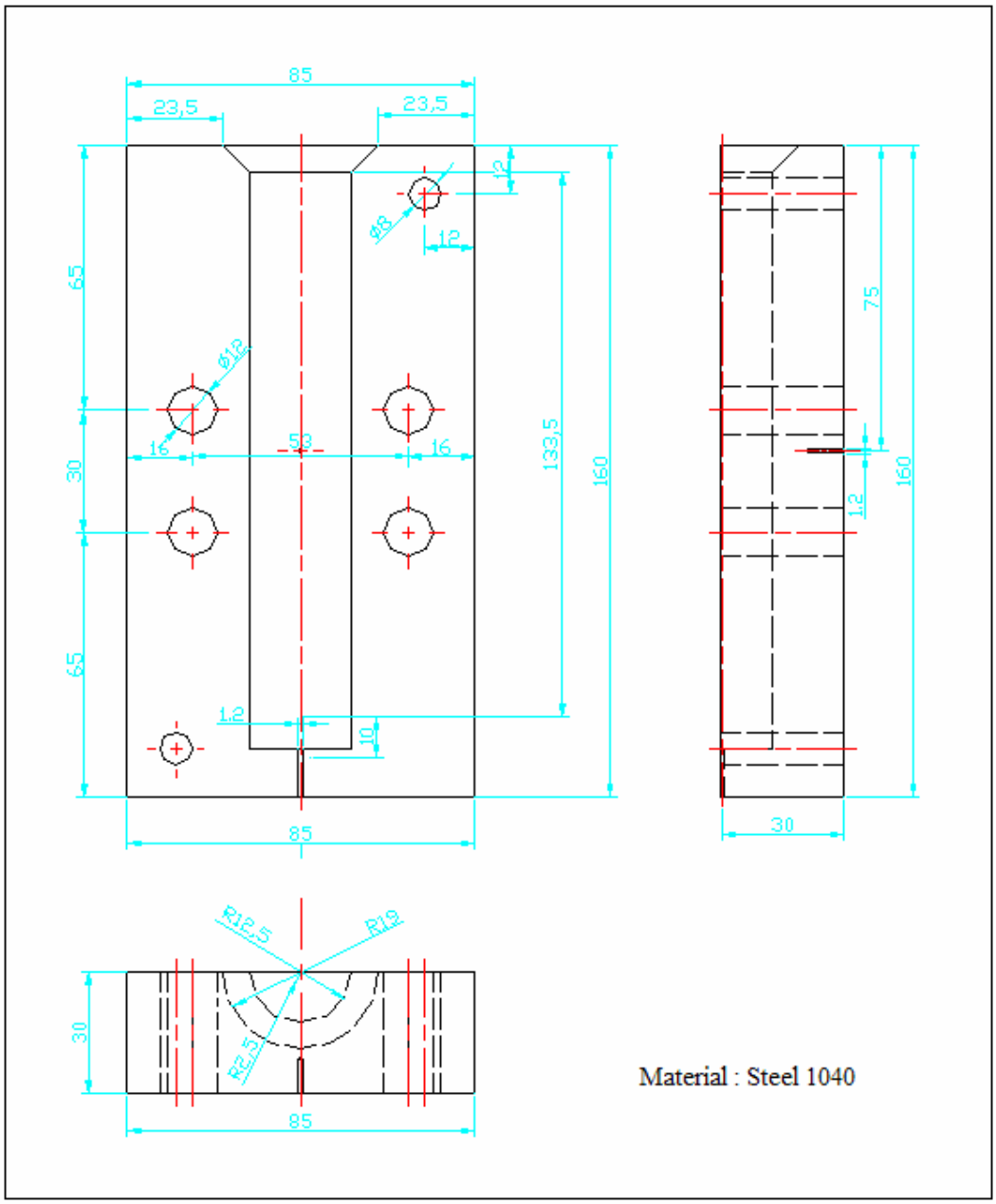

Figure B.1. Technical drawing of first half of the squeeze casting die

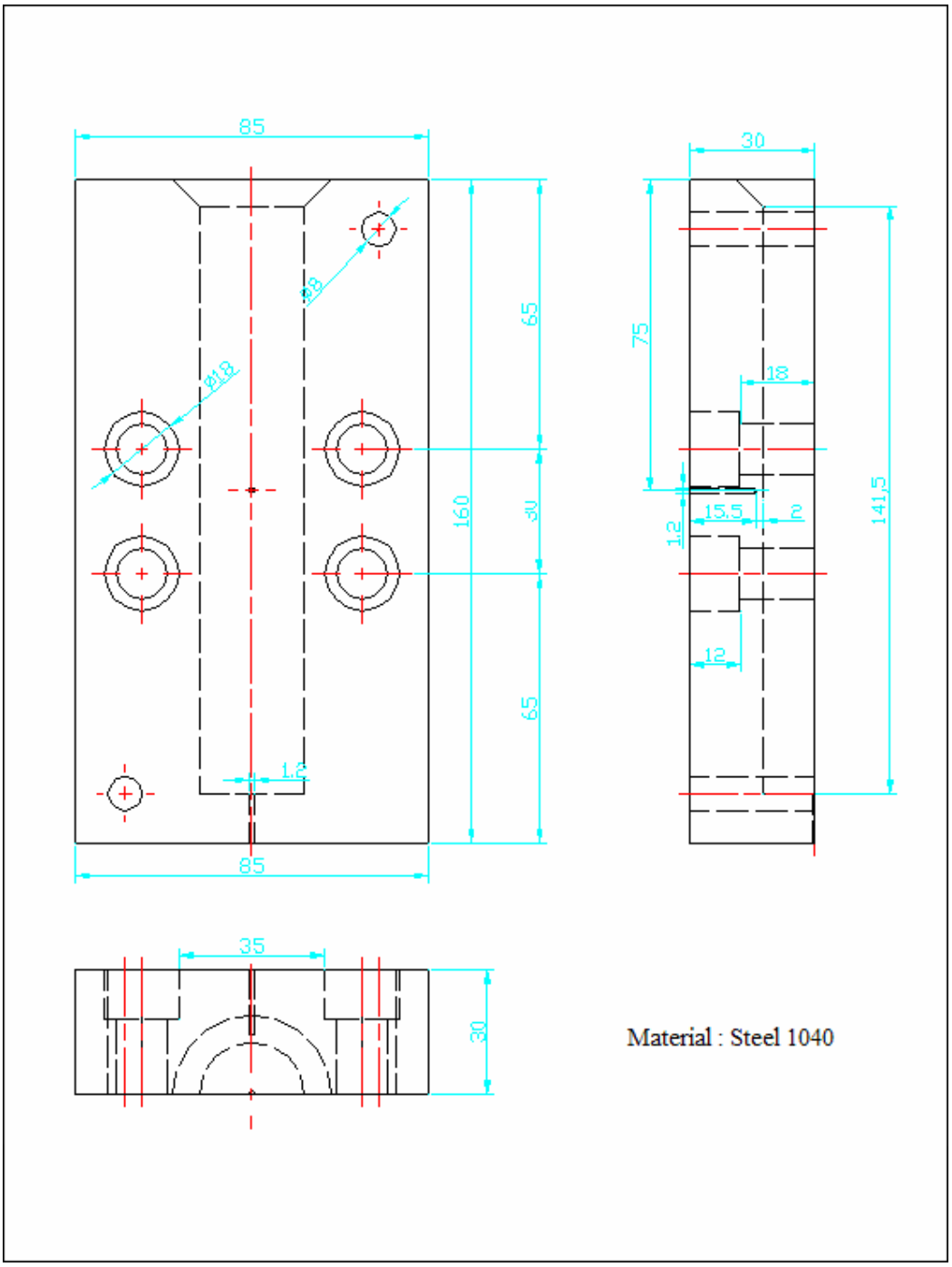

Figure B.2. Technical drawing of second half of the squeeze casting die

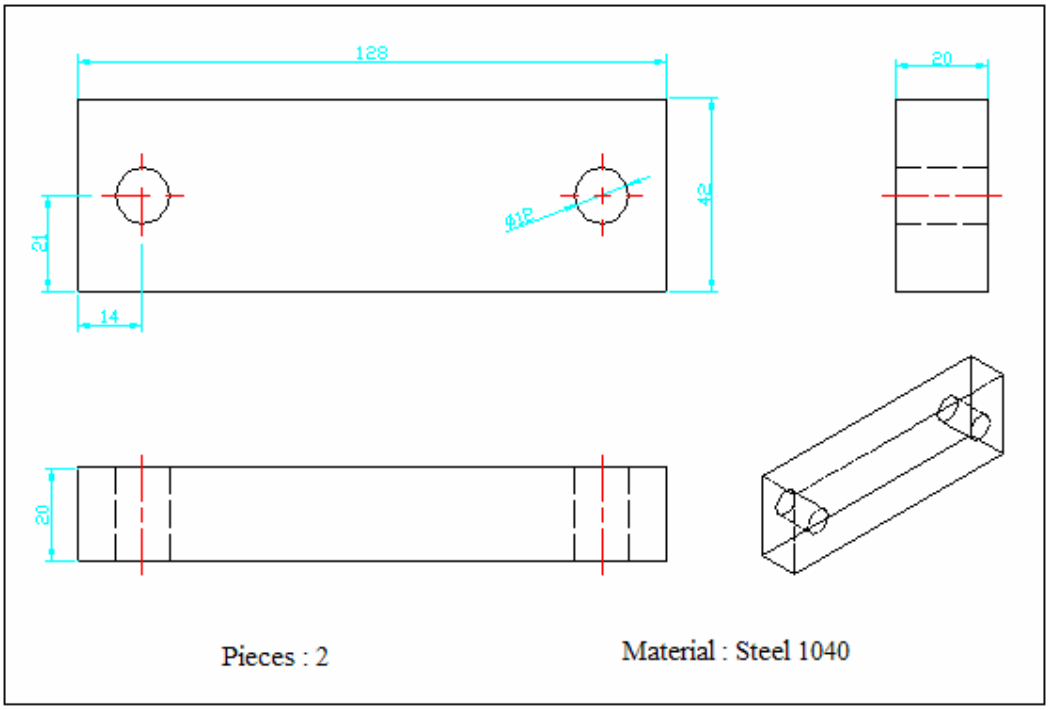

Figure B.3. Technical drawing of rear plate of the squeeze casting die

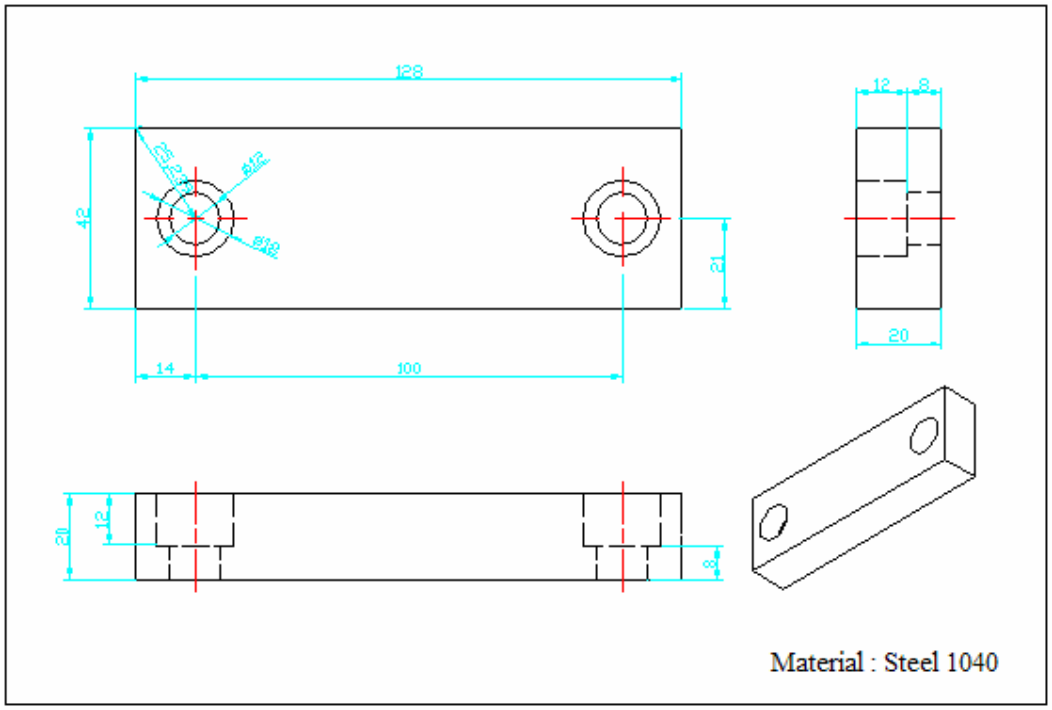

Figure B.4. Technical drawing of front plate of the squeeze casting die

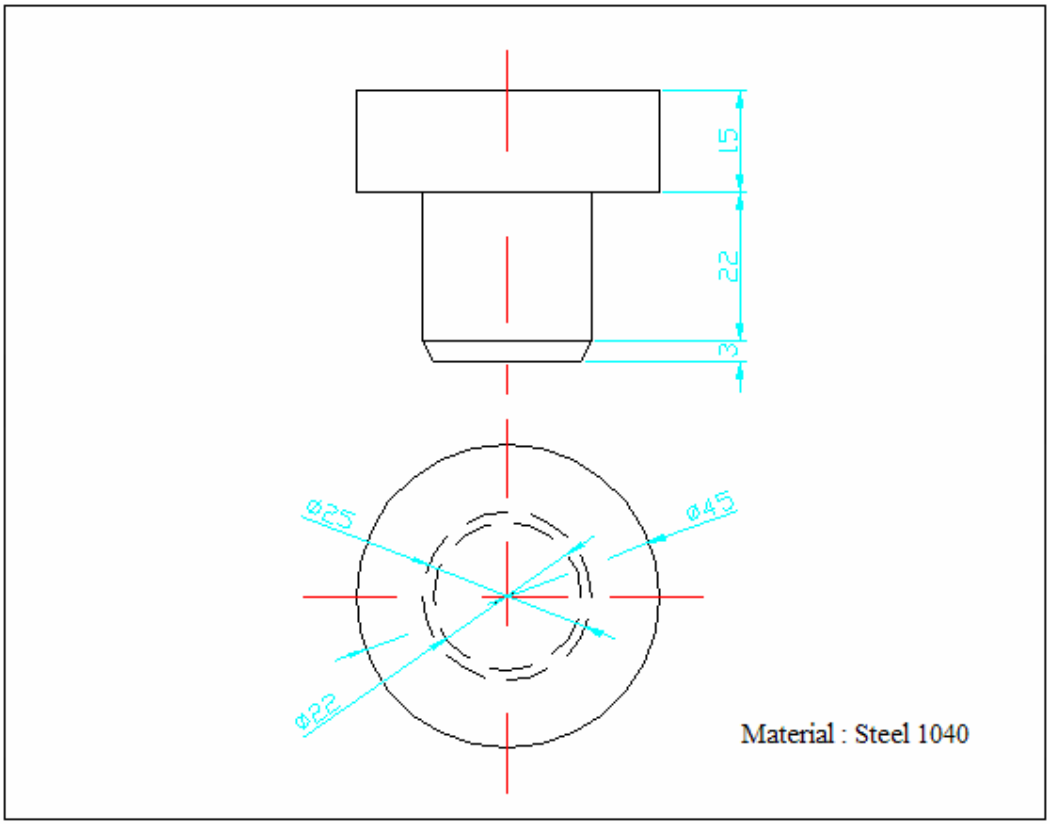

Figure B.5. Technical drawing of punch of the squeeze casting die